RECEIVED
LAWRENCE
RADIATION LABORATORY

AUG 12 1974

LIBRARY AND
DOCUMENTS SECTION

LBL-2694
c.2

OPTICAL STUDY OF METAL ION-NERVE INTERACTIONS

Daniel Axelrod
(Ph.D. Thesis)

May 1974

Prepared for the U. S. Atomic Energy Commission
under Contract W-7405-ENG-48

TWO-WEEK LOAN COPY

This is a Library Circulating Copy which may be borrowed for two weeks. For a personal retention copy, call Tech. Info. Division, Ext. 5545

LAWRENCE BERKELEY LABORATORY
UNIVERSITY OF CALIFORNIA
BERKELEY

LBL-2694
c.2

DISCLAIMER

This document was prepared as an account of work sponsored by the United States Government. While this document is believed to contain correct information, neither the United States Government nor any agency thereof, nor the Regents of the University of California, nor any of their employees, makes any warranty, express or implied, or assumes any legal responsibility for the accuracy, completeness, or usefulness of any information, apparatus, product, or process disclosed, or represents that its use would not infringe privately owned rights. Reference herein to any specific commercial product, process, or service by its trade name, trademark, manufacturer, or otherwise, does not necessarily constitute or imply its endorsement, recommendation, or favoring by the United States Government or any agency thereof, or the Regents of the University of California. The views and opinions of authors expressed herein do not necessarily state or reflect those of the United States Government or any agency thereof or the Regents of the University of California.

LBL-2694

OPTICAL STUDY OF METAL ION - NERVE INTERACTIONS

Daniel Axelrod
(Ph.D. thesis)

Department of Physics and Laboratory of Chemical Biodynamics
Lawrence Berkeley Laboratory, University of California
Berkeley, California 94720

May 1974

OPTICAL STUDY OF METAL ION – NERVE INTERACTIONS

Table of Contents

Chapter I. INTRODUCTION 1

Chapter II. REVIEW OF PHYSIOLOGY 6

A. Biological Membranes: Structure and Function 6

B. Axon Membrane 10

C. Axon Action Potential 11

D. Action Potentials and Metal Ions 14

E. Models 24

F. Spectroscopic Experiments on Nerve 39

Chapter III. METAL IONS: CHEMISTRY AND SPECTROSCOPY 52

A. Na^{+}, K^{+}, and Ca^{+2} Chemistry 52

B. Spectroscopically Interesting Chemical Substitutes for Ca^{+2} and K^{+} 56

C. Atomic Structure and Spectroscopy of Europium and Terbium 58

D. Experimental *in vitro* Eu^{+3} Fluorescence Spectra: Results and Discussion. . . . 70

E. Fluorescence of Transition Metal Complexes 76

Chapter IV. GARFISH NERVE: ANATOMY AND PHYSIOLOGY 78

A. Garfish Olfactory Nerve 78

B. Care of Garfish 80

C. Dissection of Olfactory Nerve 81

D. Ringer Solutions 87

E. External Stimulation and Recording of Garfish Nerve Trunks 88

Chapter V. GARFISH NERVES IN RARE-EARTH RINGERS . . 90

A. Rare-earths as Physiological Substitutes for Ca^{+2} 90

B. Fluorescence Spectra of Nerves 93

Chapter VI. TRANSIENT FLUORESCENCE CHANGE STUDIES. 101

A. Experimental Apparatus 101

B. Transient Changes of Rare-earth Fluorescence 107

C. Transient Changes of Intrinsic Fluorescence 110

Chapter VII. FLUORESCENCE CHANGES IN RESTING NERVE 113

A. Uptake of Eu^{+3}: Time Course 113

B. Diffusion of External Solution into Nerve Trunk 118

C. Eu^{+3} Uptake: Quantity 119

D. Effect of High $[K^+]$. 120

E. Effects of Proteases and Neuraminidase . . . 122

F. Effect of Phospholipase-c (Plc) 123

G. Effect of Dimethylsulfoxide (DMSO) 126

H. Energy Transfer Between Bound Rare-Earth Ions 128

I. Protein Fluorescence Quenching by Transition Metals 132

Chapter VIII. CONCLUSIONS AND DISCUSSION 133

Acknowledgments 138

References 139

ABSTRACT

Calcium ions are intimately involved in the process of nerve conduction. Obstacles to gaining information about the precise molecular mechanisms have been the minute quantities and fast transience of Ca^{+2} interaction, and Ca^{+2}'s spectroscopic invisibility. In order to probe the ion-nerve membrane interaction, rare-earth ions were substituted in place of Ca^{+2} in the bathing solution of garfish olfactory nerve trunk. Low concentrations of rare-earth ions maintain excitability of nerve in Ca-free solutions, and restore excitability to nerves previously bathed in solutions free of any polyvalent ions. Furthermore, two of the rare-earth ions, Eu^{+3} and Tb^{+3}, show a much enhanced fluorescence upon chemical binding. We observed the fluorescence of Eu^{+3} and Tb^{+3} as a measure of rare-earth (and by analogy, calcium) binding to nerve, both resting and firing, and subjected to treatments with various enzymes, chemical agents, and abnormal salt concentrations. The main results are: (1) Rare-earth ions bind to proteins, NADH and possibly other molecules in the nerve; (2) The total bound rare-earth ion fluorescence changes by less than 0.01% upon firing; (3) Most of the observed binding is a slow, continual uptake of rare-earth ion, probably into the axoplasm, rate-limited by permeation through the axon membrane.

A detailed discussion of the luminescence properties of rare-earth ions, a review of membrane and neuron physiology, and suggestions for the handling and dissection of garfish are included.

CHAPTER I.

INTRODUCTION

A complicated multicellular organism consists of many types of differentiated cells. Each cell has a specific function but also must rely on the specialized chemical work of the others in order that the whole organism remain viable and self-sustaining. As a result, information on the state of the organism and of the environment must be processed and transmitted among these specialized cells so that they can function together cooperatively. In higher animals, processing and transmittal of intercellular information is carried on in a rapid and well-determined manner by another specialized cell, the nerve cell or neuron. The neuron (see Fig. 1) has three specific functions.

(1) It receives electrical signals from other sensory organs or nerve cells and computes an analog sum of these inputs. This summation occurs in the membrane of the cell body. If the sum is greater than a fixed threshold value, the neuron "responds".

(2) The "response" is the transmittal of information along the length of the neuron, often in digital form, manifested by a propagating all-or-none electrical pulse called an "action potential". The propagation of the action potential occurs in the membrane of the axon.

(3) The information is then transferred to one of the inputs of another nerve, to a muscle, or to some other organ, via the synapse between the neuron and the succeeding cell.

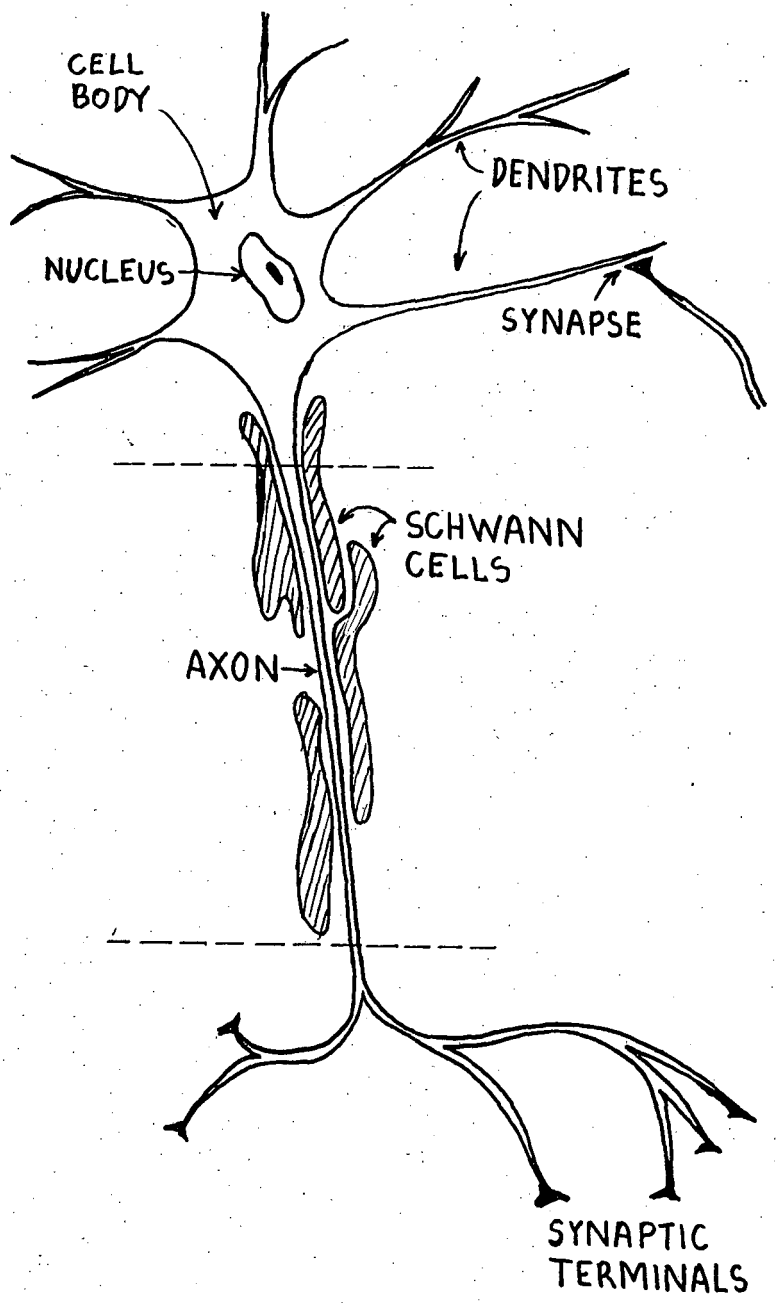

XBL 744-694

Fig. 1. A neuron. Axon preparations, indicated schematically by the area between the dashed lines, are dissected out and studied as described in this thesis.

This thesis concerns a study of the little understood molecular mechanism of the second neuronal function listed above, i.e., action potential propagation along the axon membrane.

As will be discussed in detail in the next chapter, the successful propagation of an action potential depends critically on the metal ion composition of the external solution bathing the axon (the blood in the live animal). In particular, Ca^{+2} ions in the external solution appear to exert a controlling influence on the binding or permeability of other ions, notably Na^{+} and K^{+} (45, 43). Such Ca^{+2}-dependent effects raise several questions:

(1) Does Ca^{+2} bind to the axon membrane?

(2) If so, to what macromolecules and with what chemical specificity?

(3) Does the state of Ca^{+2} binding change during excitation?

(4) If so, is such a change of binding state causal to excitation?

Some obstacles to answering these questions are the following:

(1) It is desirable to leave the nerve membrane intact to study excitation.

(2) Ca^{+2} has no electron spin resonance, and neither ultraviolet nor visible absorption or fluorescence spectra.

(3) We are interested in rapid transient chemical associations with the membrane, not integrated fluxes, so $^{45}Ca^{+2}$ tracer studies are inappropriate.

(4) The quantity of bound Ca^{+2} may be fairly small, and the fraction specific to the excitation process is probably extremely small.

The goal of minimizing the external perturbation to the delicate axon membrane is reached in this study by employing electromagnetic spectroscopic techniques, specifically fluorescence and scattering of UV and visible light. The problem of the spectroscopic "invisibility" of Ca^{+2} is avoided by chemically replacing the Ca^{+2} in the external solution with other polyvalent ions which have similar physiological effects on nerve as does Ca^{+2}, and also have more interesting chemically-sensitive spectra. These ions are the trivalent rare earths, and divalent manganese, cobalt and nickel. During and after substitution of these ions for Ca^{+2}, an appropriate spectral feature of the nerve or substitute ion is monitored for changes occurring synchronously with the passage of an action potential or changes arising from chemical, electrical, or enzymatic modification of the external solution or axon membrane. Because of the richness of some of the spectra involved, and the wide variety of ions and treatments employed, the spectroscopic approach offers hope of finding some unambiguous answers to problems concerning metal ion, and specifically Ca^{+2}, interaction with axonal macromolecules.

The thesis is divided into eight chapters, providing first a self-contained background in the relevant biology, chemistry, and physics, and followed by a presentation and discussion of experimental results. All of the literature references are listed at the end.

The literature in all aspects of membrane organization and function is huge; therefore, many of the references cited are reviews.

CHAPTER II.

REVIEW OF PHYSIOLOGY

It is virtually certain that the axonal action potential is a membrane phenomenon (the evidence for this conclusion is discussed in Section B below). In order to study macromolecular changes in neuronal membrane, it is necessary to first become familiar with the general principles of organization and function of biological membranes.

A. Biological membranes: structure and function

Biological membranes are composed primarily of proteins, lipids and carbohydrates, and to a small extent, covalent combinations of these as glycoproteins and glycolipids.

The mass ratio of proteins to lipids is usually between 1 and 2, depending on the type of membrane, and carbohydrates account for a smaller portion, about 10% of the membrane weight (11, 82, 20).

The macromolecular organization of these components has been a subject of controversy for years. The lipids and proteins of membranes are held together by non-covalent electrostatic interactions, which can include hydrophilic, hydrophobic, Van der Waals, hydrogen bond, and ionic interactions. Membrane models are designed so that the macromolecules are ordered in a state where the free energy of the system is at a relative minimum; as a rule of thumb, one tries to maximize the hydrophobic and hydrophilic interactions. One point of agreement between many membrane models is that at least

large portions of the membrane phospholipids (which comprise the bulk of the lipids) are in a bilayer array, with the two hydrophobic tails of each phospholipid molecule facing or intertwining each other in the interior and the hydrophilic head group of the phospholipid facing outward. This arrangement (as opposed to, say, the head group facing the interior) is supported by a variety of indirect chemical evidence (146) as well as thermodynamic arguments (125).

The main disagreement between models is in the placement and mobility of the proteins, and their degree of interaction with the lipids. The formerly widely accepted model of Danielli and Davson (35) consists of a continuous phospholipid bilayer sheet with globular proteins covering the lipids in layers, making a protein-lipid sandwich. Robertson (114) modified the proteins to be more sheet-like while retaining the lipid bilayer backbone (see Fig. 2a). This model, claimed to be universal (and hence called the "unit membrane"), had supporting evidence from electron microscopy and X-ray diffraction, but a major objection is that it does not explicitly account for membrane specificity of function and transport and does not agree with some chemical decomposition studies (11). Interesting features of the model are the emphasis it places on the phospholipid "backbone" (while the proteins are subordinated to a secondary role), and the two-dimensional homogeneity. As a result, succeeding related models tried to assign functional roles to the bilayer sheet, emphasizing its possible phase transitions as a liquid crystalline array (19), transport selectivity inherent in the type and orientation of the polar head

groups (8, 50, 3), and analogy with synthetic homogeneous ion-exchange membranes (44). The "unit membrane" was a popular model also because its basic structure is similar to artificial phospholipid bilayer membranes which can be produced easily in the laboratory. Artificial lipid membranes have a much higher electrical resistivity than natural membranes, but this can be drastically lowered and ionic selectivity introduced, by the addition of macrocyclic antibiotics such as valinomycin (143). These antibiotics apparently act as mobile "carriers" of ions (43), a fact which led to considerable speculation that transport across the lipid bilayer in real membranes is mediated by some unknown specialized carrier molecules (109).

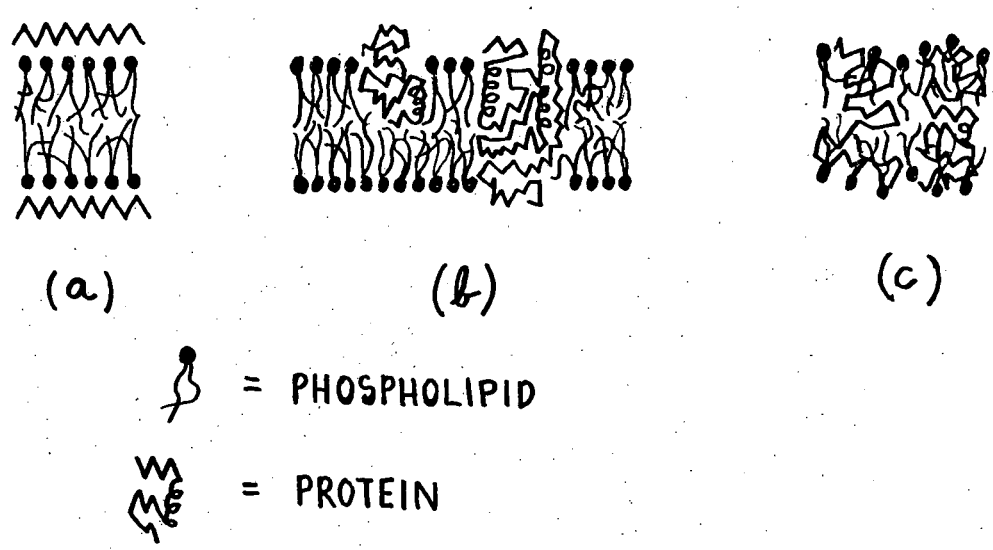

XBL 744-688

Fig. 2. Membrane models. (a) Davson Danielli-Robertson; (b) Fluid mosaic; (c) Benson.

In order to account for the specificity of biological membranes, while still retaining the bilayer backbone, some models introduce fixed "pores" through the lipid. This may consist of either a large globular protein with a "passageway" for ions through its interior extending entirely across the bilayer, or merely as a break in the continuity of the lipid bilayer (90).

A more recent model, the fluid mosaic model of S. J. Singer (126) (see Fig. 2b), and related models (15), offer more flexibility than the traditional bilayer backbone. Singer's model consists of globular proteins floating in a liquid-like phospholipid bilayer matrix "sea". Some proteins can be outside the lipid bilayer as in the "unit membrane", but others ("integral" protein) can partially or completely transect the membrane. The varying degrees of accessibility of different membrane proteins to solubilization (11) and enzymatic attack, and the growing body of experimental results indicating mobility of both phospholipids (118) and proteins (46, 30, 140), in the plane of the membrane, and fluidity in the hydrophobic interior (95), support the fluid mosaic model. Transport or specialized functions are handled by the integral proteins; the model leaves the question open as to exactly how this is accomplished in specific real membranes.

The Benson model (5) dispenses with the lipid bilayer entirely (Fig. 2c). The proteins are arranged in globular subunits with hydrophobic interiors and hydrophilic exteriors. The hydrocarbon tails of lipids intercollate into interior folds in the protein chains, with polar heads in contact with the water at the membrane surfaces. These

lipoprotein subunits are held together by hydrophobic and Van der Walls associations. Benson's model appears to be somewhat crystalline in that the protein chain subunits cannot flex nor translate freely. However, complicated and possibly cooperative conformation changes relating to transport and specific functions can be easily rationalized in this model.

B. Axon membrane

Much of the experimental work on membrane structure has been performed on erythrocyte (red blood cell) membranes because erythrocyte cells are easily obtainable and can be readily (osmotically) burst to obtain "pure" membrane preparations or "ghosts". It is of course possible that the organization of the axonal membrane is completely different from the erythrocyte membrane. Aside from the obvious functional difference in that the axon membrane is "excitable", there are several known biochemical and structure differences. Some nerve membrane (although not all) (155) contain in addition to phospholipid, "gangliosides" (~5% of the total lipid) (86). These are lipids with two hydrocarbon "tails", as in phospholipids, and an oligosaccharide head which contains many sialic acid residues. The sialic acid residues are negatively charged at neutral pH, so the presence of gangliosides in the membrane may be significant in determining membrane electrical properties. On the other hand, nerve cell membranes contain little or no collagen and certain mucopolysaccharides such as are present at the outside surface of some mammalian cells (although the ubiquitous linear mucopolysaccharide hyaluronic acid with a negative

charge at pH 7.0 is present) (86, 87). Spin-label studies on lobster walking leg nerves show that the hydrophobic region of the axon membrane is fluid (70); this fluidity is probably due to the high degree of unsaturation of the phospholipid hydrocarbon tails and the fairly low content of cholesterol in nerve membrane (155). However, no studies have demonstrated as yet translational mobility of proteins or phospholipids in nerve.

C. Axon action potential

It is interesting to examine whether one can partially deduce the nerve membrane's structure from its remarkable ability to propagate an electrical impulse. We will review the electrophysiology of axons ("axonology"), followed by a discussion of the requirements for nerve membrane modeling and a brief survey of popular models in the literature.

The most easily observable feature of an action potential is a propagating reversal of the electrical potential difference between the inside (axoplasm) and the external solution (blood) (77) (see Fig. 3). The trans-membrane voltage is relatively negative inside in the resting regions and relatively positive inside in the active region.

The trans-membrane voltage arises from a constant ion concentration gradient across the membrane, coupled with selective permeability of the membrane to certain ions. Specifically, the external solution contains a high Na^+ and low K^+ concentration, and the reverse being the case in the axoplasm. The membrane in the resting state

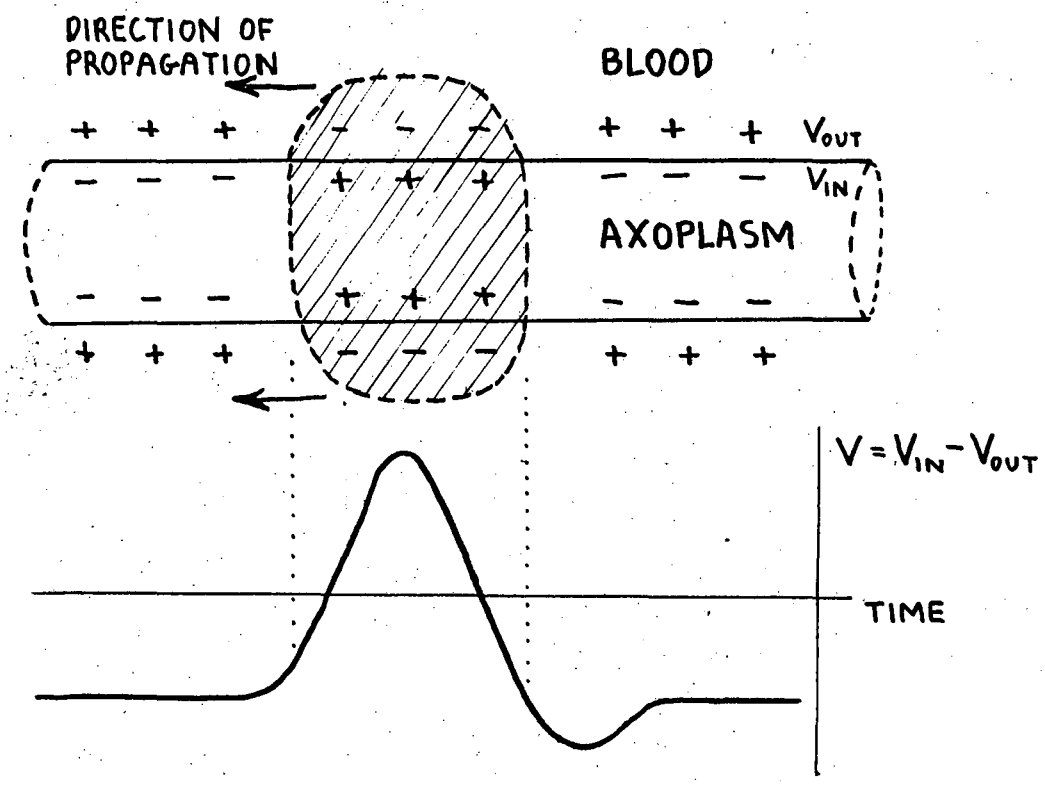

XBL 744-689

Fig. 3. The action potential. In the squid axon, the maximum height of the pulse is ~+40 mv, the resting potential ~ -90 mv, and the time duration ~ 2 ms.

is more permeable to K^+ ions, which migrate outward across the membrane down their concentration gradient to form an excess positive charge larger at the outer surface of the membrane, leaving a depletion layer of negative charge at the inner surface. The resulting negative-inside polarity of the membrane is not an equilibrium state; the concentration gradient flow of positive ions outward is maintained by a continuous chemical energy-dependent selective pumping of K^+ ions inward and Na^+ ions outward. The chemical basis of this pumping mechanism will not be discussed further. Na^+-K^+ pumping is not related directly to excitability, but only indirectly in its role of maintaining

the ionic concentration differences across the membrane.

In the "active" region, the relative ionic permeabilities are reversed. Na^+ diffuses inward through the membrane more easily than K^+ diffuses out.

The origin of membrane potential can be more complicated than explained above, particularly if one considers the membrane to be multi-layered, charged, laterally inhomogeneous, containing macromolecular dipole layers or significantly permeable to many charged species. Clearly, the existence and change of membrane potential does not clearly define an unambiguous membrane model. However, the action potential has characteristics which place more stringent demands on a membrane model. The propagating change of voltage is "all-or-none"; i.e., it always has the same time-dependent shape and magnitude. It is produced by briefly bringing the membrane potential from its resting level of about -90 mV inside to -50 mV inside: (or causing a sufficient outward current through the membrane): this stimulation can occur naturally by cable conduction from dendritic postsynaptic membranes to the action potential-generating region at the proximal end of the axon, or artificially by applying a current pulse via internal or external electrodes. Raising the axoplasm's electrical potential to a more positive value is called depolarization, and lowering it to a more negative value is called hyperpolarization. A "threshold" potential is the trans-membrane voltage above which an all-or-none action potential is produced and below which none is produced. The threshold voltage, however, is ill defined because of the phenom-

enon of accommodation. If a steadily rising stimulus current is applied, the apparent threshold level will be higher if the rate rise of the stimulus is slow; the nerve will adapt or accommodate to a slowly increasing stimulus by not firing as readily.

An action potential can propagate in either direction along the axon, so if the axon is excited in the middle of its length, two oppositely-traveling action potentials are produced. The propagation is self-reinforcing and shape-conserving: the depolarization spreads forward so that forward areas successively reach threshold and become active, but rear areas (those which have already been active) become "refractory" or inexcitable for about a millisecond, thereby preventing the action potential from spreading back to the rear.

D. Action potentials and metal ions

All of the available chemical information relevant to excitability is indirect. Much of it comes from studying the effect of varying internal and external metal ionic concentrations on the electrical properties of squid axon membrane. The literature in this field is vast; we will concentrate mostly on the effects of Na^+ and K^+ first, and then those of Ca^+. The movements of the anion Cl^- will not be discussed much because it appears not to play an important role in excitability and is relatively impermeable through nerve membrane compared to the cations.

<u>Na^+ and K^+</u>

The flux of ions through the membrane in both the resting and excited state has been measured by many workers using radioactive

isotopes (72, 135, 13). The resting influx of Na^+ is approximately equal to the resting efflux of K^+, and the flux rate for both ions increases approximately 100-fold during an impulse. Permeability coefficients can be calculated from the fluxes and the known electrochemical gradient; they confirm the greater permeability of K^+ than Na^+ in the resting state and the reverse during an impulse. Consistent with this is the observation that the resting potential depends strongly on the K^+ trans-membrane concentration difference, whereas the Na^+ concentration difference affects most strongly the "height" (i.e., the maximum voltage polarity reversal) of the action potential (77, 34).

Another class of electrophysiological experiments designed to measure specific ion fluxes are those employing the "voltage-clamp" (67). Using an electrode inserted into the axoplasm without damaging its excitable properties, one can artificially fix the membrane voltage by an external feedback circuit and monitor the time course of currents through the membrane. If one artificially depolarizes the membrane by this technique, one observes first a transient inward current (although the inside was made more positive!), followed by a steady ohmic outward current (see Fig. 4). The inward transient current, which is unique to excitable membranes, largely consists of Na ions (as measured by radioactive tracers), and the outward current consists of K^+ ions (59). (This is not surprising since the most numerous metal ions are Na^+ outside and K^+ inside.) It is clear from the voltage clamp measurements that when the membrane becomes depolarized (either by internal electrode or by an approaching action potential), an inward current develops which tends to further depolarize the membrane.

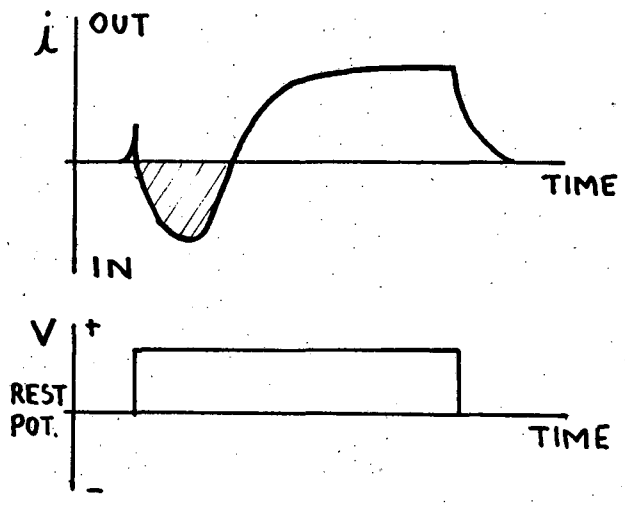

XBL 744-690

Fig. 4. The voltage clamp. Cross-hatched area is the "early inward current".

The advantage of voltage clamping is that it makes the membrane part of an external circuit where both voltage and current can be measured simultaneously, whereas the current is unknown in a straight electrical observation of an action potential. One can plot the maximum height of the inward transient current or the outward ohmic current as a function of the applied depolarization and thereby deduce that the membrane resistance falls by a factor of 100-200 in the excited region (134). Alternatively, one can measure membrane resistance under voltage clamping by imposing a small AC voltage on the applied DC "clamp" voltage (28). This AC impedance method gives the additional information that the membrane capacitance changes very little during excitation.

Using both voltage clamps and straight intracellular recording, attempts have been made to determine the specificity of the inward current for Na^+ and the outward for K^+, by substituting other metal ions for the physiologically normal ones. Tasaki (134) has shown that a nerve can remain excitable even when Ca^{+2} is the only cation outside (i.e., no Na^+ at all!) and Cs^+ is the only cation in the interior. (The axoplasm of squid axons can be extruded and replaced with some artificial solutions without destroying excitability, a technique called "internal perfusion"). Hille (60, 62), working with sciatic nerve, found that the Na^+ presumed to constitute the normal early inward current can be replaced by monovalent ions, Li^+, Tl^+, and K^+, in decreasing order of permeability, and the K^+ presumed to constitute the late outward current can be replaced by Tl^+, Rb^+, and NH_4^+ in decreasing order pf permeability. Cs^+ and Rb^+ also have been used as a successful replacements for internal K^+ (4, 134, 100) on squid giant axon, and NH_4^+ ion can carry both the early and late voltage-clamp currents at reducéd permeability on squid giant axon (7). Several monovalent organic ions can also carry the early inward current, most effectively hydroxylamine and hydrazine (60, 134).

Chemical agents have been used which block either the early or late voltage clamp current, or both (59). The fact that agents exist which can block one current component and not the other has led to the widespread assumption that the two current components each was controlled by their own specific macromolecular array in the membrane. Hence the terms "Na channel (or gate)" and "K channel" are used freely in the literature.

Tetrodotoxin (TTX) and saxitoxin (STX), extracted from Japanese puffer fish and planktonic dinoflagellates respectively, both very effectively block the early inward current--so effectively that they are the most poisonous small molecules known. The dose-response curve indicates that one TTX molecule binds to one "Na channel". Radioactive TTX has therefore been used as a marker of "Na channels" to count their density on the membrane surface of an axon. The results are variously given as $36/\mu^2$ (80), $22/\mu^2$ (52), and less than $13/\mu^2$ (101), all for lobster nerve. Biochemical purification using ^{3}H-labeled TTX as a marker have tentatively identified the TTX binding site as a protein imbedded in a phospholipid environment (6).

In addition, in vivo, TTX binding is insensitive to treatment by enzymes which destroy phospholipids (phospholipases), or carbohydrates (neuraminidase, hyaluronidase) but is degraded by pronase, which destroys proteins (53). Furthermore, TTX can be displaced from its binding site with about equal ease by all of the alkali metal ions. This may indicate that TTX does not bind to the site that is presumably selective for Na^+(53).

Tetraethylammonium ion (TEA) has the effect, when injected into the axoplasm, of blocking only the late outward current, presumably by one TEA binding to one "K^+ channel" (59). Other drugs, such as the local anesthetic procaine, depress both current components to a varying extent depending on the species of animal. Condylactis toxin (105), DDT (59) and several other drugs prolong either the early or late current component.

Another method of investigating the interaction of metal ions with nerve membrane is by using enzymes which destroy specific macromolecules in the membrane. External application of proteases (which destroy protein structure) to axons has no effect on their electrophysiological properties. However, when a solution of trypsin, a protease which cleaves certain peptide bonds in protein, is injected into a squid axon, electrical excitability is lost and a large increase in Na^+ influx is observed (102). Internally perfused pronase, (which cleaves all accessible peptide bonds in protein) also abolishes excitability (115). Phospholipases immediately and irreversibly stop electrical activity on lobster axons when applied either externally or internally, and the membrane potential difference approaches zero (115). The enzyme data is not sufficient to draw any conclusions as yet, except that if excitability is due to some specialized proteins, they seem to be "closer" to the axoplasmic surface than the external surface of the membrane.

Ca^{+2}

The effects of Ca^{+2} interaction on the nerve membrane's electrical properties is not as obvious as those of Na^+ and K^+ but it is just as important and perhaps key to eventual understanding of excitability.

Calcium ion is always present in the blood of animals in at least millimolar concentrations, but the total Ca^{+2} concentration in squid axoplasm is at least one order of magnitude lower, as monitored by $^{45}Ca^{+2}$ as a radioactive tracer (79). In addition, most of this intracellular Ca^{+2} appears to be bound to some relatively immobile macromolecules. Intracellular electrophoresis experiments show

that intracellular Ca^{+2} has a mobility of only .02 times its mobility in a free solution (69), although mobility of intracellular K^+ is close to that of free K^+ (68). In internally perfused squid axons, divalent ions in the perfusate tend to block excitability at concentrations lower than the normal external Ca^{+2} concentration, and internal Ca^{+2} is not required for excitability (134).

The effects of varying external Ca^{+2} concentration on the electrical properties of the membrane were investigated by several groups even before voltage-clamping became popular (29, 12). The observations were:

1) Increasing external $[Ca^{+2}]$* raises the threshold voltage, increases membrane resistance, and increases the rate of accomodation.

2) Reducing $[Ca^{+2}]$ has the opposite of the above effects, and frequently leads to repetitive spontaneous activity. In low $[Ca^{+2}]$, a nerve can fire even if the stimulus is a rapid change from a hyperpolarized potential to the normal resting potential.

In general, it appears that high $[Ca^{+2}]$ "stabilizes" the resting state whereas low $[Ca^{+2}]$ predisposes it to firing. This has led to the suggestion that the removal of Ca^{+2} from membrane binding sites is the first step in excitation (51, 65).

Using a voltage clamp on squid axon, Frankenhauser and Hodgkin (45) obtained the following results:

1) Decreasing $[Ca^{+2}]$ led to an increased early inward current upon

---

*[ ] refers to the concentration of the bracketed species.

membrane depolarization, and a more rapid rise of the inward current. Upon reduction of [Ca^{+2}], the I-V curve obtained by plotting the maximum inward current vs. applied clamping voltage was uniformly shifted so that a smaller depolarization was required to yield a given size inward current.

2) Reducing [Ca^{+2}] causes large increases in the size of the late outward current and its rate of rise. The delay time before the beginning of the outward current decreases.

3) If [Ca^{+2}] is reduced to very low levels, the nerve becomes refractory--the same state the nerve is in immediately after the passage of an action potential. (Partial refractoriness which reduces the inward current, can always be abolished by first hyperpolarizing the nerve before depolarizing it in the voltage clamp. When low (Ca^{+2}]-induced refractoriness is abolished in this manner, then the effect of low [Ca^{+2}] is to cause increase in the inward current, previously explained in (1)).

In other words, at very low [Ca^{+2}] concentrations, the membrane resistance is much below normal (as shown by the high outward voltage clamp current). Whether the nerve spontaneously fires or not depends on whether the lowered threshold voltage (which makes firing more likely) or the increased tendency toward refraction (which makes firing less likely) is the predominant effect at the particular [Ca^{+2}] concentration used. If one could remove all the [Ca^{+2}], the nerve might first pass through a spontaneous firing stage, but then become refractory. In addition, the Na-K energy pump will fail to maintain the requisite ionic trans-membrane concentration gradients because of the low membrane resistance.

The influx of Ca^{+2} in giant axons per unit area of membrane, as measured by $^{45}Ca^{+2}$, is about 0.1 pmol/cm^2-sec in resting nerve, about an order of magnitude lower than the influx of Na^+ (72, 69). This rate increases 100-fold during the action potential, but is still lower than Na^+ or K^+ fluxes during excitation.

The calcium influx in resting nerve is increased by raising the external $[K^+]$, or raising the internal $[Na^+]$. Are these inter-ionic effects a result of some kind of chemical competition between ions, or a voltage-dependent continuous change in membrane state? Raising external $[K^+]$ depolarizes the membrane, so its effect on Ca^{+2} influx may be either electrical or chemical. But raising internal $[Na^+]$ does not have a strong effect on resting membrane potential and may suggest ionic competition between Na^+ and Ca^{+2} for macromolecular "transport sites". Ca^{+2} flux increases in a non-linear manner with external $[Ca^{+2}]$ and reaches a saturation plateau (69), suggesting that Ca^{+2} influx may not be due to simple diffusion, as Na^+ influx and K^+ efflux appear to be.

Although no direct evidence exists showing Ca^{+2} binding to nerve membrane, one can assume such binding occurs because of the pronounced physiological effects of Ca^{+2}. Whether such binding is coordinate, ionic, or merely as a loosely held surface layer of positive charge is not known.

Ca^{+2} can also bind to organelles in the axoplasm which have little to do with excitability. For example, the mitochondria, which manufacture the chemical energy-supplying molecule adenosine triphosphate (ATP) needed in many biochemical processes and particularly

in the Na-K concentration gradient membrane pump mentioned earlier, exist in the axoplasm of several invertebrates as well as in the garfish olefactory nerve. Reynafaye and Lehninger (125) have shown that mitochondria of rat liver have a large capacity for Ca^{+2}, with both passive and active uptake; one can assume that nerve mitochondria behave qualitatively similarly.

Ionic substitution for Ca^{+2}

The nerve membrane's excitability requirement for Ca^{+2}, like that for Na^{+} and K^{+}, does not appear to be very highly specific.

Previous work by Blaustein and Goldman [9] indicated that, on voltage-clamped lobster axon, several polyvalent cations (La^{+3}, Ni^{+2}, Co^{+2}, Cd^{+2}, Ba^{+2}) could be used instead of Ca^{+2} in the Ringer solution and still maintain nerve excitability. Similar results were obtained for Ca^{+2} replacement by La^{+3} by Takata, Pickard, Lettvin, and Moore [132]. Khodorov and Peganov (81) found La^{+3}, Ba^{+2}, and Ni^{+2} physiologically similar to Ca^{+2} on frog nerves. Comparison with the calcium concentration studies on squid axons by Frankenhauser and Hodgkin [35] indicates that these polyvalent cations have a somewhat similar physiological effect to that of high $[Ca^{+2}]$. This effect is manifested in a higher stimulus threshold voltage and a broadened action potential. Because of the fairly non-specific nature of successful Ca^{+2} replacements, and because of the chemical similarity between La^{+3} and the rare-earth ions following it in the periodic table, one would anticipate that any of the trivalent rare-earth ions would be a successful substitute for Ca^{+2}.

E. Models

The time course of action potential at one point is a sort of explosive phenomenon. First, upon a stimulation strong enough to push the membrane past some threshold point of unstable equilibrium, some positive feedback system continues to alter the membrane's electrical and/or ion transport properties in the same direction as the stimulation. A second phenomenon returns the membrane to the resting state. The two functions are related by an unknown mechanism.

The forward spread of the action potential may or may not be an independent process from the positive feedback system operative at a single point on the axon membrane. Excitation may spread forward because the ionic current in the rising phase of the action potential is inwardly directed, and part of the return path of this current is outward through the membrane region just ahead of the action potential, thereby exciting the forward membrane region by some voltage or current dependent mechanism. Or perhaps the forward spread is entirely membrane phenomenon, a wave or "ripple" in the state of membrane macromolecules based on possible cooperative interactions among them.* Resolution of the action potential into two states, with one physical phenomenon involved in the rising phase and another possibly related one in the falling phase, is only the simplest, but by no means the truest, model of membrane events. One instead could conceive of a whole series of quasi-stable membrane states with appropriate

---

*To paraphrase Dean Rusk: "... falling like a row of dominos."

transitions between them, or in the extreme, a continuous range of states. So it appears that the test of a mathematical or physical model for nerve excitation is not only whether it works and satisfies electrophysiological characteristics, but whether it makes chemical sense; i.e., it must be consistent with known experimental information on the physical and organic chemistry of an action potential and the macromolecules involved.

Numerous models for the nerve membrane have been proposed. It is generally true that if one simple proposed model of excitability correctly predicts axon behavior, then infinitely many more complicated models also will do so. (This is apart from the previously discussed ambiguity of models derived from electrophysiological data alone.) And, unfortunately, in biology the simplest and most powerful model by no means is necessarily the correct one. However, nerve models do help suggest new chemical and spectroscopic experiments whose potential results may narrow the field in model competition, and they help one mentally order the available experimental data. Since this thesis is an experimental study of Ca^{+2}-nerve interaction, we will discuss first the two most popular models, followed by brief discussions of several other models assigning a specific role to Ca^{+2}.

1) Hodgkin-Huxley Model (66, 63, 64)

This model is by far the most quoted of all, and experimental results are usually phrased in terms of the model's mathematical parameters. Strictly speaking, the Hodgkin-Huxley (HH) model is an equation describing the current behavior of an axon in a voltage clamp.

The functional forms of the terms of the equation were arrived at empirically, and sufficient adjustable parameters are available to make the equations fit experimental results over a wide range of voltages and ionic conditions. In this sense, the model is "true" but adds little to one's understanding of excitation at the molecular level. However, the model implicity contains a particular physical outlook, the points of which are summarized below.

a) The permeabilities of the membrane to Na^+ and K^+ ions are specific and independent of each other.

b) These permeabilities are explicit, smooth functions of voltage and time, strongly suggesting that no abrupt phase transitions exist.

c) An all-or-none action potential can be understood by a straightforward interpretation of voltage clamp data.

In the resting nerve, K^+ permeability is much higher than Na^+ permeability; hence the resting potential is near the K^+ electrochemical equilibrium, which is negative inside. Upon stimulation of the nerve by depolarization, the Na^+ permeability becomes greater than the K^+ permeability, which leads to an influx of Na^+, thereby making the inside more positive. The Na^+ permeability is assumed to increase monotonically with the inside electrical potential, so the newly raised inside potential leads to greater Na^+ permeability and faster Na^+ influx. This is the HH version of the "positive feedback" system required of excitability models. Membrane potential then approaches the Na^+ equilibrium potential (positive inside), but never quite reaches it because a second process begins to take over: Na^+ permeability

"inactivation". This is a time-dependent process which smoothly decreases the Na^+ permeability to its original level before stimulation. Simultaneous with Na^+ inactivation, K^+ permeability smoothly rises to a level higher than the decreasing Na^+ permeability, leading to an efflux of K^+ ion, accumulation of positive charges at the exterior surface of the membrane, and a consequent return to the resting (near-K^+ equilibrium) potential. The K^+ permeability, being a function of membrane voltage as well as time, then returns to its resting level. The "Na^+ inactivation" diminishes after about a millisecond, thereby accounting for the short refractory period after the passage of an impulse. Voltage clamp data, according to the HH model, clearly show the transient activation and inactivation of Na^+ (early current) and the delayed K^+ current (late current). In the course of action potential, the specific ionic conductances take on a time dependent course illustrated in Fig. 5. Calcium is not mentioned explicitly in the HH model; presumably it functions to control Na^+ permeability. Because the HH model

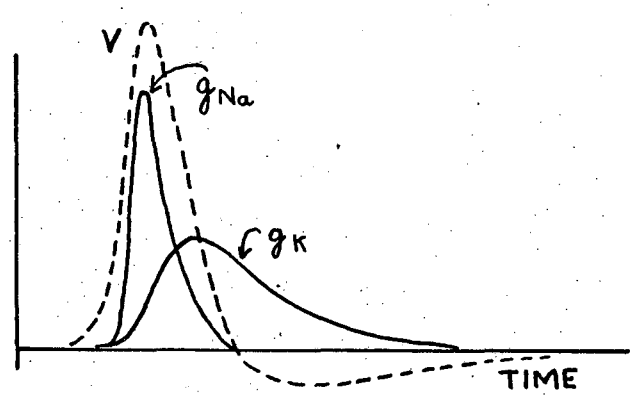

XBL 744-691

Fig. 5. Hodgkin-Huxley interpretation of voltage clamp data in terms of specific ion conductivities, applied to an action potential.

is more a mathematical than physico-chemical prediction, it is hard to find evidence against it. However, the assumption of specific, separate ionic conductance channels does appear to contradict the remarkable observation that squid axon action potentials can be produced using only Na_2PO_4 internally, and only $CaCl_2$ externally (148).

2) Tasaki model (134)

Tasaki's model differs from the HH model in the following important points:

a) At the height of the action potential, the membrane is in an "excited" quasi-stable macromolecular state which can be approached from the resting state only by an abrupt, cooperative "phase transition" of a semi-crystalline macromolecular array.

b) It proposes a specific chemical scheme for excitation, placing emphasis on the chemical interaction of Ca^{+2} and K^+ ions with the membrane, rather than on passive ionic diffusion through it.

The model proposes that the ion-conducting portion of the membrane acts like an anion-impermeable cation exchanger (130), able to transport positively charged ions via a binding and jumping mechanism on membrane-fixed negative charges, The evidence for fixed negative charges in the membrane comes from (a) the previously mentioned presence of negatively charged glycoproteins in the outer layers of the membrane; (b) the relative impermeability of anions through the axon membrane (although this varies with animal species); and (c) physiological (49, 116) and electrophoretic experiments (120) indicating the presence on the order of 1 negative charge/1600 Å surface. (However, there is

no evidence as yet that these negative charges are directly involved in excitability). The membrane potentials are due not primarily to excess ionic charge layers on the surfaces, but rather to the intra-membrane generated voltages generated by the different mobilities of cations which continuously interdiffuse in both directions (57).

The resting state of the membrane is characterized by high affinity for divalent (i.e., Ca^{+}) rather than univalent cation binding, hydrophobicity, low electrical conductivity, and a higher mobility for K^{+} ions than Na^{+} ions. The excited state is characterized by the reverse of the resting state, i.e., high affinity for K^{+} rather than Ca^{+2}, hydrophilicity, high conductivity with increased mobility of all ions present, a higher mobility for Na^{+} than K^{+}, and possibly an increase in fixed charge directly due to the removal of bound Ca^{+2}. The nerve is excited, not by triggering a voltage-sensitive increase in Na permeability as in the HH model, but instead by driving K^{+} ions into the membrane, thereby displacing bound Ca^{+2} ions which throws the membrane into the excited state. This can be accomplished by an outward current (which incidentally depolarizes the membrane), which carries K^{+} ions from the axoplasm, or by a high external K concentration (which also incidentally depolarizes the membrane). Physiological evidence on nerves is consistent with the postulated K^{+}-Ca^{+2} competition, but no direct evidence for it exists.

For example, raising the external K^{+} concentration gradually leads to an abrupt depolarization. If the Ca^{+2} content of the high $[K^{+}]$ external solution is then gradually increased, there follows an abrupt return to the normal (relatively hyperpolarized) membrane potential (134).

The cooperativity of the membrane is the Tasaki version of the required positive feedback for excitability models: the presence of K^+ in the membrane above threshold concentration will throw the membrane into a new macromolecular state where the affinity for more K^+ is greatly increased. This cooperativity presumably is due to intermolecular interactions whereby one molecule can "sense" whether its neighbors are in the Ca^{+2} or K^+ binding conformation, and thereby be compelled to assume the same conformation.

A general mathematical theory of how cooperative macromolecular interactions can lead to a membrane with two stable states has been given by Changeux et al. (18); the theory became the basis of a general excitability model in which the two states are characterized by a discontinuous change in the affinity and permeability of some ionic or molecular species (10).

The steady-state membrane potential of an excited state membrane is positive inside; the resting state is negative inside. Therefore, in a region of the membrane where excited and resting regions are adjacent, as near the advancing front of an action potential, current will flow inward in the excited region and outward in the resting region (see Fig. 6). In the excited region, well in back of the front, no current will flow, but external Ca^{+2} will gradually diffuse back into the membrane. If the external Ca^{+2} concentration is high enough (as it is in the blood), then sufficient Ca^{+2} will eventually diffuse back into the membrane to cooperatively throw it back to the resting state.

The observed action potential isn't square shaped because the excitation spreads in "patches": some patches may have a lower threshold

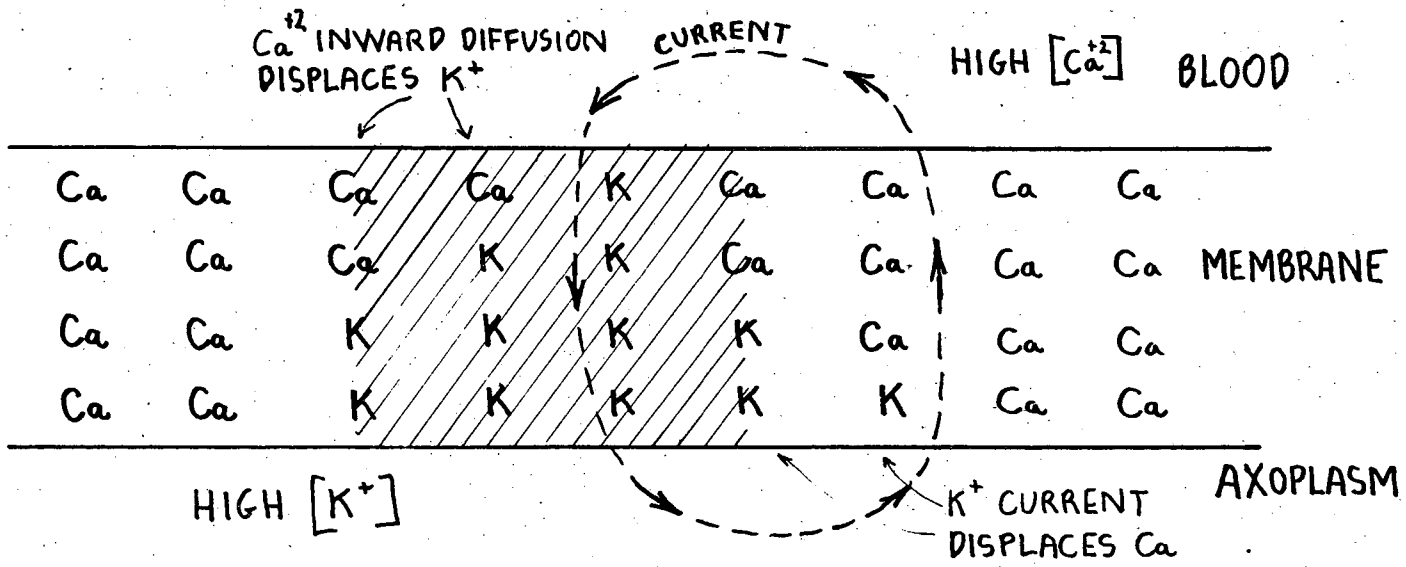

XBL 744-696

Fig. 6. Tasaki model. Shaded area is in the "active" or excited state.

for a K^+-induced "flip" than others. TTX's effect may be to slow the kinetics of this flip, thereby reducing the inward current at the front of an action potential or in a voltage clamped axon (149).

Although Tasaki's model can explain most of the observed effects of Ca^{+2} discussed earlier, particularly its role in stabilizing the resting state, it apparently does not explain why a high external Ca^{+2} concentration broadens the time course action potential. The model would seem to predict the opposite; i.e., a quicker return to the resting state. Additionally, there is no explanation for the seemingly "specific" action of internal tetraethylammonium ion in blocking the late outward current, which is one of the key experimental facts used to support the HH assumption of separate, specific ionic channels.

If the axon can exist in two stable states A and B, and an action potential is a transient switch $A \rightarrow B \rightarrow A$, then it would appear that an inverted action potential $B \rightarrow A \rightarrow B$ could propagate, with appropriate internal and external salt concentrations in a perfused axon. Such a phenomenon does exist (133), and is called the "hyperpolarizing" response. It is a transient hyperpolarization in an axon whose resting potential is depolarized by high external $[K^+]$, in response to a pulse of inward current.

The origin of the membrane potential, whether resting or active, is no doubt not as mathematically simple as is generally assumed in equations (134, 62) relating membrane potential to ion permeabilities and mobilities. The membrane is probably not homogeneous, neither in the lateral nor transverse directions, so assumptions of a constant transverse electric field across the membrane (often invoked by HH

supporters) or similarity to polymeric ion-exchange resins (as proposed by Tasaki supporters) are not accurate.

3) Other models

What follows is a brief review of some other excitability models prescribing a specific function for Ca^{+2} ions.

a) Tobias phospholipid model (142)

This model is similar to the Tasaki model in describing the first step of excitation as a replacement of membrane bound Ca^{+2} by K^{+} from the axoplasm. Tobias postulates that the critical ion exchange occurs at the phosphate and/or carboxylic groups at the polar ends of the phosphatidylserine molecules in the membrane. The phospholipids then undergo an orientational change, inducing a conformational change in the lipoprotein membrane structure which is expressed in the electrophysiological properties of the excited state. The evidence for the theory, which puts phospholipids at the critical triggering step, is entirely indirect. Ca^{+2} binds to negatively charged (at neutral pH) phospholipid monolayers (37) and K^{+} can replace Ca^{+2} bound to phospholipids (97). In addition, some of the properties of the excited state--increased membrane conductance and water permeability--are mimicked in phospholipid artificial membranes by the introduction of K^{+} and the removal of Ca^{+2}.

Another model which also places heavy emphasis on the role of oriented phospholipids is that of Wei (150). However, Wei's model does not specifically mention ion-binding: excitation is induced by a voltage-induced "flip-flop" of the oriented phospholipid head group's electrical

dipoles, i.e., a reversal of dipole orientation which propagates along the axon by a direct, cooperative electrostatic interaction among dipoles.

b) Nachmansohn acetylcholine receptor model (103)

The genesis for Nachmansohn's model is the apparent ability of acetylcholine (AcCh) to electrically excite post-synaptic membranes; indeed, acetylcholine is commonly thought to be the transmitter substance in synapses (77). Exposure to acetylcholine can directly excite lobster walking leg nerve trunk (39), but not most other nerves, presumably because they are wrapped with sheaths containing acetylcholinesterase, which cleaves the ester bond of any incoming acetylcholine molecule.

In the model, AcCh is bound to some protein in the resting state membrane. Excitation leads to the intra-membrane release of AcCh. As in synaptic transmission, the AcCh is then captured by a protein receptor, which undergoes a conformation change. In order to explain the important physiological effects of Ca^{+2}, Nachmansohn assumes the receptor protein binds Ca^{+2} which is released upon the AcCh-induced conformational change. The release of Ca^{+2} triggers other conformational changes characterizing the excited state. Return to the resting state occurs by membrane-bound acetylcholinesterase hydrolysis of the transferred AcCh. Evidence for this rather complex series of events is that inhibitors of acetylcholinesterase block electrical activity of axons, as do organophosphates, which are known to reversibly bind to acetylcholine receptors in post-synaptic membrane.

c) Passive key model (88)

This model, proposed by Lettven, Pickard, McCulloch, and Pitts, is probably the simplest physico-chemical scheme for explaining excitability in terms of the separate channel concept associated with the Hodgkin-Huxley model. Ionic transport is assumed to take place by way of small pores or channels. The cation channels are of two types, the K^+ channel which is large enough to pass hydrated K^+ (1.7 A radius) but not hydrated Ca^{+2} (2.8 Å radius), and the slightly larger Na^+ channel which passes hydrated Na^+ (2.4 Å) and K^+ with ease and hydrated Ca^{+2} with difficulty. In the resting state, Ca^{+2} will block the Na^+ channels by binding to the walls of the channel interior, but upon a depolarization, the membrane ultrastructure changes slightly so that Na^+ can "knock" Ca^{+2} out of the channel, allowing Na^+ ions to flow through the channel until another Ca^{+2} again randomly becomes locked in the channel, thus cutting off Na^+ flow. The K^+ channel is assumed to be blocked by Ca^{++} at its outer end with a strength related to the local electric field. A large depolarization will loosen this blocking, allowing K^+ ions to flow outward, thereby repolarizing the membrane and allowing Ca^{+2} to again resume its blocking of K^+ channels.

No doubt this model is not literally true since membrane "pores", if they exist, would be highly irregular, bumpy gaps in macromolecular arrays. But the model does predict the previously mentioned effects of Ca^{+2} in shortening the refractory period and of La^{+3} (hydrated radius 3.1 Å) as a "super-calcium" replacement.

d) Weiss molecular "springs" model (152)

This model, sort of a "three-state theory", envisions membrane lipoproteins in a spring-like helical conformation which is contracted in the resting state, with Ca^{+2} bound to outer sites and K^+ bound to inner sites. An outward excitation current displaces the Ca^{+2}, causing the "springs" to expand, which raises the Na^+ permeability. Ca^{+2} diffuses back into the membrane with Na^+, causing the "springs" to recontract into a conformation favorable to binding and passage of K^+ ions. The K^+ current displaces Ca^{+2} from inner sites to outer sites, and the membrane thereby reverts to the resting state.

e) Calcium adsorption layer models

In their classic paper on the effect of Ca^{+2} on axon electrical properties, Frankenhaeuser and Hodgkin (45) suggest that Ca^{+2} ions may be adsorbed at the outer edge of the membrane, creating a local electric field inside the membrane which adds to the resting potential; i.e., adsorbed calcium ions might alter the distribution of other charge configurations in the membrane without changing the observed membrane potential. In this way, one can preserve the Hodgkin-Huxley idea of purely voltage-sensitive macromolecular configurations without referring to the specific binding chemistry of Ca^{+2}. Deadsorption of Ca^{+2} would be electrically equivalent to depolarization.

A more recent model involving an Ca^{+2} adsorption layer is that of Offner (107). In the model, permeability to Na^+ and K^+ is controlled by an electrical field barrier at the membrane interface with the axoplasm and external solution, as well as a layer of bound Ca^{+2} at the

external interface. The theory is based on the premise that univalent cations cannot pass a region of the external membrane surface in the immediate vicinity of an absorbed Ca^{+2} ion. Depolarization has two effects: it lowers the external interface's electrical barrier to permeation by Na^{+}, and it causes Ca^{+2} to be deadsorbed. These combined effects cause a large influx of Na^{+} ions, which then accumulate in the membrane interior, unable to pass the internal interface barrier as the membrane polarization becomes positive inside, thus leading to "Na current inactivation". Outward K^{+} current is essentially an ohmic current, delayed because of the initial electrostatic barriers at the inner membrane interface and the diminishing Ca^{+2} adsorption at the external interface.

f) Goldman multi-state model (50)

Goldman's theory proposes a precise mechanism by which the conformation of a macromolecule critically involved in excitation can be modulated by univalent and divalent ion binding, and by membrane electric field. If the hypothetical macromolecule has a dipole moment near the outer membrane surface, the resting membrane electric field will orient the dipole with the positive charge embedded in the membrane and the negative charge exposed to electrostatic interaction with ions; when the membrane is depolarized, the dipole will rotate more freely. The conformation of the macromolecule depends upon the electrostatic attraction between the singly-charged positive and negative ends of the dipole, assumed to be connected by a flexible molecular chain. These charges attract each other when no counter-ions

are present; they do not interact when the negative charge is electrostatically bound to a univalent cation, and they repel when the negative charge is bound to a divalent cation. If one assigns a specific affinity for Na^+, K^+, or Ca^{+2} to each of these conformations, as well as appropriate electric field-dependent rate constants for transitions between them, one can work out a mathematical model which successfully predicts much physiological data. Specifically, Goldman assumes the resting state is that in which one end of the dipole is buried in the membrane and Ca^{+2} is bound to the other end. Depolarization allows the dipole to emerge from the membrane, release Ca^{+2} and bind Na^+ and then K^+ in successive conformational states.

The models discussed, as well as many not mentioned, differ on several key points which cannot be resolved on electrophysiological evidence alone. These differences include:

1) Is the electrical behavior a voltage dependent or ionic-environment-dependent phenomenon?
2) Are the ionic distributions and flows in and around the membrane in a steady state throughout the duration of the action potential so that the electrical changes "keep up" with changes in membrane macromolecular structure, or does the formation equilibrium layers lag behind membrane structural changes?
3) Is propagation via a spread of current, a propagating cooperative macromolecular interaction, or a propagating heat wave (as proposed in a model by Schmidt (91))?

Most of the models prescribing a definite function for Ca^{+2} indicate that it is bound in the resting axon and unbound during some part of the excitation process. One property of Ca^{++} (as opposed to Na^{+} and K^{+}) is that, as a divalent ion, it has the ability to cross-link negative charges on separate molecules, thereby restricting their motion, and also it can bind strongly to dipolar or negatively charged layers in the membrane, thereby neutralizing or reversing their charge and altering their electrical behavior.

A major effort of this thesis is to find experimental evidence for a change in the binding state of Ca^{+2} during excitation, primarily by spectroscopic means. The following brief review of previous spectroscopic experiments on nerve axons completes this chapter.

F. Spectroscopic experiments on nerve

Spectroscopic experiments on firing nerves have examined changes in the absorption, scattering, birefringence, intrinsic and extrinsic fluorescence, and spin resonance. An excellent recent review of these and other non-electrophysiological changes is given by L. B. Cohen (23). Some of these spectroscopic changes are clear evidence of alterations in membrane structure during excitation, although the critical structural changes which impart excitability to a membrane still have not been revealed by spectroscopic techniques.

1) Absorption

Kayushin et al. (78, 124) and Makarov and Krasovitskaya (93) reported changes in ultraviolet absorption of light in crab and cuttlefish nerves. At 245 nm, the absorption decreased approximately 40%; at

265 nm, the decrease was from 5-80%; at 280 nm, the absorption increased from 5-50%. (In all cases, the crab gave larger changes than the cuttlefish nerve.) These observations apparently are not corrected for scattering changes during firing. The changes at 245 and 280 nm may be connected with protein conformational changes involving cysteine and tryptophan residues, respectively, and at 265 nm with ATP modulated by transient pH changes in the medium. Attempts to measure absorption changes in frog and squid nerve thus far have been unsuccessful (23).

No changes in visible absorption synchronous with an action potential have been reported.

Infrared absorption changes in frog nerve have been measured by Sherebrin et al. (121, 122). Correlating these with the wavelengths of known molecular vibrational bands, the authors deduce that P-O-C stretch, C-H deformation, and carbonyl stretch are involved in excitation.

Somewhat related to infrared absorption measurements have been measurements of heat emission during the passage of an action potential in a rabbit nerve trunk (71), using a thermopile in direct contact with the nerve. The rising edge of the action potential emits 24 μcal/gram of heat energy, and the falling edge re-absorbs 22 μcal/gram.

2) Scattering

Light scattering changes at 90° on the order of 2×10^{-7} times the resting scattering for squid nerve have been observed by Cohen

et al. (27); a transient increase follows the course of the action potential, followed by a longer-lasting increase. Scattering studies in voltage clamped axon (27) indicate that these changes depend primarily on the integrated current through the axon membrane, with only a smaller dependence on membrane potential. Tasaki et al. (138) obtained an increase in 90° scattering of monochromatic visible light of $0.8\text{-}5.7\times10^{-5}$ times in intensity at rest, on the nerve trunks of lobster, crab, and squid; the change was independent of visible wavelength.

3) Birefringence

Nerve membrane is birefringent, i.e., its optical index of refraction depends upon the orientation of the plane of polarization of transmitted light. This birefringence can arise from two sources: (1) homogeneous ordered arrays of molecules whose oriented chemical bonds are anisotropic in their polarizabilities, and (2) heterogeneous but ordered arrays (such as stacks of rods or layers) of two or more materials having different indices of refraction. The physical theory of birefringence is reviewed by Kaplan (76). Changes in birefringence (or more correctly optical retardation, which is the product of birefringence and thickness) were first reported by Cohen et al. (25) to produce a fractional light intensity change of 5×10^{-6} in firing squid axon. More careful voltage-clamping birefringence results on this axon (26) led to the results that (1) the birefringence change apparently is potential-dependent, but in a non-linear manner; (2) it is a phenomenon of the axon membrane rather than the axoplasm or Schwann cells, and (3) the increase in membrane optical retardation during an action potential over its resting retardation is about 0.2%. The observed

changes could be connected either with re-orientation of some molecules during depolarization (the Kerr effect) or a change in membrane thickness due to electrostriction. Kaplan (76) investigated the effects of various destructive enzymes on birefringence changes in lobster giant axon in order to identify the possible macromolecular source of the effect. His results indicate that glycoproteins, hyaluronic acid, and possibly glycolipids and proteins may be involved. But since birefringence changes can be modified extensively by enzymatic treatment without affecting the action potential, the birefringence effect does not appear to be directly attributable to the macromolecules controlling the ionic permeability, binding, or mobility changes characteristic of excitation.

4) Intrinsic fluorescence

Masters (94) claims to have observed a .01% transient change of protein fluorescence from the amino acid tryptophan in a firing garfish olfactory nerve. However, he admits that the possibility of an experimental artifact was not entirely eliminated; furthermore, my own experiments on the same preparation did not reproduce Masters' results. No other reports of changes in the fluorescence of intrinsic nerve membrane chromophores synchronous with the action potential exist in the literature. However, Ungar and Romano (144) have applied trains of 10^5-10^6 stimulations and claimed reductions of fluorescence up to 30%--although this change, if true, may not be synchronous with membrane excitation events, but instead associated with the energy-dependent pumping mechanisms. The temperature dependence of

tryptophan (protein) fluorescence in nerve shows abrupt changes in two narrow temperature intervals; these fluorescence changes can be correlated with abrupt changes in impulse propagation properties in the same temperature intervals (22). Such results indirectly indicate changes in the supramolecular structure of protein or protein lipid arrays during excitation.

Study of intrinsic NADH fluorescence in the nerve (mostly located in the axoplasmic mitochondria) (41) show a decrease in NADH concentration after repetitive firing, probably by oxidation to non-fluorescent NAD (84). The phenomenon is probably associated with the increased rate of energy-dependent membrane pumping due to the partially exhausted concentration gradient and accumulated influx of Ca^{+2}, but not directly associated with excitability mechanisms.

5) Extrinsic fluorescence from membrane probes

The fluorescence spectra and quantum yield of many molecules are sensitive to the viscosity, pH, solvent polarity, and specific chemical neighbors in their microenvironment. An excellent review of the theory of extrinsic fluorescent probes is given by Radda and Vanderkooi (111). Some of these molecules bind to or accumulate in axon membrane. In recent years, literally hundreds of fluorescent dyes were used to examine changes of membrane-bound dye fluorescence synchronous with the action potential. As in observation of all other optical changes in axons, the changes are very small, and signal averaging over hundreds or thousands of nerve firings must be performed.

The first dye employed for these experiments was 1-anilino-8-naphathalene sulfonate (ANS) which fluoresces intensely only in a low polarity (i.e., hydrophobic) environment, such as the lipid interior of a membrane. With ANS added to the external solution, fractional fluorescence increases of 5×10^{-5}/impulse were observed synchronous with firing (110). Voltage clamped studies using ANS externally (24) show the changes to follow closely the rectangular shape of the applied potential with just a slightly slower rise time; i.e., the changes appear largely "voltage dependent". Similar experiments were performed by several groups using many other dyes (see ref. 23 for a review) and in all cases, the fluorescence change follows the time course of the potential in firing and voltage-clamped nerve. The only differences in effects among the dyes are: (1) ANS is the only dye which reversed the sign of its effect when applied internally rather than externally, possibly because most other dyes diffused through the membrane more rapidly than ANS; (2) most types of dyes show an increase of fluorescence during depolarization, but pyronin dyes show a decrease; (3) some dyes gave a fractional fluorescence change larger than 10^{-4} whereas other days showed no fluorescence change. In fact, one of the dyes, merocyanin (injected internally), gives a fluorescence change large enough to observe without signal averaging, and therefore may be useful in optical examination of in vivo firing patterns of neural nets (4). Most of the dyes' fluorescence varies linearly with voltage clamp potential, although at least two dyes show a quadratic dependence.

The origin of the fluorescence changes is not clear, but they do not necessarily reflect membrane structural changes during excitation. More "trivial" explanations exist, as follows:

(1) The dyes may have an electric field-sensitive fluorescence, due to Stark effect-type energy level shifts which change the probability of radiationless decay vs. fluorescent decay. The average electric field in a membrane is very strong indeed ($\sim 10^5$ V/cm). The slow rise time of the fluorescence changes observed in the axon may be too slow for this trivial explanation to account for the observed effect, but the rise time of a trans-membrane potential step is not a well controlled experimental parameter. The electric field dependence of these dyes in solid glasses or crystals should be examined.

(2) The potential changes across the axon membrane may be acting to change the total quantity of dye in the membrane, or at least the concentration profile of dye in the membrane. For example, ANS is negatively charged; depolarization therefore would reduce the potential barrier to its penetration into the membrane interior from the outside and thereby increase the quantity of ANS in a hydrophobic environment. Exactly how each dye will act by this scheme depends on its membrane solubility and permeability, as well as the electric field profile across the membrane.

(3) For charged dyes, and those with permanent or inducible dipoles electric field changes can move dyes already bound to the membrane surface into regions of greater hydrophobicity nearer the center

of the membrane. Prediction of this effect depends on knowledge of the electric field gradient across the membrane surface.

Such trivial explanations have received support from the observation of changes in the fluorescence intensity of ANS-stained lipid bilayers (which are certainly not excitable) subjected to voltage pulses (32). However, even lipid bilayers have orientable head groups and may undergo "structural changes" with application electrical fields.

Recently, Tasaki's group has begun intensive studies of the polarized fluorescence response of 2-p-toluidinyl-naphthalene sulfonate (TNS) in squid nerve axon (136). Using exciting light polarized parallel to the axon's axis, no change in the intensity of fluorescent light polarized perpendicular to the axon axis (observed at 90° to the exciting beam) was observed. However, the intensity of fluorescent light polarized parallel to the axon's axis did decrease synchronously with the action potential. This high degree of polarization of the fluorescence change at least indicates that the TNS molecules are not free to rotate during the excited-state lifetime (< 20 ns). Physical interpretation of the intensity change is not as clear, so voltage clamp studies were undertaken to determine whether or not these changes follow the same time course as an imposed membrane potential (i.e., a "voltage-dependent" change). Tasaki et al. (137) found that hyperpolarization led to voltage-dependent fluorescent changes, which he interpreted as increased incorporation of TNS into the membrane, but depolarizations led to fluorescent changes which appeared to be current-dependent. Since his two-state excitability model predicts current-

dependent membrane structural changes, Tasaki et al. interpreted the voltage-clamped depolarization results for TNS as evidence in favor of such structural changes. The fact that the changes, but not the steady background of fluorescence, were highly polarized seems to exclude the trivial explanations for intensity change cited above. However, evidence against the interpretation exists: (1) Larger voltage-clamped depolarizations produce voltage-dependent, not current-dependent, responses (possibly indicating a "trivial mechanism" for fluorescent change masks the current-dependent effect); and (2) Cohen (23) claims that his experiments on the same preparation fail to show any current-dependent effects.

6) Extrinsic spectral changes from Ca-sensitive probes

Most closely related to the project described in this thesis are optical spectroscopic techniques used to monitor Ca^{+2} flux or binding to membranes. Three such techniques have been used: (1) Absorption studies using the reversible Ca^{+2}-binding dye, murexide; (2) chemiluminescence studies using the highly specific Ca^{+2}-binding protein, aequorin; (3) fluorescence studies using the Ca^{+2}-binding antibiotic chlortetracycline.

Murexide (ammonium purpurate) is a water-soluble dye whose color changes from deep red to orange upon binding Ca^{+2}. Relative to the strength of Ca^{+2}-binding to membranes, murexide-Ca^{+2} binding is relatively weak and also kinetically fast. By use of a double-beam spectrophotometer, rapid changes of free-Ca^{+2} concentration down to about 10 μM can be observed. Murexide has been used as an indicator of Ca^{+2} concentration in solution to examine Ca^{+2}-binding to isolated

sarcoplasmic reticulum vesicles from muscle (108). Calcium release and reabsorption in the sarcoplasma of muscle during the course of muscle contraction has been observed by intracellular use of murexide (73). To my knowledge, it has never been used to measure trans-membrane Ca^{+2} flux during axon excitation, possibly because concentration change measurements in the μM range are several orders of magnitude too coarse for this application.

Aequorin is a chemiluminescent protein extracted from jellyfish (123) which emits a photon upon binding to Ca^{+2}, probably by changing its conformation to a lower energy state. Following the emission of light, the protein is apparently inactivated and the Ca^{+2} released. Light emission takes place within 10 milliseconds after rapid mixing of aequorin with Ca^{+2}(89), making the time resolution of this technique rather poor for fast chemical kinetic studies. However, the sensitivity is one to two orders of magnitude better than that of murexide; aequorin luminescence can easily detect changes of low Ca^{+2} concentrations down to about 0.1 μM (the luminescence does not vary linearly with $[Ca^{+2}]$, however). Baker et al. measured Ca^{+2} influx into squid axoplasm with injected aequorin (1). They found the resting intracellular concentration of free (i.e., unbound) Ca^{+2} to be about 0.3 μM. No attempt was made to observe signal-averaged luminescence changes synchronous with stimulation, apparently because of the slow time response of aequorin. However, a train of stimulations at 50-200 impulses/sec did produce an increase in luminescence which was dependent in a non-linear manner on external $[Ca^{+2}]$, frequency of stimulation, and total time of stimulation. Difficulties in calibrating aequorin luminescence with free Ca^{+2}

concentration, and with locating the precise source of the increased Ca^{+2}, precluded calculation of a figure for Ca^{+2} influx more reliable than that already known from ^{45}Ca studies. Voltage-clamping with repeated square depolarization pulses produced an increase in luminescence; this increase was plotted against the length of the depolarization pulse to give a rough estimate of the time course of Ca^{+2} entry following a depolarization step. The probable time course for Ca^{+2} influx corresponded with the time course of the early inward current observed in voltage-clamping, a result which sheds no light on the possible impulse triggering or stabilizing role of Ca^{+2}. In all cases, the increase of luminescence returned to its original level in 10-30 sec after depolarization or stimulation was terminated. The authors speculate that this slow decay is due to uptake of excess free axoplasmic Ca^{+2} by mitochondria in the axon.

The last Ca^{+2}-sensitive optical probe I will discuss is chlorotetracycline (CTC), an antibiotic fluorescent chelator of several divalent ions (17). CTC binds to Mg^{+2}, Ca^{+2}, Sr^{+2}, and Zn^{+2}, giving enhanced fluorescence, possibly by some conformational change, and to the paramagnetic ions Mn^{+2} and Co^{+2}, giving reduced fluorescence presumably because the metal ion spin increases singlet--triplet intersystem crossing in the CTC ring system. CTC has the following interesting properties which make it useful as a probe for specifically membrane-bound Ca^{+2}: (1) The affinity of CTC for divalent ions is highest in a medium with low polarity, and (2) the fluorescence of the Ca-CTC complex is enhanced when the medium has a low polarity. The fluorescence of the unchelated antibiotic is also polarity-dependent, but much less so

than the metal chelate. Membrane-solubilized CTC in chemical equilibrium with Ca^{+2} bound to intra-membrane sites therefore will offer the strongest contribution to the fluorescence of a CTC-Ca-membrane system. CTC fluorescence has been used to observe the uptake of Ca in mitochondria and isolated sarcoplasmic reticulum (16). Hallett et al. (56) have applied the CTC fluorescence technique to nerve, in order to probe Ca-binding changes in nerve membrane during stimulation. Both squid giant axon (stained internally) and lobster walking leg nerves (stained externally) show a 10^{-4} fractional increase of fluorescence. (This result, interpreted naively, would seem to run counter to the Tasaki two-state model, which predicts a decrease of Ca^{+2} binding in the excited state.) Increasing external Ca^{+2} concentration increases the size of the transient signal but does not significantly affect the resting background CTC fluorescence. A transient decrease in fluorescence is produced synchronously with the hyperpolarizing response (see page 32) in KCl-depolarized axons. Various control experiments indicate that the bulk of the transient and steady background CTC fluorescence was due to Ca-CTC in an apolar environment. In the voltage clamp, CTC-stained squid axons produced an apparently voltage-dependent fluorescent response to both hyperpolarizing (decreased fluorescence) and depolarizing (increased fluorescence) voltage pulses. In fact, tetrodotoxin, which eliminates the inward current, did not affect the voltage-clamp fluorescence response.

The interpretation of these results is ambiguous, both because (1) possible "trivial" voltage-dependent responses exist (mentioned earlier) due to the field-dependent movement of the charged Ca-CTC

complex, and (2) it is not clear where in the membrane (on the outer surface, in the middle, or on the inner surface) changes in Ca concentration are occurring which might be producing the optical signal.

In the original experiments described in this thesis, the first of the problems encountered in CTC experiments is avoided because the Ca^{+2} probes used (rare-earth ions) are also substitutes for Ca^{+2}; any transient optical signal therefore is not likely to be a trivial artifact of dye or Ca-chelate movement independent of the action of Ca^{+2} itself. The second problem, that of interpreting non-trivial results, remains, but the richer spectroscopic properties of rare-earth ions offer a "handle" to the solution of the problem.

7) Magnetic resonance probes

Hubbell and McConnell (70) examined the ESR spectrum of a nitroxide spin-label, 2, 2, 6, 6-tetramethylpiperidine-1-oxyl in rat vagus nerve and lobster walking leg nerve. The spectra showed rapid tumbling of the label, presumed to be due to fluidity in the hydrophobic regions of the membrane, but no attempt was made to examine spectral changes during nerve firing. However, Calvin et al. (14) used biradical spin labels which were expected to give a conformation-dependent as well as motion-dependent signal in lobster nerve. The membrane-bound biradical appeared to become more elongated than the same biradical in free solution, but a rather high tumbling rate was still observed in the resting state membrane. An attempt to observe spectral changes synchronous with nerve firing was made, but no such change could be observed.

CHAPTER III.

METAL IONS: CHEMISTRY AND SPECTROSCOPY

This chapter is not intended to be a general review of the huge field of metal ion binding chemistry or spectroscopy. Rather, it will be limited to: (1) a brief discussion of chemical differences among univalent and divalent cations, with the goal of showing possible ways by which nerve membrane can distinguish Na^+, K^+, and Ca^{+2} from one another; (2) a discussion of the chemical similarities of rare-earth ions to Ca^{+2}; (3) a detailed discussion of the atomic structure and spectroscopy of free rare-earth ions, especially Eu^{+3}; spectral changes upon chemical binding; and a presentation of the spectra of some bound-Eu^{+3} chemical systems prepared in this laboratory; and (4) a very brief discussion of transition metal complex fluorescence.

Spectroscopy has been applied very successfully, both in theory and experiment, to the coordination chemistry for non-metallic complexes via ligand field theory. However, such an approach is not necessary to explain any of the results of this thesis, and therefore no attempt will be made to discuss that field in detail.

A. Na^+, K^+, and Ca^{+2} Chemistry*

Metal ions bind to negatively charged anionic groups or the negative ends of permanent or induced dipoles. Each of these groups, which may or may not be part of the same molecule, is a "ligand".

---

*An excellent review of the biochemistry of Group IA and IIA cations has been given by R.J.P. Williams (153).

Ligands are arranged around the central metal ion in a near-symmetrical arrangment, with ligand electronic orbitals overlapping the outer p, d, or hybrid atomic orbitals of the metal, which in the case of Na^+, K^+, and Ca^{+2} are completely unoccupied by metal electrons. The number of ligands (or "coordination number") characteristic of the binding of a particular metal ion is a function of its size, charge, and nature of the ligand: the coordination number of Na^+ is typically 6, K^+ is 8, and Ca^{+2} is 8. When bound to the nerve membrane, ligand positions not used in binding to macromolecular groups are "hydrated", i.e., associated with the negative oxygen end of the water dipole.

The most important phenomenon in metal-nerve interaction is the apparent selectivity of several membranes for different ions, i.e., Na^+-K^+ concentration gradients are created, cationic permeabilities are selective and relatively variable, and Ca^{+2}, but not Na^+ or K^+ apparently has some control function. One of the simplest ways to understand the difference in ionic chemistry is to consider only the charges and radii of the metal ion and its possible anionic ligands. This model is called the "radius ratio effect" (153). The theory reasonably assumes that small cations bind to anionic ligands more strongly (i.e., with lower free energy) than do large cations of the same charge. In other words, Na^+ (crystal radius 0.95Å) bind to anions more strongly than does K^+ (1.33Å). The reason for this difference is simply that smaller cations can approach the anion more closely before Pauli repulsion becomes important, thereby maximizing the cation-anion electrostatic attraction. However, in the environment of the nerve,

we do not have "free" M^+ ions binding to anions; the so-called "free" cations are really in a complex with water; i.e., hydrated ions $M^+(H_2O)_n$. The free energy change upon ligand binding should be measured relative to the hydrated metal ion state rather than the gaseous metal ion state, because metal-membrane binding is really a competition between membrane anions and water. If this is done, one can show that metal complexes with anions of small weak acids (i.e., those that donate their excess electrons easily, such as the oxygens in CO_2^-, CO_3^{-2}, OPO_3^{-2}, PO_4^{-3}) show a higher stability for Na^+ rather than K^+, relative to water complexes, whereas complexes with anions of large strong acids (those that tend to "hold" their excess electrons, such as OSO_3^-) favor K^+ over Na^+. The nominally neutrally-charged oxygen in alcohols or ethers can be an electron donor, as can neutral nitrogen in amine and imidazole groups. For a molecule containing several anionic ligands bound to one metal ion, the definitions of "large anion" and "small anion" is somewhat imprecise, because they depend not only on the size of the negatively charged atom in a molecular group, but also on the shape of the whole molecule containing the anionic groups. In an extreme case, all of the ligands may be attached to one molecule. The "hole" in the molecule in which the metal ion becomes situated may be just the right size only for a particular metal. Thus, some macrocyclic antibiotics are highly selective: valinomycin prefers K^+ to Na^+, whereas actinomycin prefers Na^+ to K^+ (99).

Most ligand systems which easily bind Na^+(0.95Å) also easily bind Ca^{+2} (0.99Å) because of the near equivalence in size of the two ions and the higher charge of Ca^{+2}. In general, Ca^{+2} binding is

stronger and less hydrated than that of Na^+ and K^+. Ca^{+2} possibly can "crosslink" groups on separate macromolecules and thereby increase the stability and "stiffness" of a membrane structural state. Conversely, the loss of Ca^{+2} might "destabilize" the membrane, predisposing it toward formation of new macromolecular structures or "phase transitions". Ca^{+2} ligands can include not only negatively charged and neutral oxygen and nitrogen, but also sulfur.

In the membrane, metal ions can be expected to bind to the charged or dipolar head groups of the phospholipids. The phosphate group oxygen of all the phospholipids, the amino nitrogen and carboxylic oxygen of phosphatidyl serine, and the amino nitrogen of phosphatidyl ethanolamine, are possibly binding ligands for Ca^{+2} binding. Metal ions also can bind to the carboxyl oxygen, imidazole nitrogen, and sulfhydroxyl sulfur of the side-chain groups of protein residues. Because of the specific three-dimensional shape of the protein peptide chain, a metal ion can form a connective bridge between amino acids quite distantly separated along the peptide backbone. The specificity and affinity of protein binding sites for metal ions then becomes a function of protein tertiary structure, which determines the size and accessibility of the binding site and the combination of metal binding ligands offered by the site. The negatively charged oxygens on the sialic acid residues of glycoprotein may also bind metal ions.

B. Spectroscopically Interesting Chemical Substitutes for Ca^{+2} and K^{+}

The trivalent lanthanides have approximately the same radius and the same coordination number as Ca^{+2}. Since radius, rather than charge, seems to have the strongest effect on whether an ion can be an isomorphous replacement for another ion, we would expect that the trivalent rare-earths would bind to the same macromolecular sites as Ca^{+2}, although perhaps rare-earth binding would be stronger and less specific. However, the biochemical function of Ca^{+2} probably depends on strength of binding as well as the specific ligands, so competition for the same binding site between rare-earths and Ca^{+2} does not predict, a priori, functional replacement in any particular system. Europium, Eu^{+3}, and terbium, Tb^{+3}, ions have the ionic radii 0.97 Å and 1.00 Å respectively, compared with 0.99 Å for Ca^{+2}.

Lanthanum, which is the first element in the chemically homologous "lanthanide series" (rare-earths), has frequently been used in biological and chemical systems to either substitute for Ca^{+2}, or to block Ca^{+2} interactions, presumably by irreversible binding to the same or nearby sites. La^{+3} very effectively competes with Ca^{+2} for binding to phospholipid monomolecular films (117). In addition to the previously mentioned studies on action potentials (see page 23), La^{+3} has been shown to interact with nerve membrane by inhibiting $^{45}Ca^{+2}$ efflux from squid giant axon. The rate of rise of an action potential in muscle membrane is dependent on external [Ca^{+2}]; the effect is competitively blocked by La^{+3}, Zn^{+2}, Co^{+2}, Fe^{+2}, Ni^{+2}, Mg^{+2} and Sr^{+2}

in decreasing order of effectiveness (55). Krasnow (83) observed non-competitive inhibition of Ca^{+2} binding to sarcoplasmic reticulum by La^{+3} and Gd^{+3}. Calcium ion is required for transmitter release in synapses, and La^{+3} blocks the effect of Ca^{+2} in the stellate ganglion of squid without substituting for it (98); it is not clear whether La^{+3} and Ca^{+2} are competing for the same site or the blocking is more indirect. However, a somewhat opposite effect of La^{+3} was observed in frog neuromuscular junction, where La^{+3} increased (and Mn^{+3} decreased) the normal rate of apparent spontaneous transmitter release (75). Rare-earth ions have been found to functionally replace Ca^{+2} in the activation of certain enzymes, specifically trypsinogen and α-amylase (36, 128). Finally, La^{+3} powerfully inhibits Ca^{+2} uptake by mitochondria (96) and inhibits Ca-stimulated ATP translocation across inner mitochondrial membranes (129).

Divalent europium ion has ha radius of 1.12 Å and the same charge as Ca^{+2}, but unfortunately it oxidizes to the trivalent state in room-temperature water in about 30 min. For this reason, no extensive experiments were performed with Eu^{+2} on nerves.

Some use of first row divalent transition metal ions will be made in this thesis. Although these are generally smaller than Ca^{+2}, and also have a partially filled outer d shell, some transition metal ions have been used as substitutes, inhibitors, or probes of Ca^{+2} binding sites, as reviewed above.

Vanadyl (IV) ion, VO_2^{++}, has been used as an EPR probe of metal binding sites in proteins (21) but its use is not feasible for <u>in vivo</u> nerve studies since VO_2^{++} precipitates out as vanadyl hydroxide

above pH 3.7.

K^+ (1.33 Å) might be expected to be replaced by Tl^+ (1.40 Å), and indeed has been employed as a K^+ substitute in several enzyme systems (153). In general, thallium binds to ligands more strongly than K^+. However, there are some obvious chemical differences. For example, Tl Cl is only slightly soluble in water, and forms the species $Tl\ Cl_n^{-(n-1)}$ for $n \leq 4$ in solution (33), whereas KCl is highly soluble and completely ionized. The permeability of nerve membrane to Tl has been measured (61, 54); it is approximately 1.8 times that of K^+ in squid nerve.

C. Atomic Structure and Spectroscopy of Europium and Terbium

Some of the rare-earth ions, particularly europium, are used as Ca^{+2} substitutes in the work described in this thesis, primarily because of their chemical environment-sensitive fluorescence,* observable at room temperature in solution. In particular, water solutions of $SmCl_3$, $EuCl_3$, $TbCl_3$, and $DyCl_3$ exhibit a rich spectrum of narrow fluorescence and absorption bands, whereas the other rare-earths with partially filled 4f subshells only fluoresce in crystals or solid glasses. The spectra and energy levels of rare-earths in crystals is discussed thoroughly by Dieke (40); the chemistry and spectroscopy of rare-earth complexes is presented by Sinha (127), and a modern theoretical treatment of rare-earth spectroscopy is given by Wybourne (154).

---

*Strictly speaking, the observed luminescence is not fluorescence because the excited state is not a singlet.

The electronic configuration of the trivalent rare-earth ions is the xenon core ($1s^2\ 2s^2\ 2p^6\ 3s^2\ 3p^6\ 3d^{10}\ 4s^2 4p^6\ 4d^{10}\ 5s^2\ 5p^6$) with a partially filled $4f^n$ subshell. For Eu^{+3}, n = 6, and Tb^{+3}, n = 8. The +3 valence arises from two missing 6s electrons and a missing 5d or 4f electron. All of the optical spectroscopy we will discuss arises from $4f \rightarrow 4f$ transitions. We will concentrate on the structure of Eu^{+3} since its spectra, and that of Tb^{+3}, are the most sensitive to chemical environment of all the rare-earth ions.

The most outstanding features of rare-earth solution spectra are the weakness and narrowness of the bands. The bands are weak because any $\ell \rightarrow \ell$ atomic transitions are symmetrically forbidden, and they are narrow because the 4f subshell is shielded from external chemical or collisional influences by the 5s and 5p electron clouds farther out from the nucleus. These two phenomena are critically important in determining the chemical sensitivity of the spectra.

The "Laporte" selection rule forbidding $\ell \rightarrow \ell$ transitions can be derived simply as follows:

The probability of an electric dipole transition between two electronic states A and B is:

$$\langle A\,|\vec{R}\,|B\rangle^2 \qquad \text{where}$$

$\vec{R} = e\sum_k \vec{r}_k$, with k summation over all the electrons. We will make the initial approximation that the electrons are influenced only by <u>central</u> forces, <u>i.e.</u>, attraction by the nucleus and repulsion by spherically symmetric shielding electron clouds from lower filled electronic shells. This approximation specifically excludes inter-electronic spin-

orbit coupling and coulombic interactions, both of which are significant in rare-earth ions. We only consider here the N electrons in the unfilled 4f shell. In this case, we can write A and B as linear combinations of the determinental functions of single electron wave functions $u_{n\ell m m_s}(\vec{r})$.

$$u_{n\ell m m_s}(\vec{r}) = K_{\ell m} R(r)\, P_\ell^{|m|}(\cos\theta)\, e^{im\phi}\, \alpha_{m_s}$$

where $P_\ell^{|m|}(\cos\theta)$ are the associated Legendre polynomials; the normalization for the angular part hs been absorbed into $K_{\ell m}$; and the spin function is α_{m_s} with $m_s = \pm 1/2$. For a 4f electron, there are 14 different degenerate $u_{n\ell m m_s}(\vec{r})$ functions, which we abbreviate as $u_i(j)$ where $i = 1, \ldots, 14$ and the function is evaluated at the space and spin coordinates of the jth electron. The transition dipole matrix element $\langle A | \vec{R} | B \rangle$ will contain a linear combination of terms, all of the following form:

$$e \sum \left\langle \begin{vmatrix} u_1^*(1) \ldots u_1^*(N) \\ \vdots \\ u_N^*(1) \quad u_N^*(N) \end{vmatrix} \; | \vec{r}_k | \; \begin{vmatrix} u_1'(1) \ldots u_1'(N) \\ \vdots \\ u_N'(1) \quad u_N'(N) \end{vmatrix} \right\rangle$$

where the $u_1 \ldots u_N$ and $u_1' \ldots u_N'$ are chosen from the set of 14 4f $u_{n\ell m m_s}$ functions, and N is the number of 4f electrons (N=6 for Eu^{+3}).

The $u_i(j)$ single electron functions, being eigenfunctions of a centrally symmetric Hamiltonian that commutes with the space parity operator (which transforms $\vec{r}_k \to -\vec{r}_k$), all have a definite parity, given by

$(-1)^{\ell}$ ($\ell = 3$ for f electrons). Moreover, since the determinants are just homogenous sums of products of functions, all with the same parity for 4f configurations, the determinants have a definite parity. The product of the two determinants in the expression above will then always have positive parity; i.e., invariance under $\vec{r}_k \rightarrow -\vec{r}_k$. But the operator $\vec{r}_k$ obviously has negative parity, so the whole integrand $|u_i^*(j)| \cdot \vec{r}_k \cdot |u_i'(j)|$ has negative parity. Therefore, integration over all space, as called for the matrix element, will yield a result equal to zero. This proves that when both $|u_i^*(j)|$ and $|u_i'(j)|$ have the same parity, as they do for $4f \rightarrow 4f$ transitions, the transition is forbidden.

What kind of effects can break this forbiddenness? Any perturbation which "mixes" the 4f subshell with a subshell of another parity, say the unfilled 5d orbitals, will destroy the strict parity forbiddenness described above. The three most important perturbations to consider in rare-earth ions are: (1) spin-orbit coupling, (2) electronic Coulomb repulsions, and (3) ligand fields. A complete treatment of these is most conveniently performed using tensor operators and coefficients of fractional parentage to reduce multi-electron states of N electrons to products of single electron states and multi-electron states of N-1 electrons (74). A complete, rigorous derivation of the effects of the perturbations is too long for the purposes of this thesis, but the outlines are discussed below.

1) Spin-orbit coupling

The spin-orbit perturbation is

$$H_{so} = \sum_i \xi(r_i)\vec{s}_i \cdot \vec{\ell}_i$$

where the summation is over all the electrons in incompletely filled shells.

The magnitude ξ of this perturbation varies roughly as the fourth power of the atomic number; the lanthanides are just about the heaviest elements which still can be treated most easily in the Russell-Saunders (L-S) coupling scheme before switching to basis states in intermediate coupling or j-j coupling schemes for the heavy atoms.

A general theorem for the scalar product of two tensor operators, $\overline{\overline{T}}$ and $\overline{\overline{U}}$, each acting on different "parts" of the system (like orbital coordinates and spin coordinates) is

$$\langle \alpha j_1 j_2 j m | \overline{\overline{T}}^{(k)} \cdot \overline{\overline{U}}^{(k)} | \alpha' j_1' j_2' j' m' \rangle = \delta(j,j')\,\delta(m,m').$$

$$(-1)^{j_1' + j_2 + j} \begin{pmatrix} j_1 & j_1' & k \\ j_2' & j_2 & j \end{pmatrix}. \tag{1}$$

$$\sum_{\alpha''} \langle \alpha j_1 \| \overline{\overline{T}}^{(k)} \| \alpha'' j_1' \rangle \langle \alpha'' j_1' \| \overline{\overline{U}}^{(k)} \| \alpha' j_2' \rangle$$

where α denotes all quantum numbers not explicitly mentioned; subscripts 1 and 2 refer to the two systems of coordinates upon which $\overline{\overline{T}}$ and $\overline{\overline{U}}$ act, respectively; the Wigner 6-j and reduced matrix element notations are used; $j = j_1 + j_2$ by vector addition; and k is the rank of the tensors $\overline{\overline{T}}$ and $\overline{\overline{U}}$.

Using L-S coupled states in Eq. (1), we can obtain the following expression for a matrix element of H_{so}:

$$\langle \alpha SLJM_J | H_{so} | \alpha' S' L' J' M_J' \rangle = \sum_i \xi(r_i) \langle \alpha SLJM_J | \vec{s}_i \cdot \vec{\ell}_i | \alpha' S' L' M_J' \rangle \qquad (2)$$

$$= (-1)^{S'+L+J} \delta(J, J') \delta(M_J, M_J') \begin{Bmatrix} S & S' & 1 \\ L' & L & J \end{Bmatrix} \sum_{\alpha''} \langle \alpha S \| \vec{s}_j \| \alpha'' S' \rangle \langle \alpha'' L \| \vec{\ell}_j \| \alpha L' \rangle .$$

The δ-functions immediately give the mixing rules:

$$\Delta J = 0$$

$$\Delta M_J = 0 .$$

The Wigner 6-j symbol gives the rules:

$$\Delta S = 0, \pm 1$$

$$\Delta L = 0, \pm 1 .$$

We may mix shells with different principal quantum numbers. The reduced matrix element $\langle \alpha'' L \| \vec{\ell}_j \| \alpha L' \rangle$ gives us one important restriction, as follows: If the $|\alpha L'\rangle$ ket consisting of an ℓ^N configuration, it can be decomposed by coefficients of fractional parentage (c.f.p.) into linear combinations of the product of a single electron ℓ-state with an L-S coupled state of N-1 other equivalent ℓ electrons:

$$|\ell^N L'\rangle = \sum_{\bar{L}} |(\ell^{N-1}) \bar{L}, \ell; L'\rangle \langle (\ell)^{N-1} \bar{L}, \ell; L' | \ell^N L'\rangle$$

where the last factor on the right is a c.f.p., and the ket $|\bar{L}, \ell; L'\rangle$ on the right can be easily expanded by Clebsch-Gordon coefficients

representing the vector addition of $L' = \bar{L} + \ell$. If we now assume that the bra $\langle a'' L |$ of Eq. (2) is an $\ell^{N-1}\ell'$ configuration, then the reduced matrix element $\langle a''(\ell^{N-1}\ell')L \| \vec{\ell}_j \| a(\ell^N)L \rangle$ will become a linear combination of terms of the form

$$\langle \ell' \| \vec{\ell} \| \ell \rangle$$

which is zero <u>unless</u> $\ell' = \ell$.

<u>Therefore, the spin-orbit coupling interaction will not mix a state derived from the $4f^n$ configuration with a state from any other configuration</u>. Spin-orbit coupling therefore <u>cannot</u> lead to a breakdown of the parity forbiddenness of $4f \rightarrow 4f$ transitons.

2) <u>Coulomb interaction</u> (configuration interaction)

The form of this interaction is

$$H_i = \sum_{i<j} \frac{e^2}{r_{ij}} .$$

We can convert $1/r_{ij}$ into tensor operator form (146)

$$\frac{1}{r_{ij}} = \sum_k f_k(r)\, P_k(\cos\omega)$$

where ω is the angle between electrons i and j and $f_k(r)$ is a function of r which will not be important in the calculation below. The spherical harmonics addition theorem gives

$$P_k(\cos\omega) = \frac{4\pi}{2k+1} \sum_q Y^*_{kq}(\theta_i\phi_i)\, Y_{kq}(\theta_j, \phi_j).$$

If we absorb the normalization into the tensor operator $\bar{\bar{C}}_q^{(k)} \equiv (\frac{4\pi}{2k+1})^{1/2} \cdot Y_{kq}$ and note that $\bar{\bar{C}}_q^{(k)} = (-1)^q \bar{\bar{C}}_{-q}^{(k)}$, we get $P_k(\cos\omega) = \bar{\bar{C}}_i^{(k)} \cdot \bar{\bar{C}}_j^{(k)}$. The perturbation matrix element connecting one state of ℓ^N configuration with another of $\ell^{N-1}\ell'$ configuration is proportional to:

$$\sum_k \langle \alpha(\ell^{N-1}\ell')SLJM_J | \bar{\bar{C}}_i^{(k)} \cdot \bar{\bar{C}}_j^{(k)} | \alpha' \ell^N S' L' J' M_J' \rangle .$$

Using fractional parentage coefficient expansions once on the bra and twice on the ket will convert this expression to linear combination of matrix elements describing the interaction of an $\ell\ell'$ configuration with an ℓ^2 configuration. The general theorem of scalar products (Eq.(1)) can now be applied to each of the matrix elements of this linear combination. The result involves products of reduced elements of the type

$$\langle \ell \| C^{(k)} \| \ell \rangle \langle \ell \| C^{(k)} \| \ell' \rangle \qquad \text{where}$$

$$\langle \ell \| C^{(k)} \| \ell' \rangle = (-1)^{\ell} [(2\ell+1)(2\ell'+1)]^{1/2} \begin{Bmatrix} \ell & k & \ell' \\ 0 & 0 & 0 \end{Bmatrix}.$$

The Wigner 3-j symbol allows $\ell + k \geq \ell' \geq \ell - k$, with the restriction that $\ell + k + \ell'$ is even, but since we eventually sum over all k, there is essentially no restriction at all for mixing ℓ's. Therefore Coulomb interactions can mix $4f^N$ configuration states with other states from any other configuration composed of unfilled or partially filled shells, including configurations of even parity. The parity forbiddenness of a nominally $4f \rightarrow 4f$ transition thereby is broken; it gains strength from a slight admixture of 5d state into the 4f state.

3) Ligand field perturbations

Because the 4f subshell is imbedded in the rare-earth atom well beneath the 5d and 6s "valence" shells, 4f electrons participate in chemical bonding only very slightly. The effect of ligand attachment then can be approximated by adding a perturbation potential term to the Hamiltonian whose symmetry is that of the metal complex, and whose strength is left as an empirical parameter to be fit by experimental data. This technique is the "crystal-field" approximation of ligand field theory. The form of the crystal field potential may be written as:

$$V = \sum_{k,q,i} B_q^k \bar{\bar{C}}_{qi}^{(k)} \tag{3}$$

where i is a sum over all the electrons. The radial dependence of V is absorbed into B_q^k. Since the spherical harmonics form a complete set of functions on the surface of a unit sphere, it is clear the Eq. (3) is quite general. The particular linear combination of $\bar{\bar{C}}_q^k$'s required by a given ligand symmetry can be arrived at by operating on the spherical harmonics by elements of the symmetry group (see Ref. 2). However, for the purposes here, it is only necessary to note that the $\bar{\bar{C}}_q^k$ for even k have even parity, and C_q^k's for odd k have odd parity. Therefore, the crystal field potential V for a complex which has inversion symmetry may only use C_q^k's of even k, and V for a complex with no inversion symmetry <u>must</u> use at least some C_q^k's of <u>odd</u> k.

The perturbation matrix element for the crystal field potential between $\ell^{N-1}\ell'$ and ℓ^N configuration states is

$$\sum_{kqi} B_q^k \langle a(\ell^{N-1}\ \ell')\, SLJM_J | \bar{\bar{C}}_{qi}^k | a'(\ell^N) S' L' J' M_J' \rangle .$$

As before, we use fractional parentage coefficients to separate out one-electron data, but this time only once on the ket. We can apply the Wigner-Eckart theorem to each term of the resulting linear combination of matrix elements. Each term then will contain the reduced matrix element

$$\langle \ell' \| C^k \| \ell \rangle = (-1)^{\ell} [(2\ell+1)(2\ell'+1)]^{1/2} \begin{Bmatrix} \ell & k & \ell' \\ 0 & 0 & 0 \end{Bmatrix}$$

as before. The Wigner 3j symbol is zero if the arithmetic sum $\ell + k + \ell'$ is odd. For even k <u>only,</u> meaning we are describing a complex with inversion symmetry, ℓ and ℓ' differ by an even number. Physically, this means that the crystal field will only mix ℓ subshells of the same parity: <u>i.e.</u>, odd with odd, even with even. Such mixing will not break the parity forbiddenness of nominally 4f → 4f transitions. However, if k is odd, then the crystal field <u>can</u> mix an ℓ subshell with an ℓ' subshell of opposite symmetry and break the parity forbiddenness of the $\ell \rightarrow \ell'$ transition. Nominally 4f → 4f transitions become allowed, leading to the following critically important conclusion:

Complexes of trivalent rare-earths with no center of symmetry will probably show an intensified 4f → 4f fluorescence.

The "probably" hedge is because other factors must also be considered: changes in radiationless decay rate, amount of mixing between the particular 4f level and a 5d level, shifts in the relative position of excited levels giving rise to fluorescence, and strength of the crystal field. As a result, some fluorescent bands will be more enhanced than others.

Another effect can enhance fluorescence: the ligands shield excited 4f levels from de-excitation due to solvent collisional interactions.

Enhancement of rare-earth fluorescence upon binding can also occur because of absorption spectrum changes. The absorption spectrum of Eu^{+3} does not show any dramatic changes upon EDTA binding (see page 70) except for (1) a uniform ~1 nm shift of all peaks toward the red, probably due to isotropic spreading of the electron cloud, and (2) the appearance of a new absorption peak at 465 nm. The bands are all narrow, with half-widths of the order of 2 nm. The strongest absorption, at 393 nm ($^7F_0 \rightarrow {}^5L_7$), has a maximum extinction coefficient of only $\epsilon = 2.9$ liter (moles cm)$^{-1}$; Eu^{+3} fluorescence intensity is very weak, partly because of the extremely low absorption cross-section.

If the Eu^{+3} ion is the only absorbing chromophore in a system, then its fluorescence excitation spectrum will be qualitatively similar to its absorption spectrum. However, if energy transfer can occur from another absorbing species, then the Eu^{+3} excitation spectrum will take on features of the energy donor's absorption spectrum. This process can take place by intramolecular energy transfer (127) (see Fig.7), in which the absorbing chromophore, located near the binding site of Eu^{+3}, is excited by a photon and decays into its lowest triplet state. The energy is then transferred to the metal $^5D_1$, which may decay to

the ^5D_o lowest excited state. Fluorescence from ^5D_o or $^5D_1$ to any of the ^7F levels (except J = 0) may result. The critical transfer step is enhanced by overlap of the triplet state and $^5D_1$ state orbitals and by their closeness in energy. This type of transfer is different from "Förster" dipole-dipole transfer common from fluorescent singlet levels of donor chromphores to allowed dipole transitions of an acceptor.

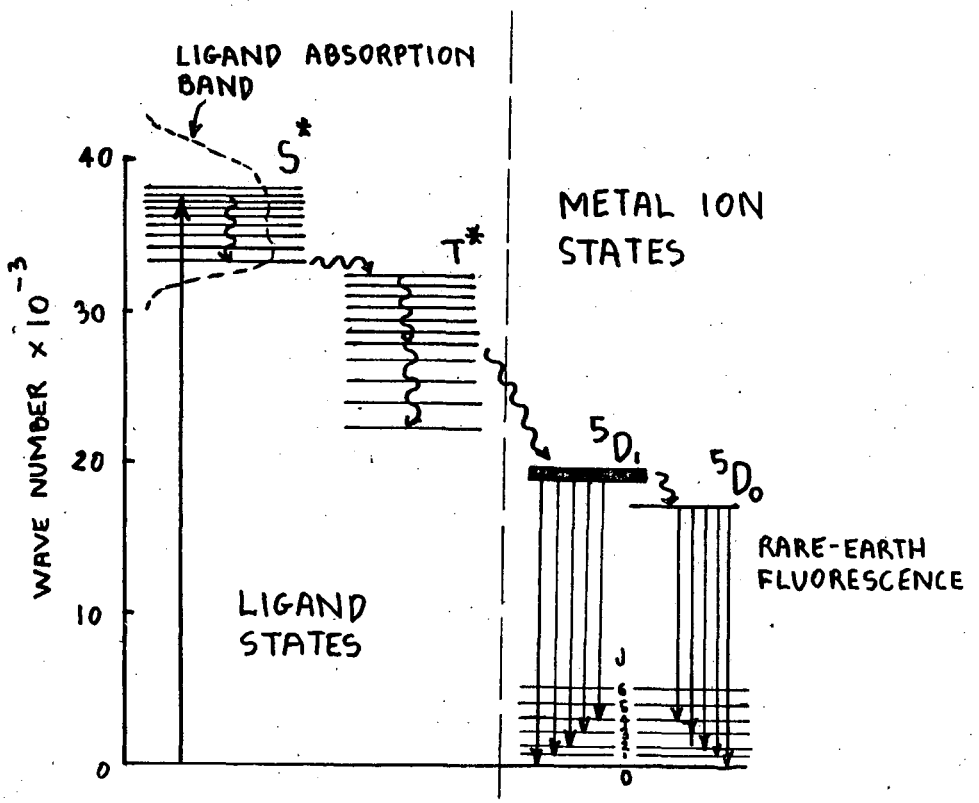

XBL 744-692

Fig. 7. Schematic drawing of intramolecular energy transfer to Eu.

Rare-earth ions can transfer energy to each other via a dipole-quadrupole interaction. Nakayawa and Shionoya (104) have calibrated the efficiency of this transfer as a function of the separation of the ions in inorganic solid glasses for various pairs of ions. The transfer, which has a $1/R^8$ dependence, has a critical distance of 12 Å or less, depending on the ions.

The energy transfer properties of rare-earth ion probes bound to the metal binding sites of the protein transferrin were studied by Luk (91). He found that Tb^{+3} fluorescence was greatly enhanced by energy transfer from nearby tryptophan residues in the protein, but Eu^{+3} received no transferred energy from tryptophan.

D. Experimental *in vitro* Eu^{+3} Fluorescence Spectra. Results and Discussion

(1) Eu-EDTA

We now examine the fluorescence emission spectrum of 25 mM aqueous solution of $EuCl_3$ *vs.* 25 mM $EuCl_3$-EDTA (Fig. 8). EDTA (ethylenediaminetetraacetic acid) is well known powerful chelating agent of many polyvalen cations. It offers up to six ligands (4 oxygen and 2 nitrogen) in binding to rare-earths: A possible structure is

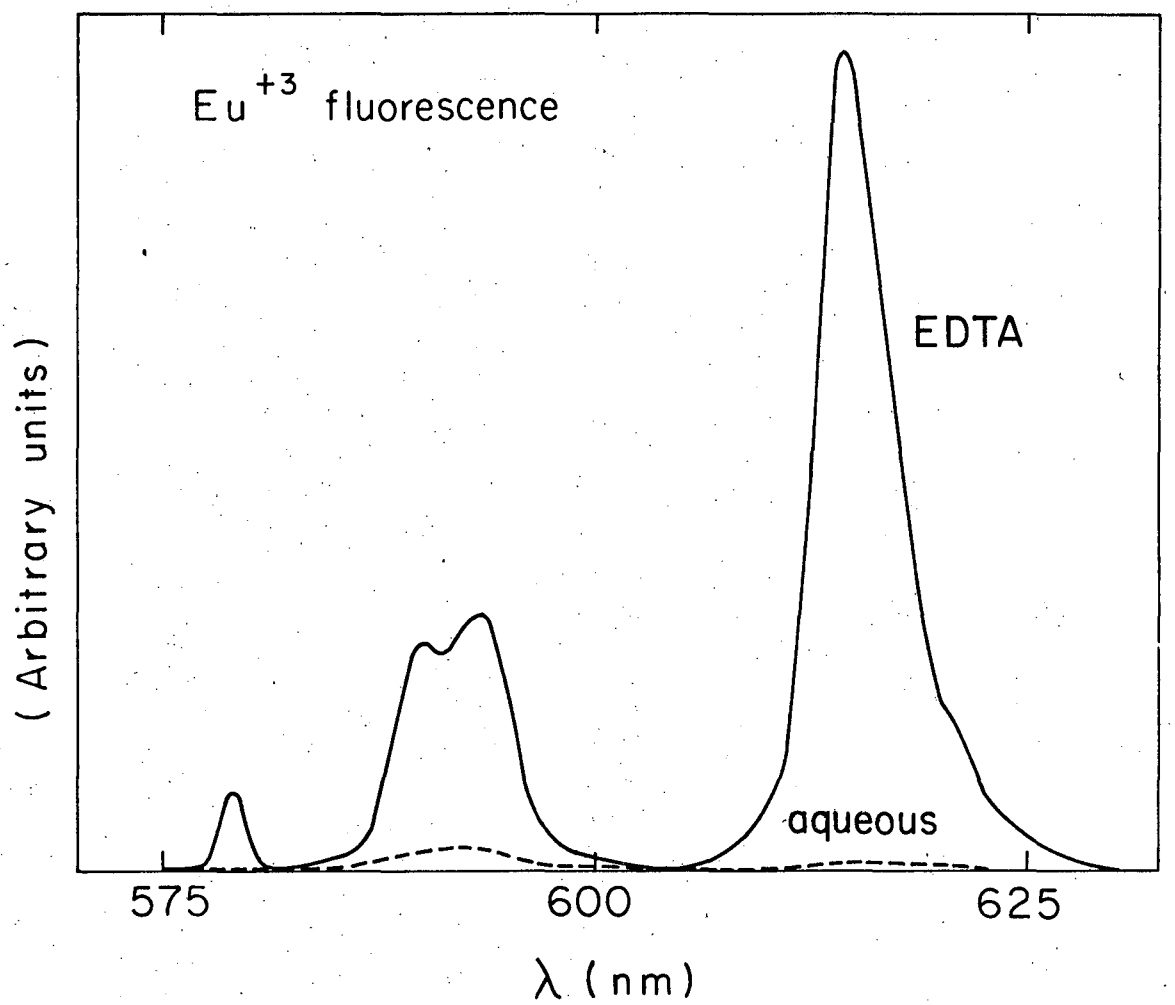

XBL738 - 3787

Fig. 8. Fluorescence emission spectra of $EuCl_3$ (25 mM) aqueous solution (dashed line) vs. Eu (25 mM)-EDTA (50 mM) solution (solid line). Resolution = 2.0 nm, λ = 614 nm, λ_a = 393 nm.

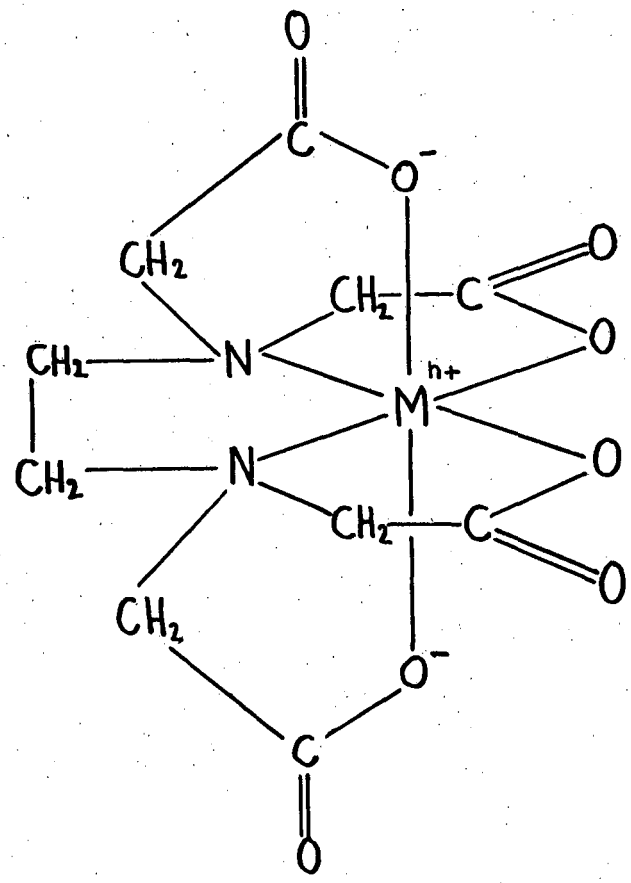

XBL 744-693

Fig. 9. Structure of metal ion - EDTA complex.

The structure clearly has no center of symmetry.

Figure 8 shows two main bands, at 590 nm and 614 nm. In the "free" Eu^{+3}, the 590 band is more intense than the 614. In Eu-EDTA, both bands are more intense, but now 614 nm is more intense than the 590 band. This reversal of intensity is characteristic of many Eu^{+3} complexes, and when it exists it can be taken as a definite indication that Eu^{+3} is bound to ligands more strongly than its association with HOH as a hydrated ion. The 614 nm band is believed to be a $5D_o \rightarrow 7F_2$ electric dipole transition (nominally $4f \rightarrow 4f$). There is some evidence

(40, 47) that the 590 nm band ($5D_o \rightarrow 7F_1$) is a magnetic dipole transition and therefore weak but allowed, and relatively insensitive to chemical environment.

The mixing of the 4f orbitals with 5d orbitals is probably only slight, even in complexes. Evidence for this is as follows: First, the energies of the states change little upon complexation. Secondly, the fluorescence yield of $EuCl_3 \cdot 6H_2O$ solvated crystals at 77° K is only 0.009; I am not aware of a value for $EuCl_3$ aqueous solution at room temperature, but it is probably even less than 0.009. Thirdly, the fluorescence lifetime of $EuCl_3$ aqueous solution at room temperature is extremely long; 0.12 ms (47). We would expect that upon complexation the lifetime would decrease as the transition becomes more probable, but surprisingly, the lifetimes of most Eu^{+3} complexes are longer than that of the aqueous ion (127). Clearly, the shielding effect of complexes and chelates (which both lengthens lifetime and increases intensity) is often as important as the loss of centro-symmetry.

(2) Eu-Phosphatidylserine Dispersions

I have measured the fluorescence spectrum of Eu^{+3} bound to phosphatidylserine vesicles (PS, a phospholipid present in nerve membrane) prepared by sonication of PS and addition of $EuCl_3$ unbuffered solution. The concentration of Eu^{+3} was 2 mM, with a twofold excess of PS. The fluorescence spectrum, measured in the MPF-2a, showed the reversal of peak intensity characteristic of bound Eu^{+3}, though to not as great a degree as Eu-EDTA. During the course of measurement, gradual precipitation of Eu-PS occurred, apparently because the binding of PS

to Eu^{+3} in "clumps" is more stable than closed PS vesicles. At lower Eu^{+3} concentrations, this precipitation was slower, but the fluorescent signal became too weak to observe. It is possible that impurities in the PS--used from a commercial preparation without purification--also were binding Eu^{+3}.

(3) Eu-Glycerylphosphorylserine

In order to avoid the insolubility problem, fluorescence of Eu^{+3} bound to glycerylphosphorylserine (GPS) was measured. GPS is the polar head group of PS, the part of PS to which Eu^{+3} is expected to bind. The concentrations were 2 mM Eu^{+3} and 3 mM GPS. At pH 5.2, the fluorescence indicated no binding; at pH 6.4, the 614 nm was slightly enhanced, and at pH 7.6, the 614 nm peak was larger than the 590 nm peak, indicating Eu-GPS binding. Higher pH values led to a heavy precipitate.

(4) Eu-NADH : Energy Transfer

I have observed the fluorescence of mixtures of $EuCl_3$ with reduced nicotinimide adenine dinucleotide (NADH), a molecule involved in energy metabolism in the mitochondria. NADH itself absorbs in a broad band centered at 350 nm and fluoresces in a broad band centered at 445 nm. A mixture of 1 mM Eu^{+3} and 3 mM NADH at pH 6.5 shows very weak Eu^{+3} fluorescence--about the same intensity as 1 mM $EuCl_3$ alone--indicating little Eu-NADH binding. However, at pH 7.8, the Eu^{+3} fluorescence emission spectrum (Fig. 10a) is enhanced by three orders of magnitude with a peak intensity reversal characteristic of binding.

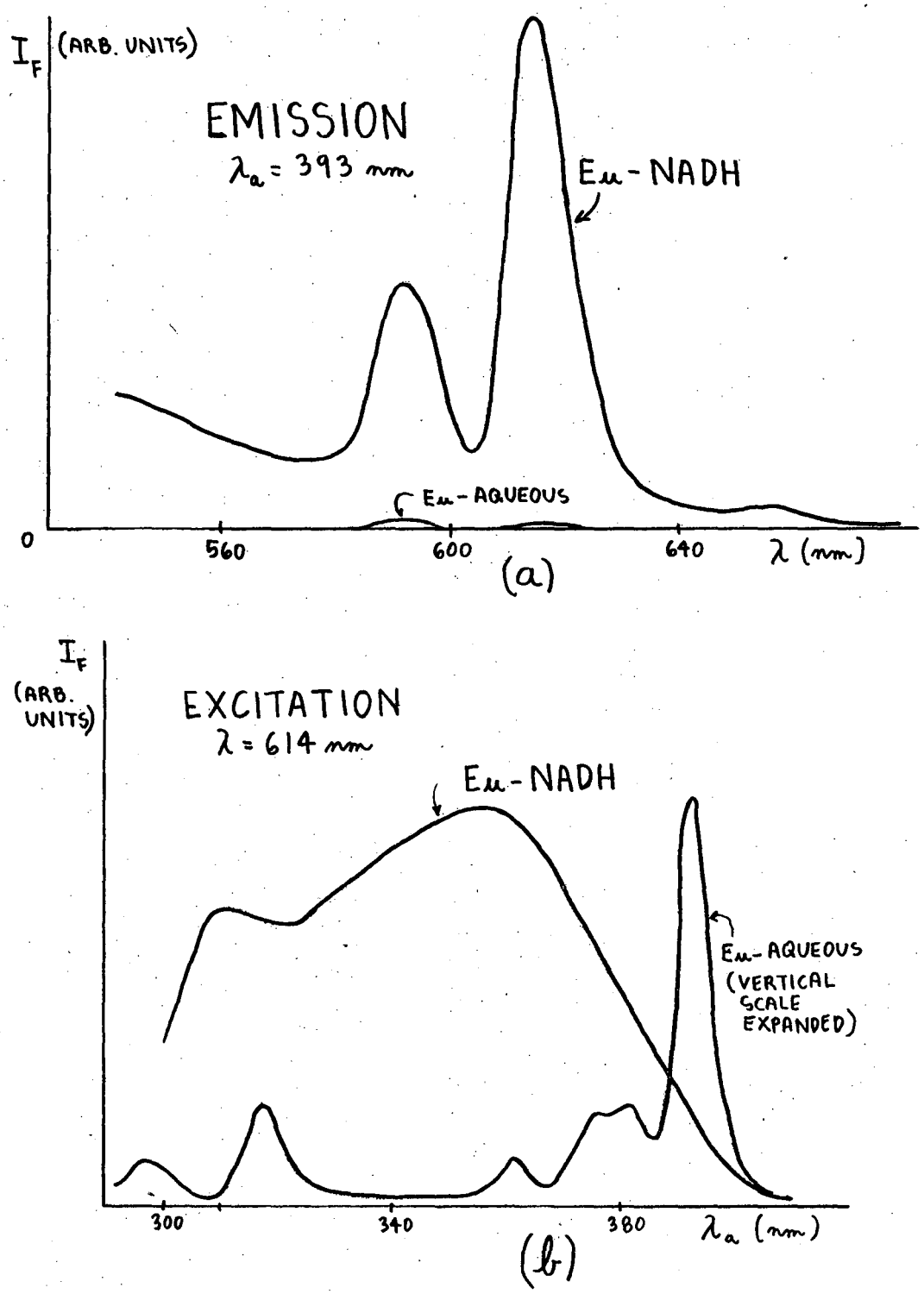

XBL 744-697

Fig. 10. Fluorescence spectra of Eu-NADH vs. Eu-aqueous.

The fluorescence excitation spectrum (Fig. 10b) for the 614 nm emission peak, shows a strong transfer of photon energy absorbed by NADH. This excitation spectrum was obtained point-by-point by measuring the height of the 614 nm Eu peak over the background fluorescence "tail" of the NADH emission. At the higher pH, a precipitate forms in the Eu-NADH mixture. Observation of NADH fluorescence of a precipitate suspension vs. the supernatant showed that the precipitate contained NADH, i.e., it was not simply $Eu(OH)_3$. Complexes of Tb-NADH, prepared and studied in the same manner, showed little fluorescent enhancement and no measurable excitation transfer.

E. Fluorescence of Transition Metal Complexes

Transition metals tend to quench the fluorescence of organic chromophores near ligands. This occurs by three mechanisms: (1) Förster energy transfer from the organic chromophore to the metal d orbitals, where the energy is lost to vibrational, rotational, and translational modes via radiationless decay; (2) ligand orbital coupling to metal d orbitals of the same symmetry. The metal orbitals contain a large degree of spin-orbit coupling, which then stimulates singlets to triplet intersystem crossing in the organic chromophore. This usually quenches fluorescence, but may enhance phosphorescence in the solid state; (3) the interposition of many new molecular vibronic states from the metal d orbitals beneath the lowest ligand state enhances the possibility of internal conversion.

This chapter obviously does not summarize metal ion chemistry and spectroscopy, but it lays the groundwork for the applications on nerve to be described in following chapters.

CHAPTER IV

GARFISH NERVE: ANATOMY AND PHYSIOLOGY

A. Garfish Olfactory Nerve

The nerve preparation used for the bulk of these studies is the olfactory nerve of the long-nosed garfish, Lepisosteus (Fig. 11). Easton (42) has performed extensive studies on the electrophyiology and thin-section electron microscopy of this nerve. The garfish olfactory nerve is a trunk of approximately 1.3×10^7 individual parallel axons. The population of axon diameters is strongly peaked at the diameter of 0.2 μm, with a population "spread" from about 0.12 to 0.45 μm. In other words, the great bulk of the fibers are of uniform size and apparent type. As a result, the impulse conduction velocities of the fibers are approximately equal (20 cm/sec).

The structure of the olfactory nerve trunk gives it a uniquely high ratio of axon membrane to Schwann cell membrane area (see Table I). Individual axons are unmyelinated (i.e., not wrapped by a Schwann cell "sheath"); instead, groups of several hundred axons are encircled once by a Schwann cell layer. There is relatively little connective tissue, which makes the trunk quite fragile.

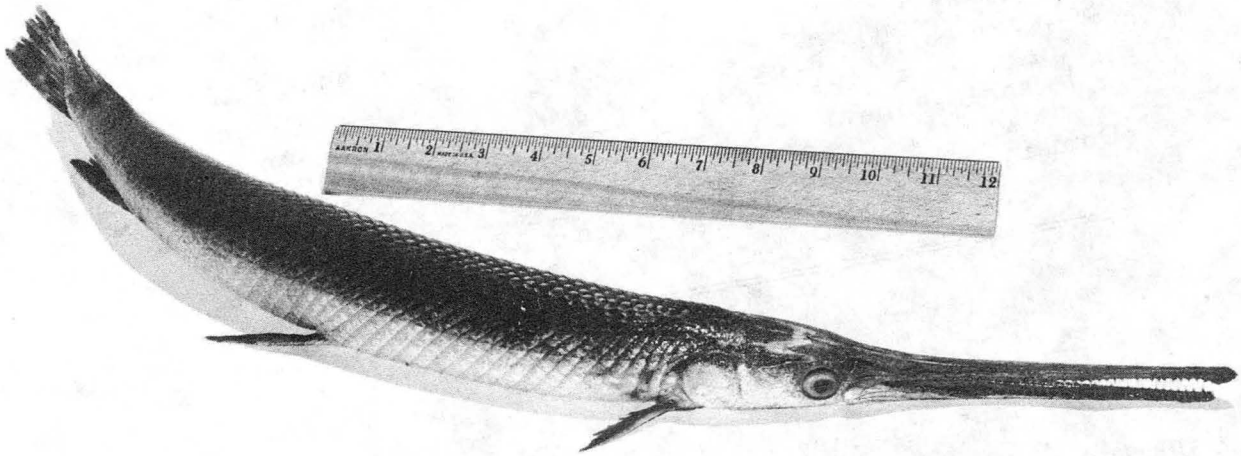

CBB 7310-6130

Fig. 11. Long-nosed garfish.

Table I. Relationships of axon and Schwann cell surfaces and volumes in olfactory nerve. (From Ref. 42)

Measurement	Whole nerve
Number of fibers	1.3×10^7
Cross-sectional area	0.0154 cm^2
Axon surface area	1000 cm^2/cm
Axon volume	0.0065 cm^3/cm
Schwann surface area	320 cm^2/cm
Schwann volume	0.0013 cm^3/cm
Domain volume excluding collagen	0.1 cm^3/cm

B. Care of Garfish

One must obtain written permission from the California State Department of Fish and Game to import garfish into California. The Department requires special precautions be taken—the storage tank must be covered and locked, and the water must be drained onto the ground rather than into the sewer system--in order that the hardy and aggressive garfish do not become established in California streams and threaten other species.

Long-nosed garfish were obtained from: Mr. Eldon Sauegling, Box 50A, Route 1, Guttenberg, Iowa 52052 (Phone (319) 252-2300). The 1.5' - 3' long fish were netted in the Mississippi River, packed in groups of three in a large plastic bag half-filled with water which was closed off with a pocket of oxygen gas above the water. The

bags were placed in a large, sturdy styrofoam boxes packed with ice. Boxes were driven immediately to Des Moines, Iowa Airport for direct air shipment to San Francisco International Airport, where I personally picked them up. The total time from packing in Iowa to unpacking in Berkeley was about 12 hours. This route of shipment was found to be absolutely essential; any method taking longer than 18 hrs. invariably killed at least half of the fish from suffocation.

Garfish were kept in an 8×8' covered wooden tank filled to a depth of 1 ft. with non-circulating, non-temperature-controlled fresh water, through which air was bubbled (although garfish can breathe air, too). Water was changed approx. once a month. The garfish ate fresh water live minnows; they did not eat any dead fish. In the winter they ate very little, if at all; during the rest of the year they could eat arbitrarily large number of minnows but could also survive without food for at least a month. What appeared to be a fungus infection caused some fatalities in the summer, but this apparently could be retarded by addition of 25 teaspoons of NaCl to the tank. In summary, once garfish are successfully imported, they are extremely easy to maintain.

C. Dissection of Olfactory Nerve

A garfish can be captured from the tank by "netting" it in a large plastic bag whose closed end was punched with small holes, with the open end clipped around the rim of a 20 cm diameter bunsen-burner steel ring with a handle. The handle of the ring was fastened to a long pole. By maneuvering the ring-plastic bag combination "net" beneath the water surface, one can usually catch a garfish head-first into the

bag. The net then should be pulled quickly out of the water and the excess water allowed to drain through the holes. The garfish (which will be flopping around quite a bit) should be kept in the bag as it is laid on a wood chopping block. As the fish is held in the bag by one hand, the head of the garfish is chopped off at about the position of the front gills by one blow from a sharp axe held in the other hand. The body of the garfish may continue to twitch, but it should be wrapped in another plastic bag and frozen for later incineration.

The two olfactory nerves, which can be seen as black stripes along the length of the bony upper jaw, are dissected from the head as follows: Using a pair of heavy cutting pliers, the lower jaw is bent back and cut off (Fig. 12). The terminal 1 to 2 cm of the upper jaw, containing the olfactory epithelium (i.e., the tip of the "nose") is clipped off. One can then remove the two rows of upper teeth, supported by the bony "maxillae", by clipping the two maxillae at the proximal end (i.e., the end near the brain) transversely to the long upper jaw bone (the "rostrum"). The maxillae can then be easily pulled away from the rostrum, as in Fig. 13.

Using the edge of a small triangular or square file, one files transverse notches every three cm. or so in the underside of the rostrum along its entire length. These notches are used as breaking points as the rostrum is carefully bent backward and cracked by hand, as in Fig. 14. After each break, the broken-off distal segment of the rostrum is pulled away longitudinally; the two olfactory nerves should become exposed, intact, and still connected proximally. Each rostrum section surrounding the nerve is slid off in this manner until

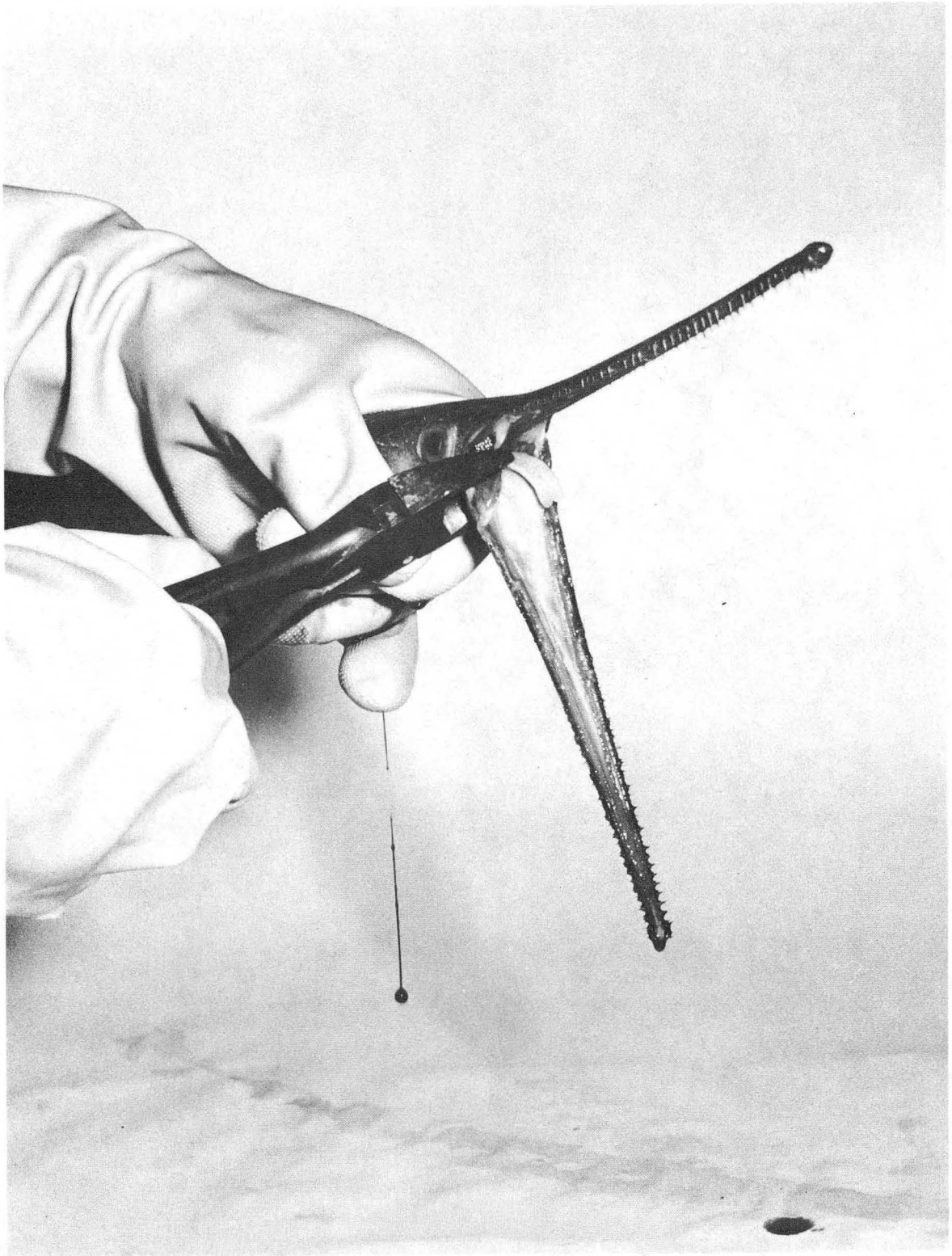

CBB 7310-6136

Figs. 12-15. Olfactory nerve dissection.

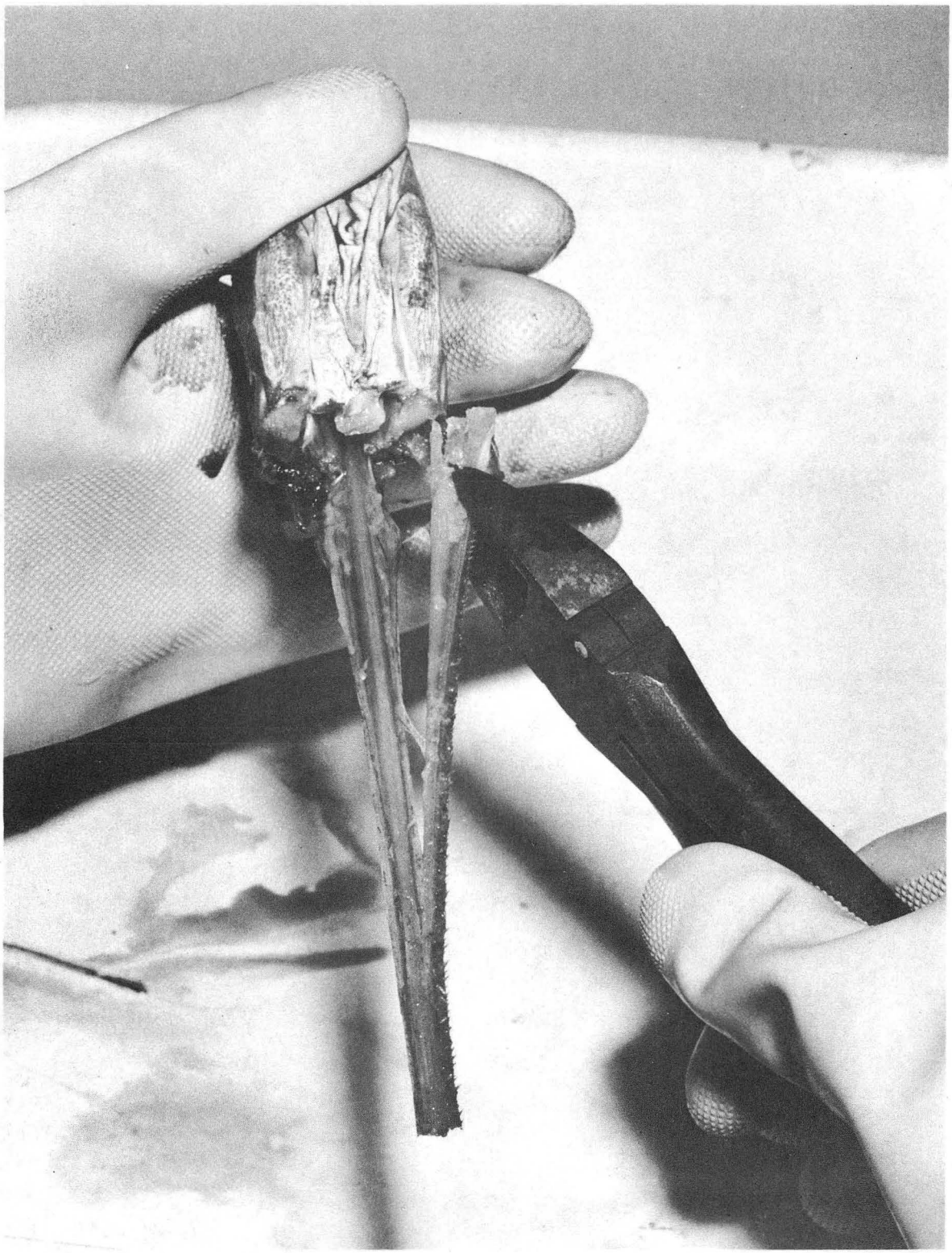

CBB 7310-6134

Fig. 13

CBB 7310-6138

Fig. 14

CBB 7310-6140

Fig. 15

the full 12-20 cm. lengths of nerve, which appear black, dangle from the head, at which time they can be cut off and dropped into a beaker of Ringer solution (Fig. 15).

A black sheath, which contains blood vessels, and the white, myelinated trigeminal nerve, both run parallel to the translucent and fragile unmyelinated olfactory nerve. By placing the nerve on a glass plate (in a "puddle" of Ringer solution to prevent drying), the sheath and trigeminal nerve can be easily teased away from the olfactory nerve by tweezers. The unmyelinated olfactory nerves (two are obtained) can be stored for up to two days in Ringer solution at 0°C without loss of excitability. If only a short length of nerve is needed for an experiment, the desired length can be cut off with a scalpel or scissors and the remainder stored.

D. Ringer Solutions

The composition of the Ringer solutions used in the experiments described in the succeeding chapters were variations of those prescribed by Easton, which were based on a chemical analysis of garfish blood. Table II shows the compositions of the various Ringers and the names by which they are identified.

Instead of bicarbonate buffer, I used HEPES buffer, and isotonicity was maintained with sucrose. The pH of the rare-earth Ringer solutions were lower than Ca-Ringer solution to prevent precipitation of rare-earth hydroxides. The concentration of rare-earth ions in rare-earth Ringer was about 1/7 that of Ca^{+2} in Ca-Ringer because of the "super-calcium" effect of rare-earths mentioned in Chapter II.

Table II. Composition of Various Garfish Ringer Solutions Used (Concentrations in mM/liter).

Ringer name Salt	Ca	Ca-free	Eu	Tb	High $[K^+]$Eu	Low Eu
NaCl	204	204	204	204	3.5	204
KCl	3.5	3.5	3.5	3.5	204	3.5
$CaCl_2$	3.5	---	---	---	---	---
$EuCl_3$	---	---	0.5	---	0.5	0.05
TbCl	---	---	---	0.5	---	---
Glucose	24	24	24	24	24	24
pH (Hepes Buffer)	6.9	6.9	6.6	6.6	6.6	6.9

E. External Stimulation and Recording of Garfish Nerve Trunks

Garfish nerve axons are too small to be pierced with microelectrodes, so external stimulation is necessary. The nerve is draped across two pairs of platinum electrodes. A square voltage pulse is applied between the electrically floating stimulating electrodes, with the negative polarity preferably toward the desired direction of propagation. Most of the potential difference in an action potential is transverse across the membrane, but since the resistance of the film of Ringer solution wetting the exernal surface of the axon is non-zero, a longitudinal potential difference will appear between the excited and resting areas of the membrane. This propagating external potential difference can then be recorded by a pair of recording electrodes, yielding a biphasic record.

The situation in a nerve trunk is more complex because the separation between most axons and the electrodes is greater, and

electrical contact through the Ringer solution film is poorer. As a result, firing of all axons is not precisely synchronous, and the axons more distant from the electrodes are fired only by a high stimulating pulse voltage. In the garfish nerve, the recorded action potential is approximately biphasic because of the fairly uniform propagation velocity among all the axons. The height of the observed response probably is proportional to the number of axons actually firing and the shape indicative of the time-course response of a single axon.

The next chapter will illustrate the firing response of garfish nerve in several different Ringer solutions.

Some experiments described herein were also performed on lobster walking leg nerves, although emphasis throughout is placed on the garfish results. The dissection of these nerves is discussed in M. Kaplan's thesis (76). Studies of their morphology (38, 48) indicates that each trunk consists of approximately 10^4 axons of non-uniform diameter, with considerable enfolding Schwann cell and connective tissue material.

"I came upon a butcher,
He was slaughtering a lamb.
I accused him there,
With his tortured lamb.
He said, 'Listen to me, child,
I am what I am'".

—Leonard Cohen

CHAPTER V

GARFISH NERVES IN RARE-EARTH RINGERS

A. Rare-Earths as Physiological Substitutes for Ca^{+2}

We tested the physiological behavior of garfish nerve bathing in Ringer solutions containing either one type of polyvalent ion or none at all, by checking the nerves' excitability frequently during a period of hours. The Ringer solutions used were Ca-, Ni-, Mn-, and Eu-Ringer (see Table I, Chap. IV). The relative persistance of excitability was monitored by displaying the voltage difference between the external recording electrodes on an oscilloscope whose horizontal sweep was triggered by the stimulation pulse to the nerve.

Figure 16 shows the results for Ca-, Ca-free, and Eu-Ringers. Each trace is the action potential of the nerves bathed in the indicated solutions and elicited at the time (in hr.) shown at the beginning of the trace. The duration of each trace is 500 ms and the vertical sensitivity is 1 mv/cm. For example, the three traces on line IV of Fig. 15 show the action potential of a nerve: (1) at t = 0 hr., immediately after placement in Ca-free Ringer; (2) at t = 16 hr., still in Ca-free Ringer; and (3) at t = 24., after bathing in Eu-Ringer for the last 6 hrs.

The results for Ca-, Eu-, and Ca-free Ringers shown in Fig. 15 indicate that: (1) Garfish nerves maintain excitability in Ca- and Eu-Ringers longer than in Ca-free Ringer; (2) bathing a nerve in Ca- or Eu-Ringer previously made inexcitable by Ca-free Ringer can restore the excitability of at least some of the axon fibers in the trunk.

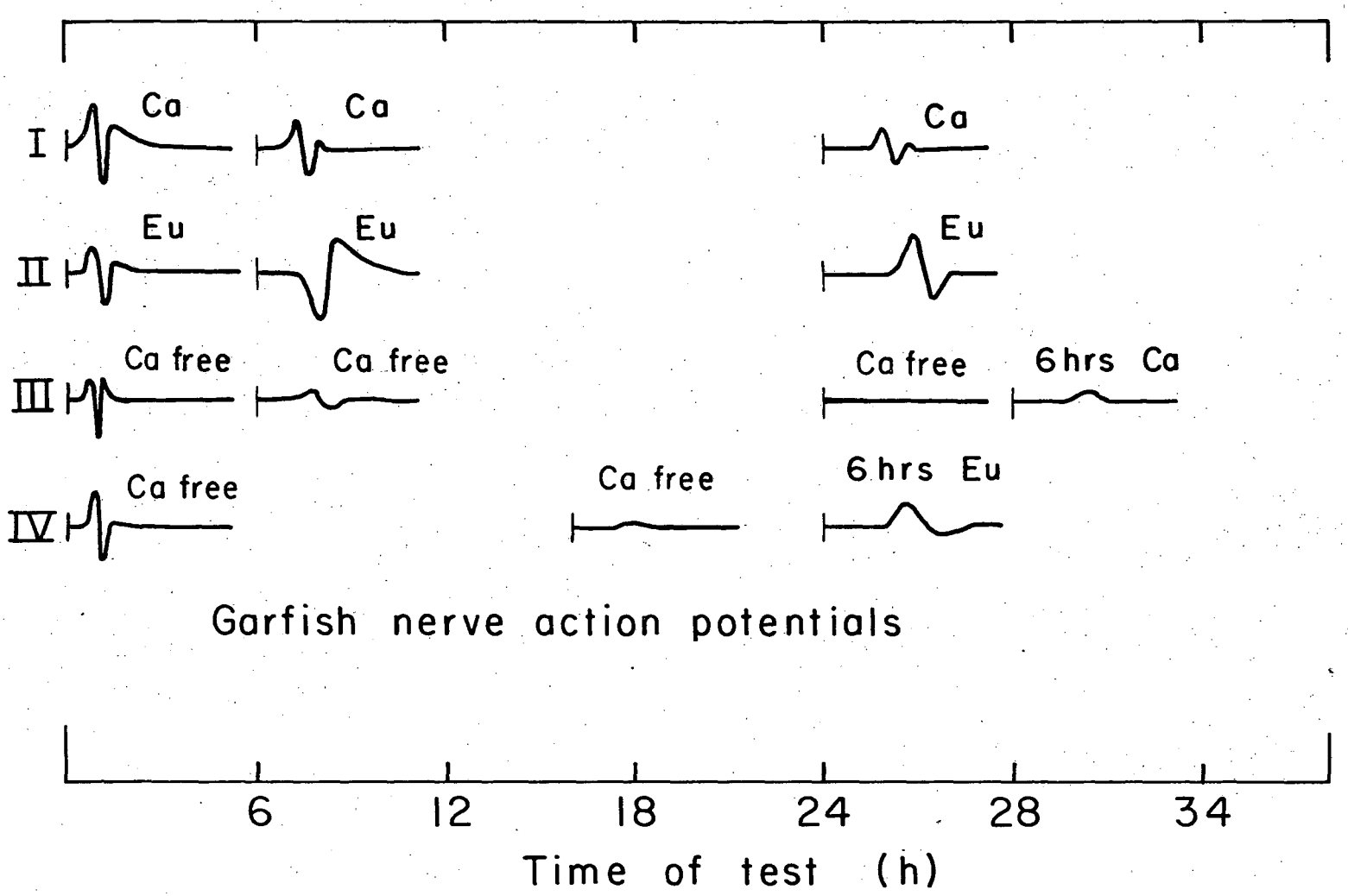

XBL738-3786

Fig. 16. Action potentials of garfish nerves bathed in Ca-, Eu-, and Ca-free - Ringer solutions.

Note that the Eu-Ringer causes a broadened and delayed action potential trace. This effect may be related to a difference between Ca^{+2} and Eu^{+3} in chemical binding constant, or a change of the nerve's gross electrical properties upon binding Eu^{+3} instead of Ca^{+2}.

Mn- and Ni-Ringers were prepared by substituting for $CaCl_2$ an equal concentration of $MnCl_2$ or $NiCl_2$. These Ringers had an effect similar to that of Eu-Ringer; i.e., maintenance of nerve excitability for times much longer than would be expected for a nerve in Ca-free Ringer. Excitability restoration after Ca-free Ringer bath was not checked experimentally for Mn or Ni-Ringer. Of all the Ca^{+2} substitutes, Mn^{+2} appeared to maintain excitability for the longest time as well as to cause the least broadening and delaying of the action potential.

Similar experiments were tried on lobster walking leg nerve. Eu^{+3} appeared to maintain excitability of the nerve, although ability to restore excitability to nerves tested by Ca-free Ringer was not clearly demonstrated. Broadening and delaying of the action potential was also observed. Use of Ca-free lobster Ringer always resulted in random firing of the lobster walking leg nerve; this was prevented by either Ca^{+2} or Eu^{+3} in the Ringer. Similar effects were observed for Mn- and Gd-Ringers on lobster nerves.

On the basis of the physiological evidence described above, I proceeded with the use of various polyvalent cations, and particularly Eu^{+3}, as an analog of Ca^{+2} in nerve-ion interactions.

An attempt was made to replace the physiological function of external K^+ with monovalent thallium ion (Tl^+ fluoresces in free aqueous solution and is quenched in complexes). However, concentrations of TlCl as low as 1 mM were found to irreversibly block the action potential.

B. Fluorescence Spectra of Nerves

The spectra described in this section were taken in a Perkin-Elmer MPF-2a spectrofluorimeter, with a HTV Type R446 photomultiplier. Filters in the excitation and fluorescence beam were used to decrease scattering artifacts and stray light transmitted through the instrument's monochromators. The sample was a 4-cm length of garfish nerve trunk pushed into a 2 × 2 mm quartz fluorescence cuvette filled with the appropriate Ringer solution. The spectra are all uncorrected for instrumental wavelength-dependent response and self-absorption of the sample, but they show the pertinent qualitative features. Quantitative data is hard to extract from this technique, because the intensity of observed fluorescence was extremely sensitive to the position of the nerve in the cuvette.

The intrinsic fluorescence emission spectrum of a fresh garfish nerve bathed in Ca-Ringer consists of three main bands, centered at λ = 330, 445, and 520 nm (see Fig. 17). The excitation bands for these are centered at λ_a = 290, 350, and 370 nm, respectively. From knowledge of the fluorescence spectra of common biomolecules (110), the three bands may be identified as originating from tryptophan residues of protein, reduced nicotine dinucleotide (NADH), and oxidized

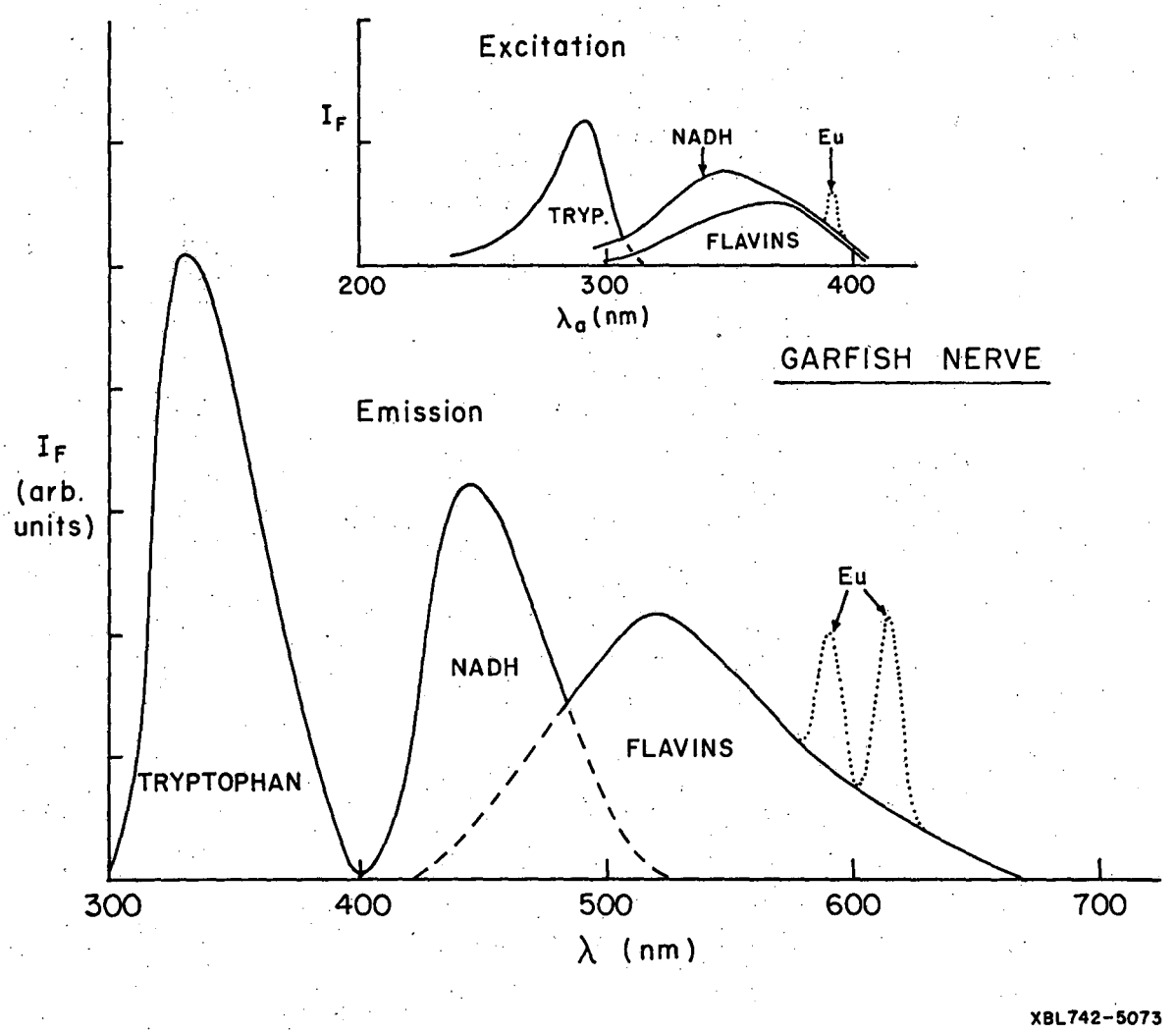

Fig. 17. Intrinsic fluorescence spectra of garfish nerve. Dotted peaks represent Eu^{+3} fluorescence in Eu-nerve.

flavins, respectively. Protein certainly exists in both the axon membrane and the axoplasm, both solubilized and in organelles. NADH and flavins are involved in the chemical energy-producing metabolism of the mitochondria organelles in the axoplasm. [It is clear from electron microscopy that mitochondria do indeed exist in the axons of garfish olfactory nerve (42) and lobster nerves (48).]

The intrinsic fluorescence spectra of a garfish nerve which has been bathed in Eu-Ringer for 24 hrs. at 0°C (abbreviated Eu-nerve hereafter), is not measurably different from the spectrum of a nerve bathed in Ca-Ringer. There is no evidence of energy transfer from rare-earth to organic chromophores or of intrinsic fluorescence quenching, although the latter effect would be hard to calibrate since the observed fluorescence intensity is highly dependent on the nerve's position in the cuvette.

The Eu^{+3} fluorescence of Eu-nerve is more interesting. The emission spectrum (lower left of Fig. 18) shows the reversal of peak intensities characteristic of bound Eu^{+3}. The fluorescence of the aqueous Eu^{+3} in the Eu-Ringer is negligible compared to the Eu^{+3} fluorescence of Eu-nerve, which indicates that virtually all of the Eu^{+3} giving rise to fluorescence in Eu-nerve is chemically bound. In addition, washing the nerve in Ca-Ringer and rechecking its spectrum leads to no decrease in Eu^{+3} fluorescence. The sloping background fluorescence is the long-wavelength tail of the nerve's intrinsic NADH and flavin fluorescence, the intensity of which is the same order of magnitude as the Eu fluorescence at 614 nm.

The excitation spectrum of Eu-nerve was obtained by plotting the height of the 614 nm emission peak above the background as a function

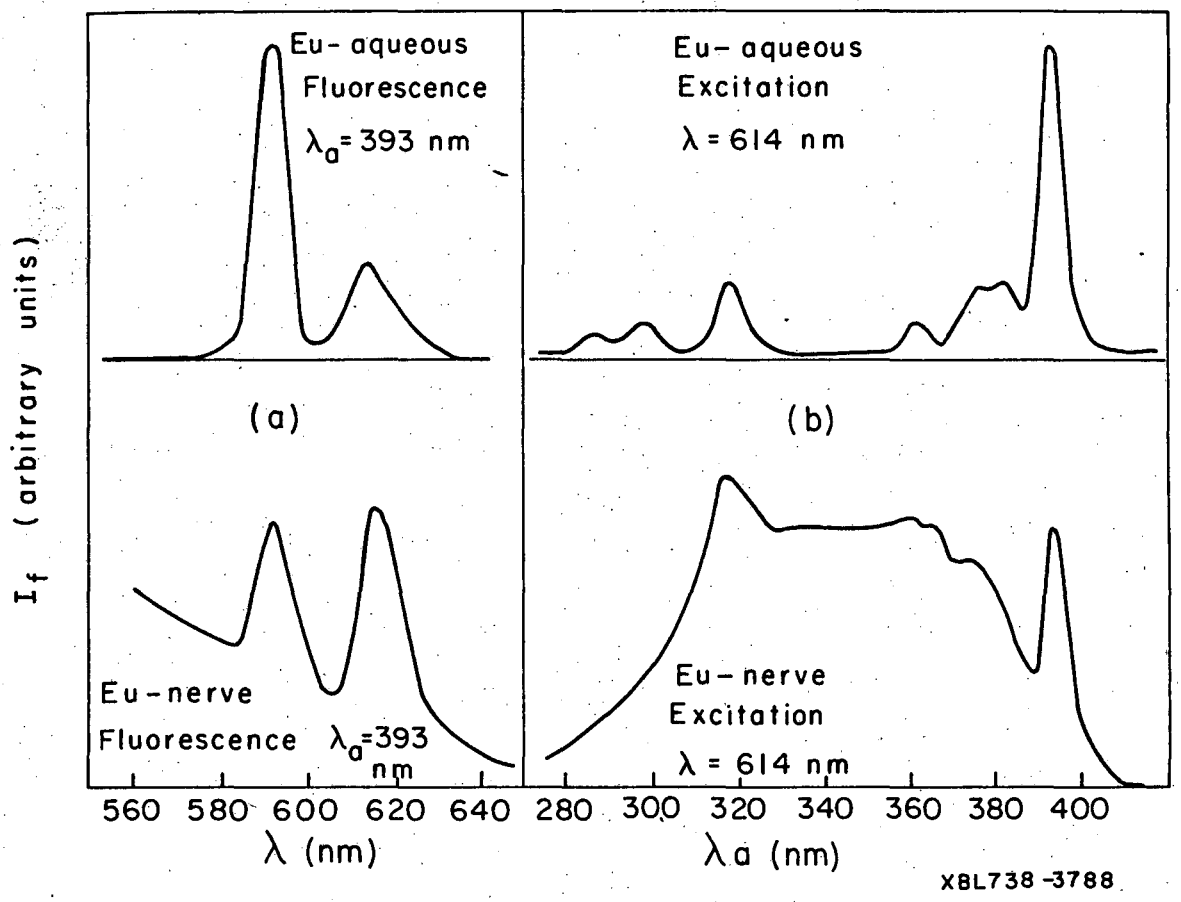

Fig. 18. (a) Fluorescence emission spectra of $EuCl_3$ aqueous solution vs. Eu-nerve. λ_a = 393 nm. Resolution = 5.0 nm. (b) Fluorescence excitation spectra (uncorrected) of $EuCl_3$ aqueous solution vs. Eu-nerve. λ = 614 nm. Resolution = 5.0 nm.

of exciting wavelength, i.e., the excitation spectrum was obtained point-by-point from a set of emission spectra curves. This was done to separate the excitation spectrum of the Eu^{+3} from the excitation spectrum of the total (Eu^{+3} + background) fluorescence. The result (lower right, Fig. 18) is qualitatively different from the excitation spectrum of an aqueous solution of $EuCl_3$ (upper right, Fig. 18). In particular, excitation in the region from 340-355 nm can produce Eu^{+3} fluorescence from Eu-nerve but not from aqueous Eu^{+3}. Energy transfer from some species absorbing in this region is indicated.

If the transfer is a "Förster" mechanism, the donor species must have a fluorescence emission band of its own overlapping Eu^{+3} absorption bands. However, if the organic donor state is a triplet level (as described in Chap. III), then the phosphorescence emission bond of the donor (which is only observable at low temperatures) must overlap an Eu^{+3} absorption band. If the transfer is a "through the band" mechanism, the donor and acceptor states must still be close in energy, but the efficiency of the transfer will depend on the degree of orbital overlap rather than the overlap of emission and absorption bands.

A likely candidate for the energy donor is NADH. This possibility is supported indirectly by the following additional facts:

(1) Ca^{+2} is believed to bind to NADH (147);

(2) Ca^{+2} accumulates in mitochondria (where NADH is present) (95);

(3) Eu^{+3} binds to NADH and NADH acts as an energy donor for Eu^{+3} fluorescence (shown in Chap. III).

Complexes of metals and flavins also exist and have been studied extensively in vitro (58).

There is no evidence of energy transfer from the tryptophan side groups of protein, although the lack of such transfer does not eliminate the possibility of Eu-protein binding. Since considerable overlap between tryptophan fluorescence emission and Eu^{+3} absorption bands exists, the lack of protein-to-Eu^{+3} transfer may indicate that triplet donor states or "through bond" mechanisms are most important in determining transfer efficiency.

The same type of experiments were performed on garfish nerve bathed in Tb-Ringer for 24 hrs. at 0° C ("Tb-nerve"). Tb^{+3} fluorescence, in general, does not show a qualitatively new emission spectrum upon complexation; all of the emission bands become intensified to the same degree. The narrow emission bands occur at 543, 486, 584, and 619 nm, in decreasing order of intensity. The Tb^{+3} emission spectrum of Tb-nerve is not qualitatively different from that of aqueous $TbCl_3$. However, the excitation spectrum of Tb-nerve, measured point-by-point from the intensity of the 543 nm Tb emission peak above the intrinsic nerve fluorescence background, is significantly different from the excitation spectrum of aqueous $TbCl_3$ (Fig. 19). The strong band centered near 290 nm indicates Tb^{+3} binding to, and energy transfer from, the tryptophan residues of protein. It is difficult to determine whether transfer from NADH exists, because Tb^{+3} has its own excitation bands in the 320-380 nm region. The fact that tryptophan is an energy donor to Tb^{+3} but not to Eu^{+3}, although the two presumably bind to the same sites because of their chemical homology, supports the

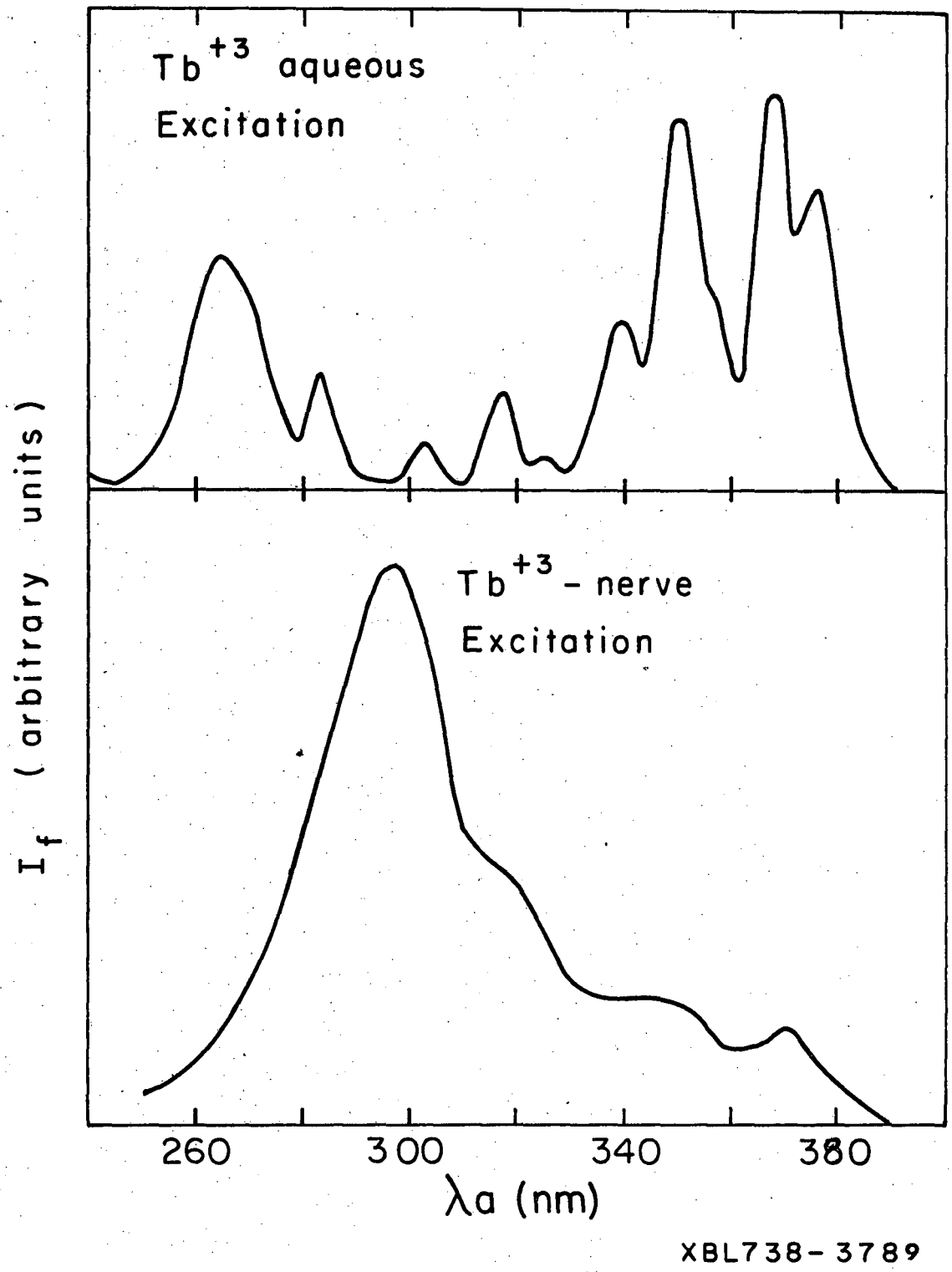

Fig. 19. Fluorescence excitation spectra (uncorrected) of $TbCl_3$ aqueous solution vs. Tb-nerve. λ = 543 nm. Resolution = 5.0 nm.

view that the transfer is by a mechanism more complicated than simple Förster transfer. Similarly to the result here, Luk (91) observed tryptophan-to-rare-earth energy transfer in Tb-transferrin (protein), but not in Eu-transferrin.

We therefore conclude that both Tb^{+3} and Eu^{+3} bind to protein and NADH and/or oxidized flavins in the nerve trunk, among other possible sites of binding.

In the early work on lobster leg nerve, a detailed study of the excitation spectra was not performed, but the emission spectrum clearly showed Eu^{+3} binding to the nerve trunk.

CHAPTER VI

TRANSIENT FLUORESCENCE CHANGE STUDIES

The heart of the project reported here was the examination of transient fluorescent changes (if any) synchronous with the passage of an action potential. The transient fluorescence of both rare-earths and intrinsic organic species was studied in a specially constructed low-noise fluorimeter with fixed excitation and emission wavelengths, provision for easy viewing and physiological support of the nerve, and ability to detect and signal-average optical changes in the millisecond time range.

A. Experimental Apparatus

The optical arrangement is shown in Fig. 20. A 900-watt Osram Xenon lamp was the light source. A flowing water filter, 20-cm long, blocked heat-producing IR wavelengths. The light was passed through interference filters and a Bausch and Lomb Hi-Intensity grating monochromator, yielding an excitation beam of 10-nm spectral bandwidth. A glass plate deflected part of the exciting light directly to a reference photomultiplier, used to monitor fluctuations in the Xenon arc. The width of the main beam impinging on the nerve was 0.5 mm after focusing and passage through a quartz side window of the black plexiglass nerve holder (see Fig. 21). The nerve was viewed at 90°, i.e., from above, through a glass window in the nerve holder's plastic cover, by a microscope. The trinocular head of the microscope could be set

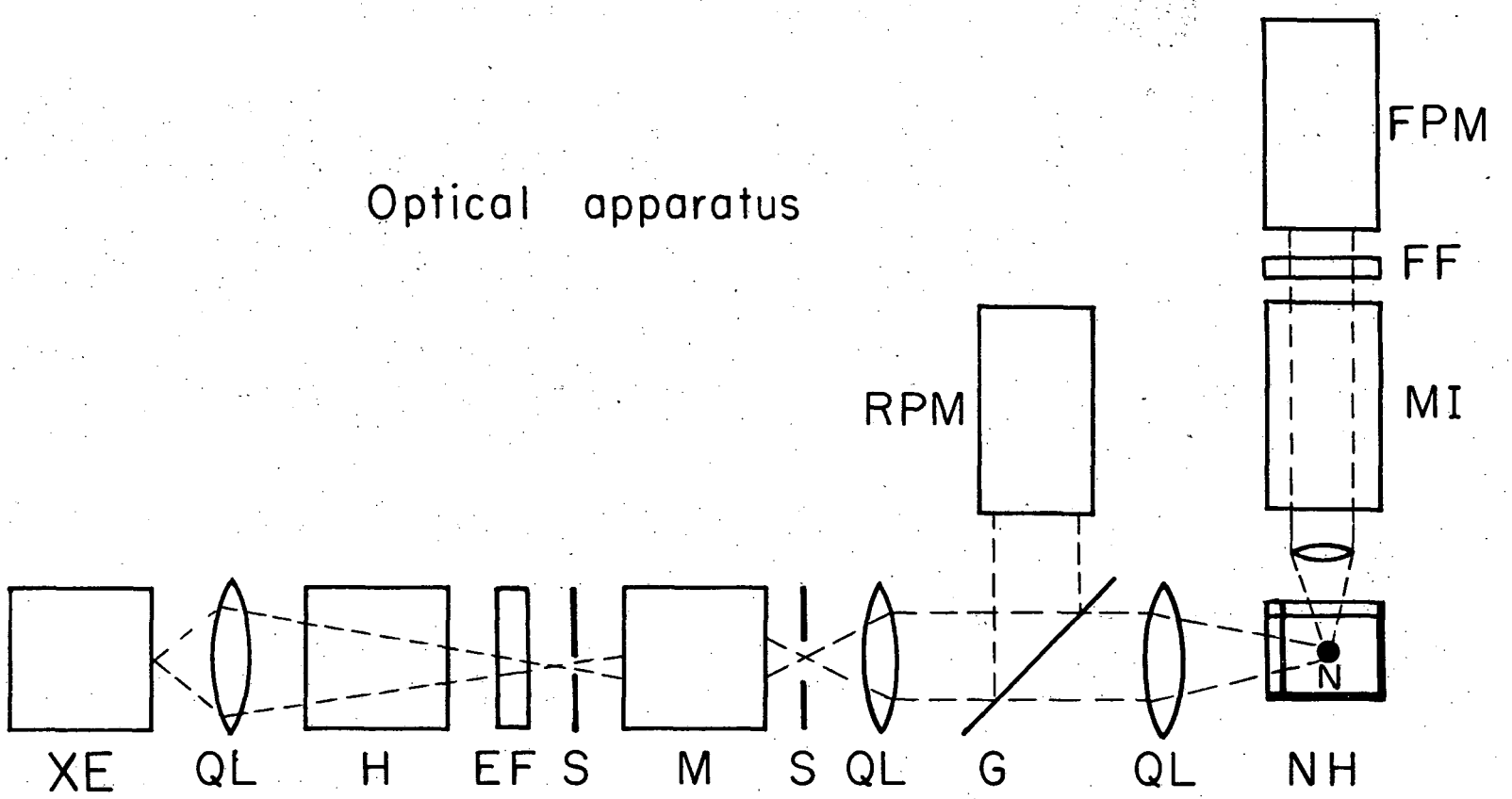

XBL738-3785

Fig. 20. Optical apparatus for observation of nerve fluorescence as a function of time. Abbreviations are as follows: EF, excitation filters; FF, fluorescence filters; FPM, fluorescence photomultiplier; G, glass plate; H, H_2O infrared filter; M, monochromator; MI, microscope; N, nerve; NH, nerve holder, QL, quartz lens; RPM, reference photomultiplier; XE, xenon lamp.

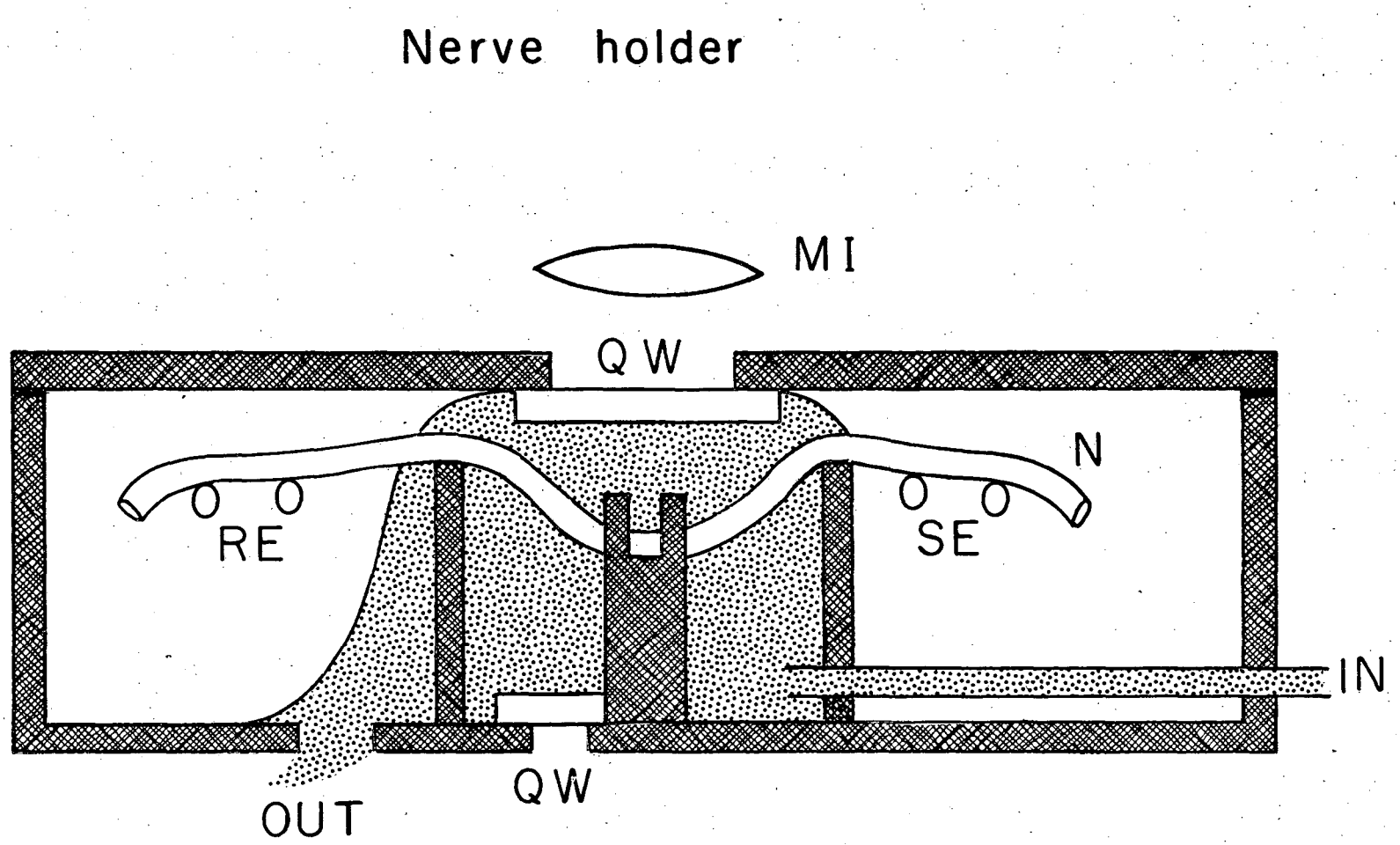

XBL738-3782

Fig. 21. Nerve holder, vertical section. Incident light for fluorescence experiments is directed perpendicularly into the paper and impinges on the nerve at the center of the middle chamber. Incident light for trypan blue absorption experiments is directed upward through the bottom quartz window. Stippled area shows path of flowing solution. Additional abbreviations are as follows: MI, microscope objective; QW, quartz window.

either to allow direct visual observation through the eyepieces or to pass the light from the objective to the emission filter array above. An EMI 9558 QA photomultiplier was used to detect the fluorescence transmitted by the filters. We selected all filters so that very little stray light or filter fluorescence was observed. The field of view of the microscope was approximately half filled by the image of the nerve, the remainder by the bathing solution. The optical setup was contained completely in a light-tight box during experiments.

The 900 W Xenon lamp was used because it produced the most intense, and yet fairly stable, near -UV exciting light. Preliminary experiments indicated that tungsten filament and deuterium arc lamps were stable but too dim and 1000 W Hg-Xe was too unstable. There is no commercially available CW laser with an output at 393 Å, the strongest excitation band for Eu^{+3} fluorescence.

The nerve holder itself was partitioned into three chambers (Fig. 21). The central chamber filled with incoming Ringer solution, which formed a minicus with the quartz window on the plastic cover and overflowed into a side chamber, whence it dripped by gravity through a hole in the floor of the side chamber. Small plastic supports and guideposts in the central chamber prevented the nerve from sagging during an experiment.

The solution flowed into the nerve holder via gravity from raised vessels; we could switch solutions rapidly by turning a valve to a new source vessel without mechanically disturbing the nerve or optics in any way. The time required for complete changeover of solutions in the nerve holder was 1-2 min; the flow rate was

approximately 1 drop/5 sec.

The electronic system was used in one of two forms: either analog or digital (photon counting) detection. In the analog form (Fig. 22), the fluorescence photomultiplier and excitation beam reference photomultiplier outputs were connected to the positive and negative inputs of a Tektronix Type 1A7A differential amplifier, respectively. The high voltage power supply to the reference photomultiplier was adjusted so that the output of the differential amplifier would not change at all when the lamp intensity was varied by ±20%. This procedure, used to cancel out the effects of lamp flicker and drift, was performed before each run on every nerve.

The duration of a garfish nerve action potential is about 40 msec. Therefore, the RC filters were set on the output of the differential amplifier to pass the frequency of 0.1 hz to 0.1 khz. This filtered output was connected directly to the input of a Computer of Average Transients (CAT) in order to signal average the photomultiplier outputs during several thousand successive stimulations of the nerve. The CAT, operated on internal triggering mode, supplied a scan starting pulse which was amplified and delayed to stimulate the nerve once during each CAT scan. The recorded data were punched on paper tape and the data contained thereon could then be added by computer to the results obtained for similar experiments on other nerves in order to further enhance the signal/noise.

In the photon counting experiments, the reference photomultiplier was not used. Fluorescent light was focused onto the center of the EMI 9558 QA photocathode, the housing of which contained electron-

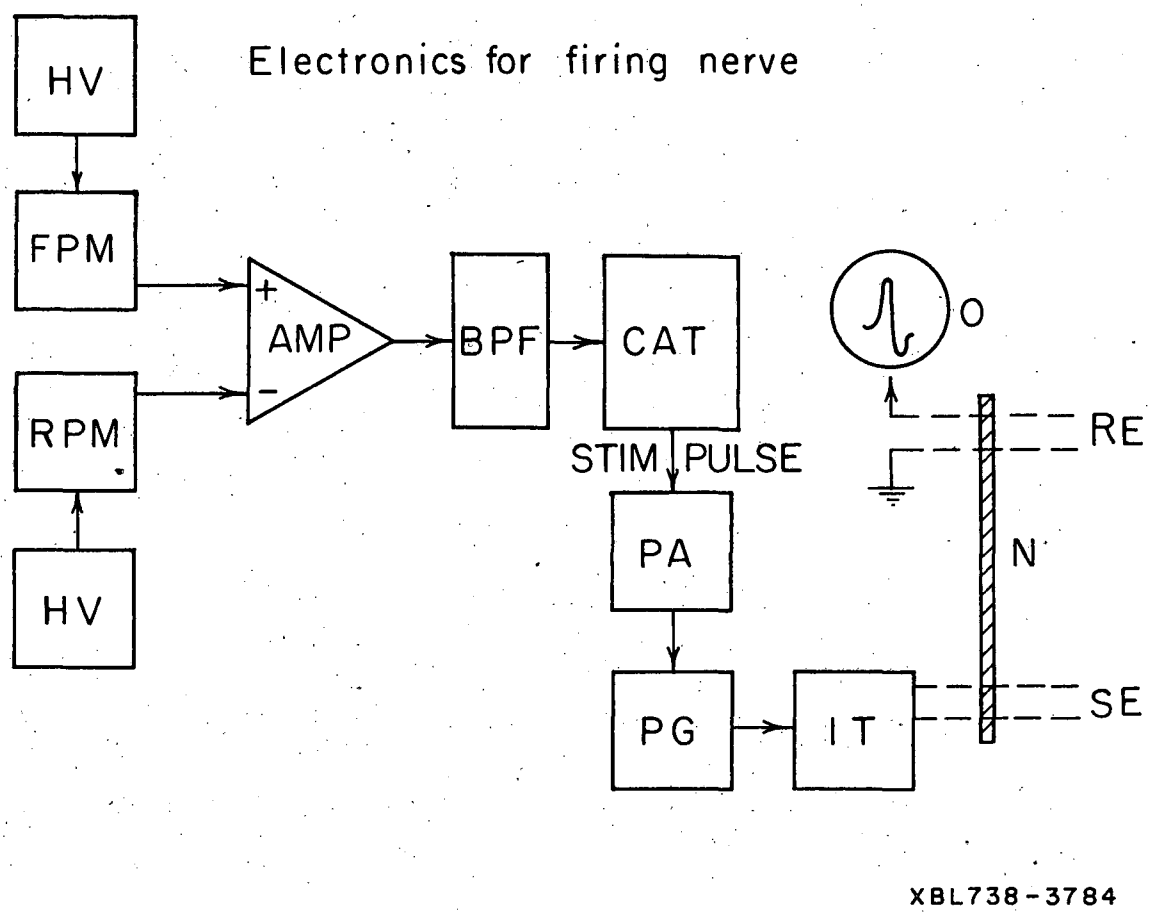

Fig. 22. (a) Electronics for observation of fluorescence during nerve firing. Abbreviations are as follows: AMP, differential amplifier; BPF, bandpass filter; CAT, signal averager; FPM, fluorescence photomultiplier; HV, high voltage power supply; IT, isolation transformer; N, nerve; O, oscilloscope; PA, pulse amplifier; PG, pulse generator with variable delay; RE, response electrodes; RPM, reference photomultiplier; SE, stimulation electrodes.

defocusing magnets to reduce the recorded dark count. The output of the photomultiplier was connected to a PAR Model 1120 "Amplifier-Discriminator" which discriminates against PM pulses smaller than a preset amplitude and shapes the remainder into -1.5 V, 50 ns duration pulses. (A count rate of greater than 10^7 counts/sec. leads to frequent pulse overlap, so photon counting must be limited to detection of low light intensities). The output of the amplifier discriminator was connected to a PAR Model 1127 "NIM Adapter" which converts the input to TTL-compatible pulses of either 50 or 300 ns duration. These TTL pulses then could be directly fed into a CAT signal averager whose analog-digital converter was replaced by a special bypass card for digital inputs. A slow-response count-rate meter was used to monitor the approximate pulse rate.

Digital detection has the advantage of eliminating all worries about AC-pickup and amplifier noise, but analog detection allowed for the use of the reference photomultiplier and higher light levels which reduces the relative size of shot noise.

For garfish nerves, the total sweep time of the 400-channel CAT was 1 sec.; the nerve was fired once/sec.

B. Transient changes of Rare-earth Fluorescence

The observed fluorescence intensity of Eu-garfish nerve at $\lambda = 614$ nm and $\lambda_a = 393$ nm* was usually on the order of 10^7 - 10^8 photons/sec. Any transient changes of Eu-fluorescence of garfish nerve as measured by the analog system, were less than the background noise level.

* λ_a and λ are the excitation and emission wavelengths, respectively.

This result was obtained both for the signal-averaged record of six nerves individually, and for the computer summation of these records, representing a total of 6,700 nerve firings.

The experimental noise level, after signal averaging and summation over the six nerves, corresponded to approximately ±0.01% of the DC output of the fluorescence photomultiplier in each channel of the CAT. At a count rate of 10^7/sec., and RC time constant of 10 ms, and 5×10^3 scans, each time constant interval would receive approximately $N = 5 \times 10^8$ counts. The shot noise magnitude of this total is $\sqrt{N}$, or approximately 2×10^4 counts. Therefore, the theoretical shot noise in each channel should be ±0.005%. This calculation indicates that approximately half the observed noise was the statistical limit-shot noise. The remainder was probably due to amplifier noise, mechanical vibrations, and excess flicker noise of the photomultiplier. Since shot noise was such a large portion of the total noise, electronic or mechanical refinements would not have greatly improved signal/noise.

Photon-counting electronics was used to examine transient Eu-fluorescent changes in thirteen other garfish nerves. Again, any changes were less than the background noise level, which ranged from ±0.05% to ±0.13%. The lack of a reference photomultiplier in photon-counting electronics increased the light source fluctuation contribution to the noise level.

In preliminary experiments, lobster nerves were used instead of garfish nerve. No reference photomultiplier was used, so the noise level was near 0.1%. Transient changes of Eu-fluorescence, if any, were hidden beneath the noise.

It was thought possible that much of the Eu-fluorescence was from Eu^{+3} bound in the axoplasm (see next chapter). In order to discriminate against this Eu^{+3} "background", transient-change experiments with analog electronics were performed on four garfish nerves bathed for less than 1 hr. in Eu-Ringer. Again, any changes were less than ±0.01%. The statistical accuracy was limited in part, by shot noise from the intrinsic organic fluorescence background.

Changes of less than ±0.02% were observed on two Eu-garfish nerves excited at λ_a = 350 nm instead of 393 nm, a procedure utilizing the energy transfer from an intrinsic organic chromophore described in Chap. V.

In experiments on two Tb-garfish nerves using analog electronics, observation of transient changes in energy transfer from protein to Tb^{+3} was attempted, using λ_a = 290 nm and λ = 543 nm. Changes, if any, were less than ±0.03%.

An effort was made to reduce the shot noise contribution from short-lifetime intrinsic organic fluorescence by "chopping" the incident light and observing the only long-lived Eu-fluorescence decay from an Eu-nerve. A special digital electronic gate was constructed, to pass only that photomultiplier output occurring when the incident light was off; a rotary wheel was used to chop the incident light into 1 ms duration, 50% duty-cycle pulses with a rise time of 10 μs. No transient changes in Eu-fluorescence synchronous to nerve firing were observed by this technique; the noise level was not improved over the best of previous experiments, partly because the observed Eu-fluorescence (in average counts/sec) was reduced by at least an order of magnitude,

and photon counting (without a reference photomultiplier) rather than analog electronics was used. In addition, a puzzling long-lifetime emission was observed with a Ca-nerve in the sample holder. Later experiments indicated that this was probably an artifact due to scattered 393 nm light inducing phosphorescent emission from epoxy glue around the edges of the windows in the sample holder, with this emission then scattering into the viewing area. Because this lingering phosphorescence during the light-off periods contributed to shot noise, chopped light experiments on Eu-nerve gave little advantage over DC-light experiments.

C. Transient Changes of Intrinsic Fluorescence

To check against the possibility that changes in rare-earth fluorescence might be cancelled by equal and opposite changes in intrinsic fluorescence, transient change experiments were performed on the three intrinsic fluorescence bands of Ca-garfish nerve.

To within ± 0.01%, the noise level, no transient changes in the protein band (λ_a = 286 nm, λ = 310 - 380 nm) were detected, using unpolarized optics and analog electronics. The static polarization of protein luminescence was measured using Polaroid HNP'H filter polarizing sheets in both the excitation and emission beam. There are four possible orientations of the two filters (polarizer and analyzer) relative to the nerve's longitudinal axis: each filter can be either parallel ($\parallel$) or perpendicular ($\perp$) to the nerve axis. The observed intensity in each case was as follows:

POLARIZER	ANALYZER	INTENSITY (counts/sec)
∥	∥	8.3×10^6
∥	⊥	1.8×10^6
⊥	⊥	7.0×10^6
⊥	⊥	3.0×10^6

(The two polarized light intensities incident on the nerve are not equal due to the polarizing effect of the monochromator). The protein fluorescence is clearly polarized, indicating restricted rotational freedom of tryptophan residues in the nanosecond time range. No transient changes in any of these four polarization configurations synchronous with firing were observed, to within ±0.02%. These experiments were each performed once in the analog mode, but without a reference photomultiplier. In addition, the incident UV light intensity was reduced by neutral density filters to avoid damaging the nerve's excitability. Therefore, the precision of the results, although sufficient to discount the possibility of a cancellation effect (due to protein fluorescence changes), could conceivably be improved.

Since the background intrinsic fluorescence of most rare-earth nerve experiments was probably from NADH and flavins, transient changes from these molecules were examined, using analog electronics. For NADH (λ_a = 352; λ = 400 - 480), no changes to within ± 0.005% were found on four Ca-garfish nerves. For oxidized flavins (λ_a = 370, λ > 500 nm) no changes to within ± 0.002% were found on two Ca-garfish nerves. Polarized light studies of NADH and flavin fluorescence were not performed.

We may conclude that the absence of observable rare-earth fluo-

rescence changes is not an artifact of an accidental cancellation of intrinsic and rare-earth fluorescence changes.

"Too much of nothing can make
a man feel ill at ease."

–Bob Dylan

CHAPTER VII

FLUORESCENCE CHANGES IN RESTING NERVE

In order to help identify the structures and molecules in nerve to which Eu^{+3} binds, changes in the fluorescence of resting nerve was observed as the external solution was varied. External Ringer solutions containing abnormal salt concentrations, certain chemical agents, and specific enzymes have known chemical and/or physiological effects, and in some cases, these effects could be correlated with Eu^{+3} binding. Ringer solutions containing two rare-earth ions or a transition metal ion were used to observe energy transfer as a measure of molecular distances.

The optical apparatus for these experiments was the same as described in Chapter VI. The electronics (Fig. 23) was in the analog mode, with the reference photomultiplier in use. We were interested in only slow time-course changes of fluorescence, the fastest of which would be due to the changeover of Ringer solutions flowing through the nerve chamber. Therefore, the differential amplifier output was DC-coupled with a 12-sec time constant. The filtered output was fed through a unity gain amplifier into a Moseley strip chart recoreder with adjustable DC offset.

A. Uptake of Eu^{+3}: Time Course

We monitored the λ = 614 nm Eu^{+3} fluorescence of Eu-garfish nerve with exciting wavelength λ_a = 393 nm, as a function of time. The nerve was not fired, but merely bathed in the nerve chamber through

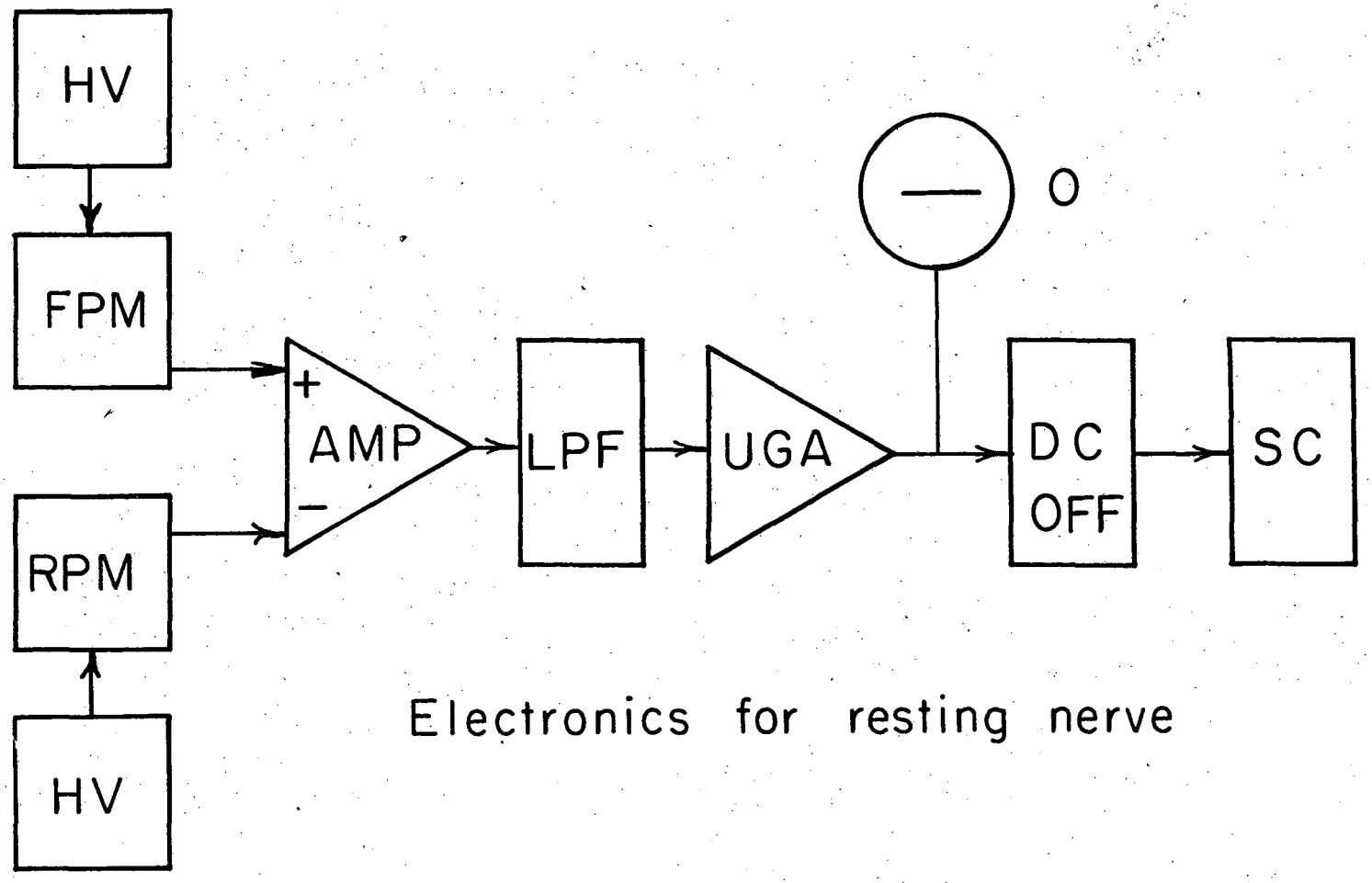

XBL738-3783

Fig. 23. Electronics for observation of fluorescence of resting nerve. Abbreviations (additional to those of Fig. 22) are as follows: DC OFF, DC offset; LPA, low pass filter; SC, strip chart recorder.

which the flowing solution could be switched from Ca-Ringer to Eu-Ringer at time zero.

The resulting curve (Fig. 24), presumably proportional to Eu^{+3} uptake, shows a fairly linear rate of uptake, at least for the first 7 hr. (The "bumps" in the curve are probably artifacts of electronic amplifier or power supply drifts or shifts in the nerve position due to vibrations.) Flow was then stopped, and then restarted 18 hr later; renewed observation showed the nerve continued to take up Eu^{+3} at an apparently undiminished rate.

Is this long-term steady uptake of Eu^{+3} by the nerve in Eu-Ringer reversed by bathing in Ca-Ringer (i.e., is Eu^{+3} binding reversible on the time scale of several hours)? Figure 25, a plot of Eu^{+3} nerve fluorescence while switching back and forth between Eu- and Ca-Ringer, shows that Eu^{+3} uptake is essentially irreversible. (The fluorescence intensity of the unbound Eu^{+3} ion in the Ringer solution itself is almost negligible in these studies.)

Perhaps several uptake processes occur simultaneously: for example, a large but very slow uptake of Eu^{+3} by the axoplasm or its organelles, and a much smaller but relatively rapid uptake by the axon membrane. In order to minimize the possible axoplasmic contributions, the same uptake experiments were performed with Eu-Ringers containing only 0.01 and 0.05 mM Eu^{+3} rather than the usual 0.5 mM Eu^{+3}. We hoped to see a relatively rapid uptake in the first few minutes, representing axon membrane uptake, followed by a long plateau when the membrane sites are saturated. However, no consistent results were observed; under conditions of very low $[Eu^{+3}]$, the Eu-nerve

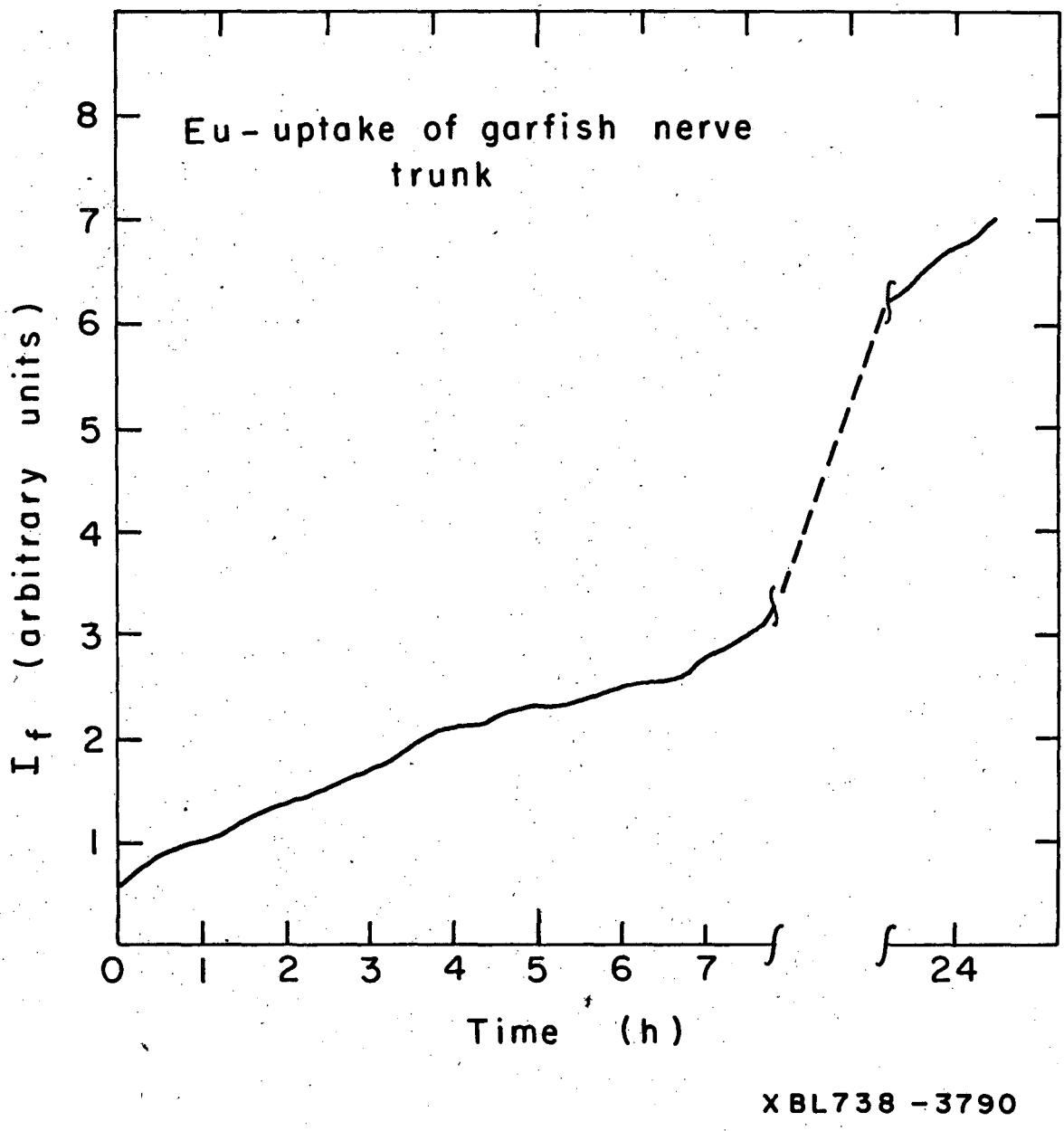

Fig. 24. Uptake of Eu^{+3} by garfish nerve trunk vs. time, measured by Eu^{+3} fluorescence at $\lambda = 614$ nm, $\lambda_a = 393$ nm.

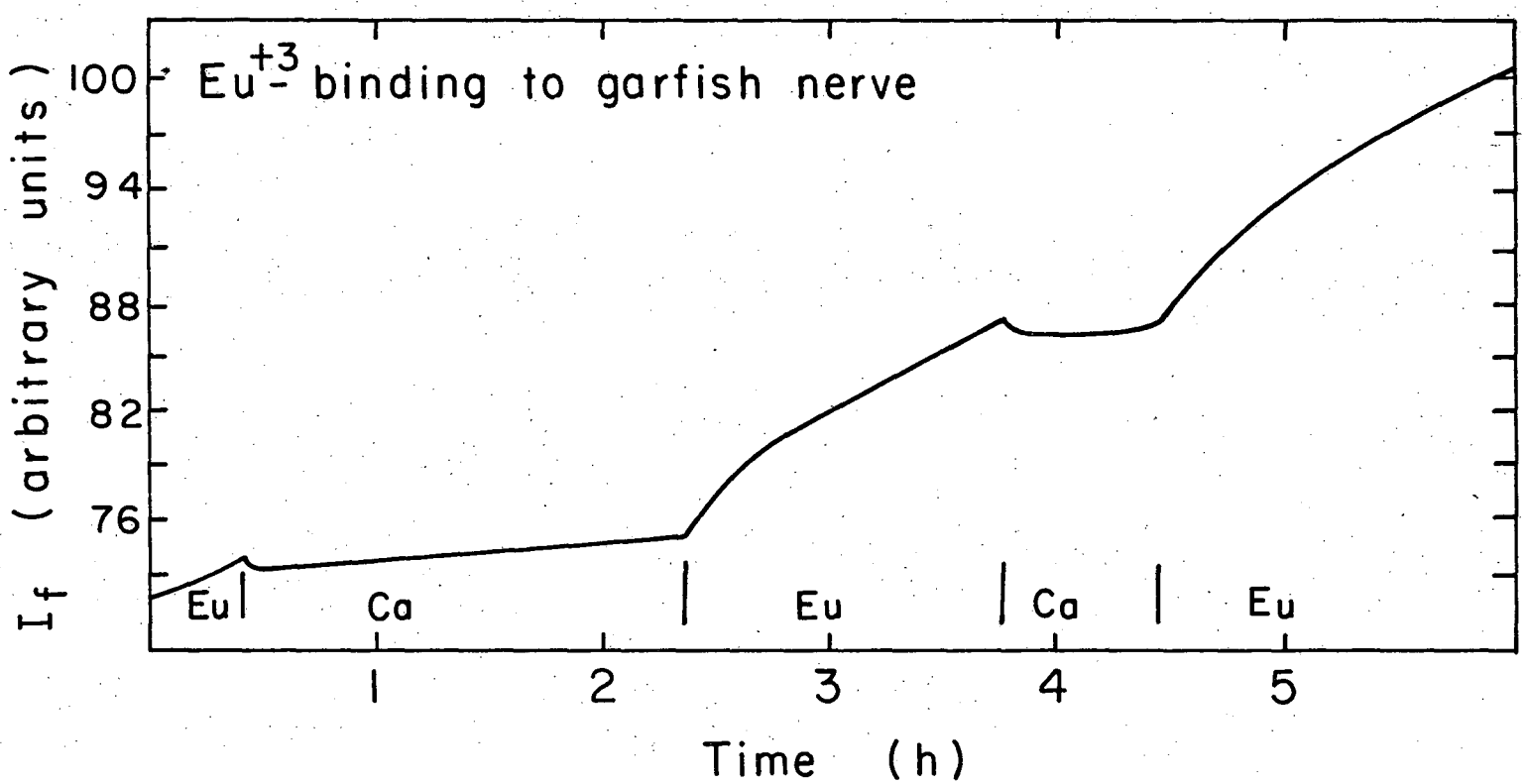

XBL738-3791

Fig. 25. Quantity of Eu^{+3} binding to garfish nerve, as measured by Eu^{+3} fluorescence at λ = 614 nm, λ_a = 393 nm, during alternation between Eu-Ringer and Ca-Ringer.

fluorescence becomes only a small fraction of the background organic fluorescence, and to within the drift noise limits of the experiment (0.5%) no clear fast initial uptake was seen.

B. Diffusion of External Solution into Nerve Trunk

We considered that the rate-limiting step for the gradual continual uptake of Eu^{+3} might be liquid ionic diffusion into the extracellular spaces between the rather densely packed individual axon fibers; i.e., perhaps it takes hours for all the axons to "see" a change of solution which affects at first only the outer axons. In order to find an upper limit to this diffusion time, we measured the adsorption of the vital biological stain trypan blue [31] to the exterior membrane surfaces of the nerve trunk as a function of time.

Two assumptions are made here: (1) that trypan blue diffuses as slowly or more slowly than does Eu^{+3}, and (2) that trypan blue binds rapidly to the exterior membrane surfaces throughout the trunk but does not penetrate to the axoplasmic regions at all. The first assumption is justified because trypan blue has a larger size and molecular weight than Eu^{+3}, and the second is a well known fact due to the large size and lipid-insolubility of the trypan blue molecule.

Adsorption of trypan blue was monitored by observing the adsorption of orange light by the whole nerve trunk as the solution flow is switched from a stain-free to stain-containing Ringer. The results of this experiment indicated that trypan blue diffuses completely throughout the extracellular spaces of the nerve trunk in about 45 min.

C. Eu^{+3} Uptake: Quantity

It is of interest to determine an approximate absolute measure of the quantity of Eu^{+3} uptake per unit time. This was done as follows. A nerve was bathed for 48 hr in cold Eu-Ringer, rinsed briefly in Ca-Ringer, and then placed in 10 ml of 5 mM EDTA (a strong chelating agent) in order to extract all the Eu^{+3} bound to the nerve trunk. Approximately 48 hr later, the nerve was removed and its Eu^{+3} fluorescence emission spectrum taken as in Chapter V. There was no evidence of bound Eu^{+3} remaining in the nerve; presumably, it had all become bound to the EDTA in the bath. In fact, the fluorescence spectrum of the EDTA bath did indeed confirm the presence of bound Eu^{+3}, and appropriate calibration of the spectrum with known concentrations of Eu-EDTA solution yielded a figure for the total Eu^{+3} originally bound to the nerve. This permitted us to calculate the rate of Eu^{+3} binding to the nerve, 0.7 ± 0.2 picomoles of Eu^{+3}/sec for a 1 cm length of garfish nerve.

We did a series of similar experiments with various Eu^{+3} concentrations in Ringer solution and found that, although the precision of the data was only ±20%, the Eu^{+3} binding rate generally increased with Eu^{+3} concentration in the Ringer bath and no saturation of binding could be found even for Eu^{+3} concentrations of up to 10.0 mM. We also noted in a separate but related experiment that Eu^{+3} uptake occurs approximately three times more rapidly at room temperature than at 0°C.

D. Effect of High $[K^+]$

The results reported in this and the following two sections are applicable to both fresh excitable nerves and nerves rendered inexcitable by repeated firings or age.

Although no transient changes of Eu^{+3} binding during firing have been observed, it is possible that bathing the nerve in a high $[K^+]$ - low $[Na^+]$ Ringer solution (see Table I) might affect Eu^{+3} binding. If, for example, Eu^{+3} binding is a function of membrane potential, high $[K^+]$ will depolarize the membrane and possibly induce a binding change. Alternatively, if the membrane acts like an ion exchanger, as suggested by Tasaki [134], the high $[K^+]$ in the membrane might displace Eu^{+3} from the Ca^{+2} binding sites.

Using the fluorescence/Ringer flow apparatus described earlier, we alternately switched solutions back and forth between "normal" low $[K^+]$ Eu-Ringer and high $[K^+]$ Eu-Ringer, as Eu-nerve fluorescence was observed at λ_a = 393 nm and λ = 614 nm. The fluorescence intensity increased approximately 1% within 5 min after introduction of high $[K^+]$ Eu-Ringer, relative to low $[K^+]$ Eu-Ringer (Fig. 26a). (This increase was superimposed on the steady rate of Eu^{+3} uptake reported in Section A). Naively, this would seem to indicate increased Eu^{+3} binding with high $[K^+]$, which contradicts our expectations. In order to check for background flavin fluorescence changes, we performed the same experiment on nerves illuminated by λ_a = 406 nm, so that Eu^{+3} fluorescence would not be excited but the broad flavin fluorescence would still appear. The result was that the same changes observed for λ_a = 393 nm (i.e., fluorescence increases upon introduction of high $[K^+]$ Ringer)

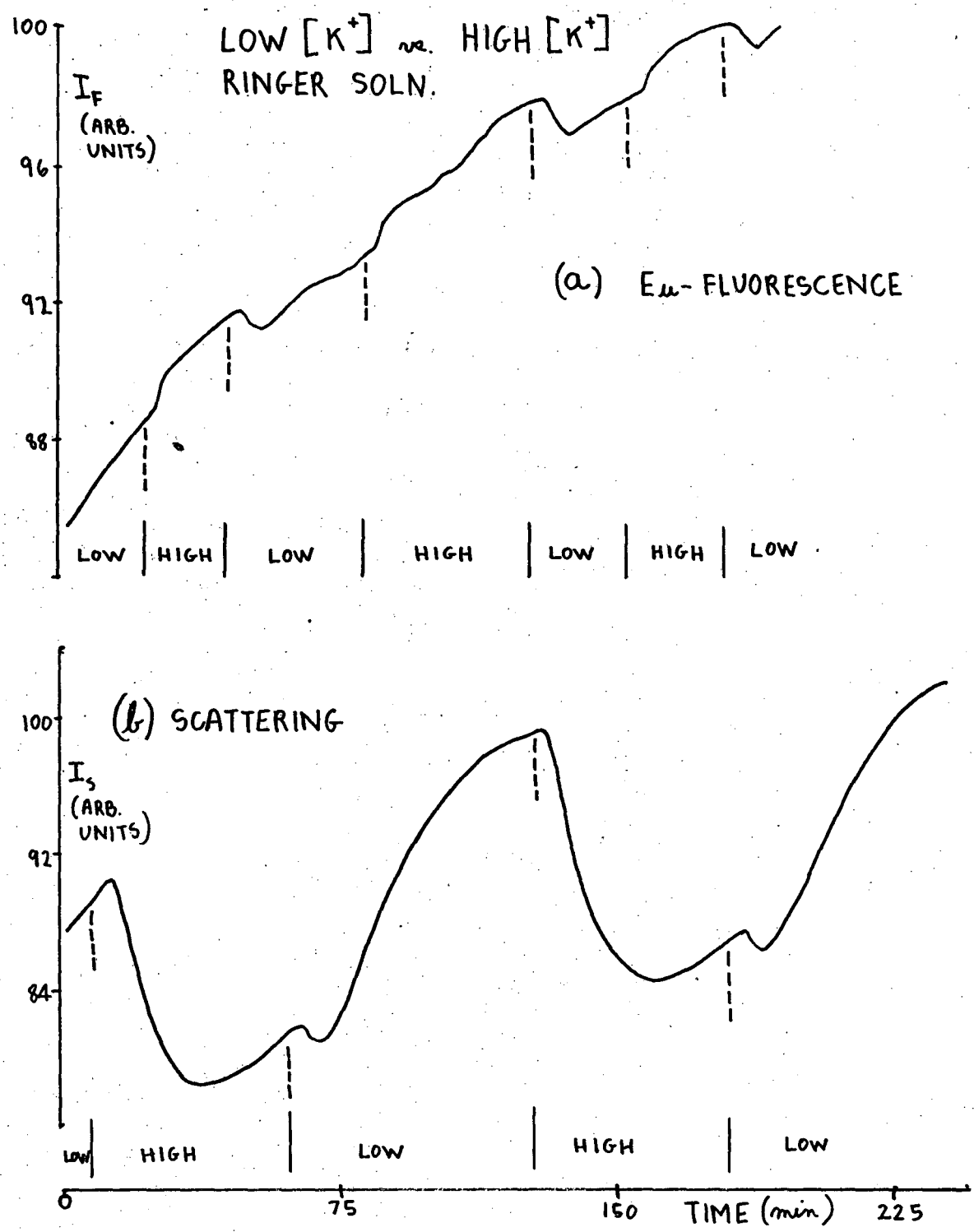

XBL 744-695

Fig. 26. Effect of low [K^+] and high [K^+] -Eu-Ringer on (a) Eu^{+3} fluorescence, λ_a = 393 nm, λ = 614 nm; and (b) light scattering, λ = 393 nm.

were also observed for λ_a = 406 nm, suggesting that background flavin fluorescence was influenced directly by external K^+ concentration. However, an alternative explanation presented itself when, instead of observing fluorescence at λ = 614 nm, we examined the time course of 90° scattered light at λ_a = 393 nm. Whenever high [K^+] solution was introduced, the scattering decreased by almost 20% (Fig. 26b). This decrease in scattering might have caused the effective incident light in the interior of the nerve trunk to become more intense, thus increasing the observed Eu^{+3} fluorescence. The observed change in Eu^{+3} fluorescence therefore may have been an artifact due to the scattering change.

High [K^+] Ca-Ringer reversibly abolishes the production of action potentials; when low [K^+] "normal" Ca-Ringer was restored after treatment of the nerve with high [K^+] Ca-Ringer, most of the axons of the axons resumed their ability to fire upon external stimulation of the nerve trunk.

E. Effects of Proteases and Neuraminidase

Experiments similar in form to the one described above were performed to study the relative Eu^{+3} binding when the solution is switched between "normal" Eu-Ringer and Eu-Ringer containing a specific enzyme destructuve to membranes. Two proteases, trypsin (1 mg/ml) and pronase (1 mg/ml), and the enzyme neuraminidase (0.1 mg/ml), which attacks the oligosaccharide side chains of glycoproteins, had no apparent effect on Eu^{+3} binding to nerve to within ±0.5%. An observable ~1% rise in fluorescence during trypsin treatment was noted, but this was an artifact due to fluorescence of Eu^{+3} bound to trypsin in the Ringer solution.

F. Effect of Phospholipase-c (Plc)

Phospholipase-c (0.2 mg/ml), which cleaves the polar heads groups of phospholipids from the diglceride portion, has a more interesting effect (Fig. 27). When Eu-Plc-Ringer was introduced, the rate of increase of λ = 614 fluorescence (λ_a = 393) became greater, possibly indicating more rapid Eu^{+3} uptake. Upon return to enzyme-free solution, the rate of increase decreased again but remained higher than it was before the first introduction of enzyme.

In order to ascertain how much of this change was an artifact of some sort, we repeated the experiments with Plc using λ_a = 406 nm, so that only background organic fluorescence would be observed at λ = 614 nm. We observed (Fig. 28) that, after a sudden increase, the rate of background fluorescence increase was greater during Eu-Plc-Ringer flow than during "normal" Eu-Ringer flow. When "normal" Eu-Ringer was returned, the increased rate of increase of fluorescence completely disappeared.

A clue to the meaning of these results was the observation that the Eu-Plc-Ringer was itself fluorescent at λ = 614 nm with λ_a = 393 nm or 406 nm, probably due to an organic impurity in the enzyme preparation used here. When the Eu-Plc-Ringer entered the nerve chamber, it caused a sudden increase in observed fluorescence, followed by perhaps a gradual permeation of the fluorescent material into the nerve trunk.

We can now interpret the results obtained by observation at the Eu^{+3} fluorescence at λ_a = 393 as shown in Fig. 27. When Eu-Plc-Ringer enters the chamber, we see a sudden increase of fluorescence from two causes: (1) Plc organic impurity fluorescence and (2) Eu^{+3}-ion

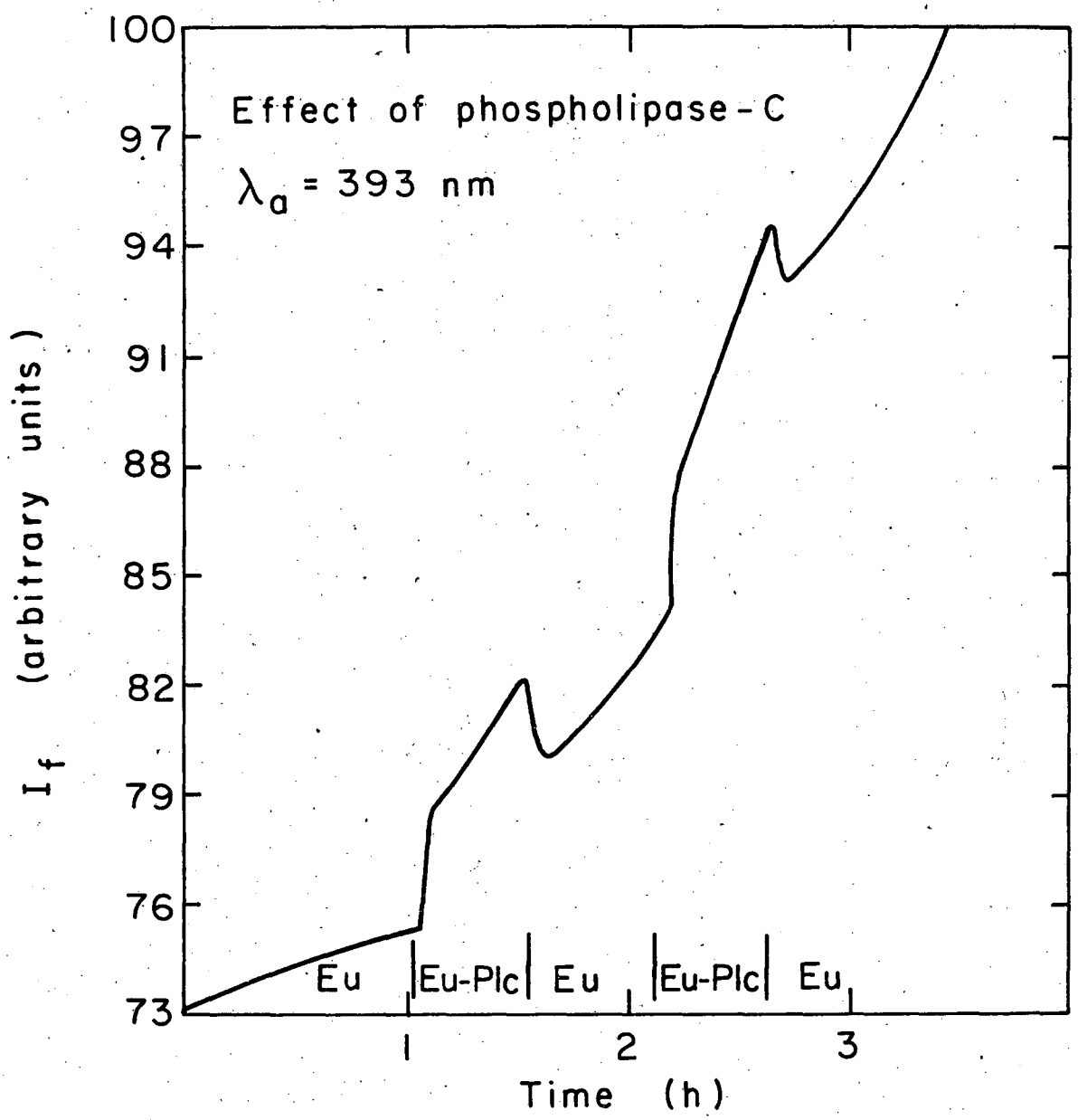

XBL738-3792

Fig. 27. Effect of phospholipase-c treatment on Eu^{+3} fluorescence in nerve. Solution is alternated between Eu-Ringer and Eu-Plc-Ringer. λ = 614 nm, λ_a = 393 nm.

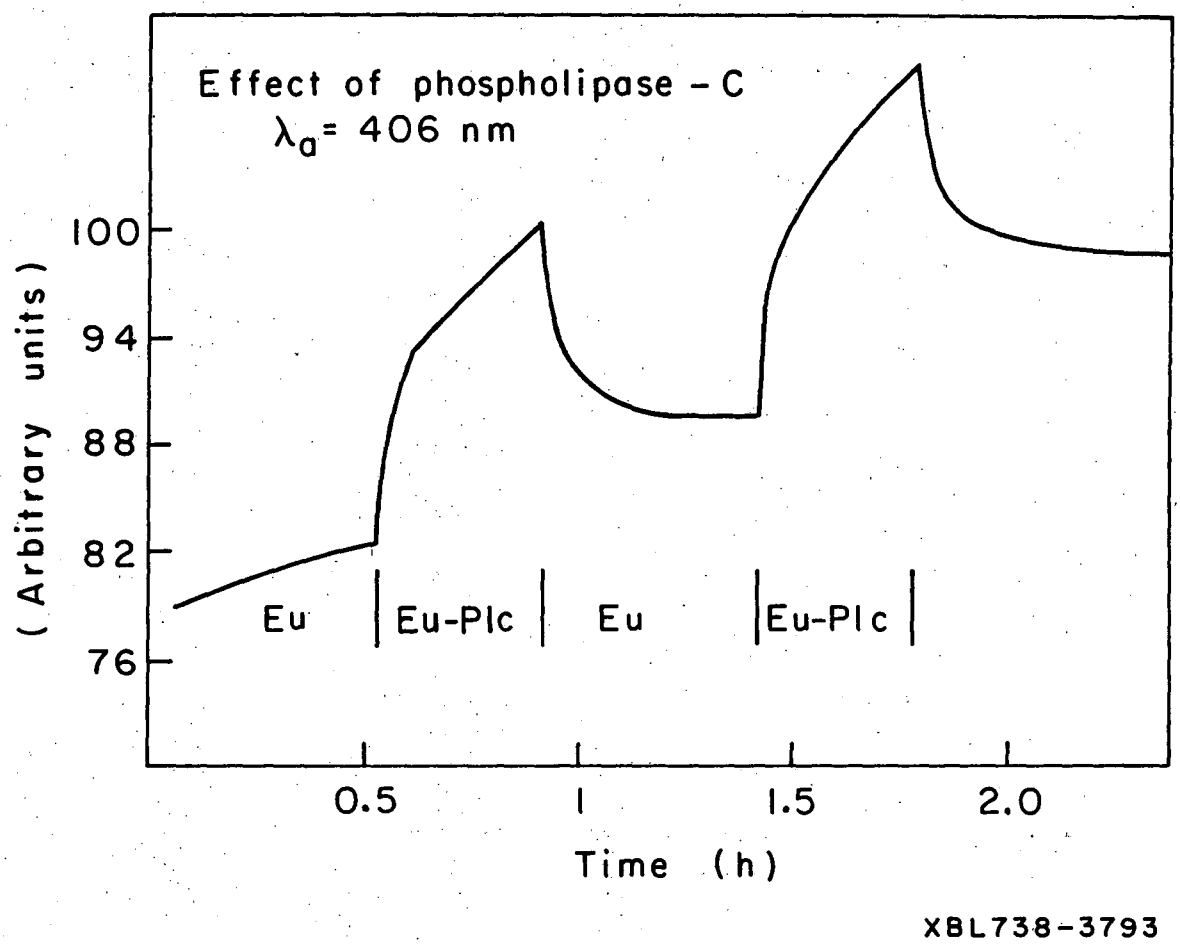

Fig. 28. Effect of phospholipase-c treatment on background fluorescence intensity in garfish nerve. Solution is alternated between Eu-Ringer and Eu-Plc-Ringer. λ = 614 nm, λ_a = 406 nm, where there is no Eu^{+3} fluorescence.

fluorescence of the Eu-Plc-Ringer. (The Eu^{+3} fluorescence in Eu-Plc-Ringer is enhanced by binding of some of the Eu^{+3} to Plc.) This is followed by a linear rapid increase in fluorescence, again from two causes: (1) Plc organic impurity fluorescence material seeping into the nerve trunk and (2) Eu^{+3} ions binding to the nerve trunk at a more rapid rate due to the enzymatic action of Plc. When the Eu-Plc-Ringer solution is again replaced by "normal" Eu-Plc-Ringer solution, we no longer observe the Eu^{+3} fluorescence, the organic impurity fluorescence, or the gradual seepage into the nerve trunk of organic impurity fluorescence of the Eu-Plc-Ringer solution. The absolute intensity of the observed fluorescence therefore drops suddenly. But this is followed by a resumption of fluorescence increase at a more rapid rate than before enzyme treatment because the enzyme has irreversibly damaged the axon membrane which increases the rate of Eu^{+3} uptake. A schematic drawing showing the interpretation of the action of Eu-Plc-Ringer set forth in this paragraph is given in Fig. 29.

Phospholipase-c was found to irreversibly abolish the ability of a garfish nerve trunk to propagate action potentials.

G. Effects of Dimethylsulfoxide (DMSO)

Dimethylsulfoxide (DMSO) is an organic solvent which is known to increase the permeability of membranes to water and aqueously solvated ions (85). We made a 0.5 mM Eu-Ringer solution containing 80% H_2O and 20% DMSO by volume, as a solvent. Using the resting state apparatus as in previous parts of this section, we found that gradual

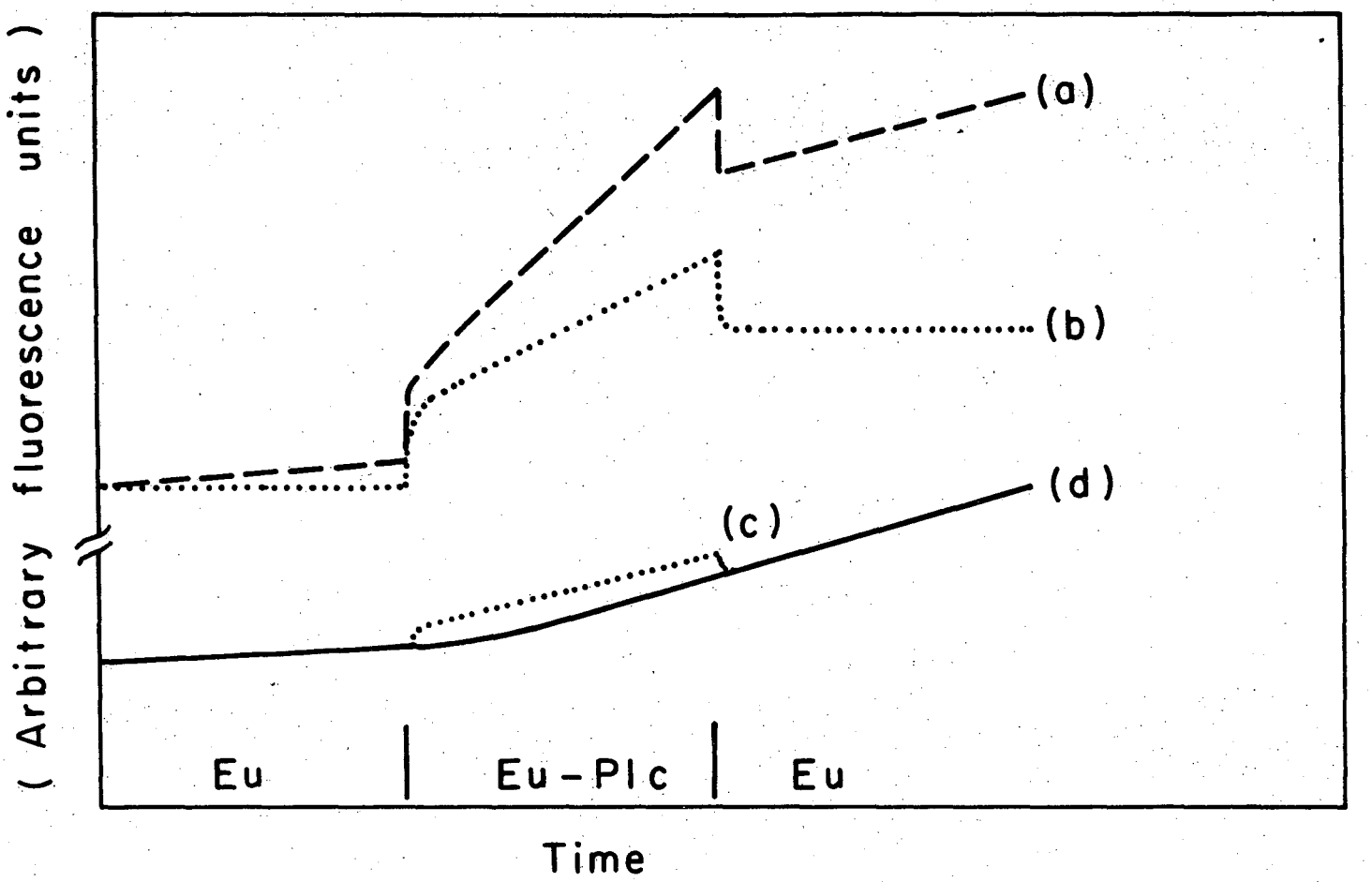

Fig. 29. Schematic drawing illustrating relationship between total fluorescence at λ = 614 nm, λ_a = 393 nm, as shown in Fig. 27, and the quantity of Eu^{+3} binding to nerve, during treatment of phospholipase-c. Curve (a), similar to Fig. 27; represents fluorescence of Ringer impurities + Eu in Ringer + Eu in nerve. Curve (b), similar to Fig. 28; represents fluorescence of Ringer impurities. Curve (c), difference between curves (a) and (b); represents Eu in Ringer + Eu in nerve. Curve (d), represents only Eu in nerve.

XBL 738 - 3794

nerve uptake of Eu^{+3} was approximately 2-4 times more rapid in the Eu-DMSO Ringer than in the "normal" DMSO-free Eu-Ringer. The change was apparently partially reversible, but this was difficult to ascertain, because re-introduction of Eu-Ringer after treatment by DMSO Eu-Ringer always caused a slight change in the mechanical properties and optical position of the nerve. A typical strip chart record is shown in Fig. 30. The possibility of optical position or background fluorescence artifacts was checked, as before, by running additional experiments with λ_a = 406 nm rather than λ_a = 393 nm; no change in rate of increase of background fluorescence was observed at λ_a = 406 nm.

H. Energy Transfer between Bound Rare-Earth Ions

Resting state fluorescence experiments, using photon-counting electronics, in which two Ringer solutions containing different pairs of chemically homologous rare-earth ions were alternately channeled through the nerve holder, were performed upon lobster walking leg nerves. The purpose of these experiments was to see whether the rare-earth binding sites are closely spaced enough for energy transfer to occur between adjacent but different bound ions (see Chapter III). This energy transfer could be measured by monitoring possible relative quenching of Eu-nerve fluorescence when Ringer solutions containing equal concentrations of Eu^{+3} and La^{+3} or Gd^{+3} [neither La^{+3} nor Gd^{+3} are good energy acceptors (104)] are alternated with Ringer solutions containing equal concentrations of Eu^{+3} and either Nd^{+3}, Tm^{+3}, or Dy^{+3} (which may accept Eu^{+3}-donated energy within a certain critical transfer distance).

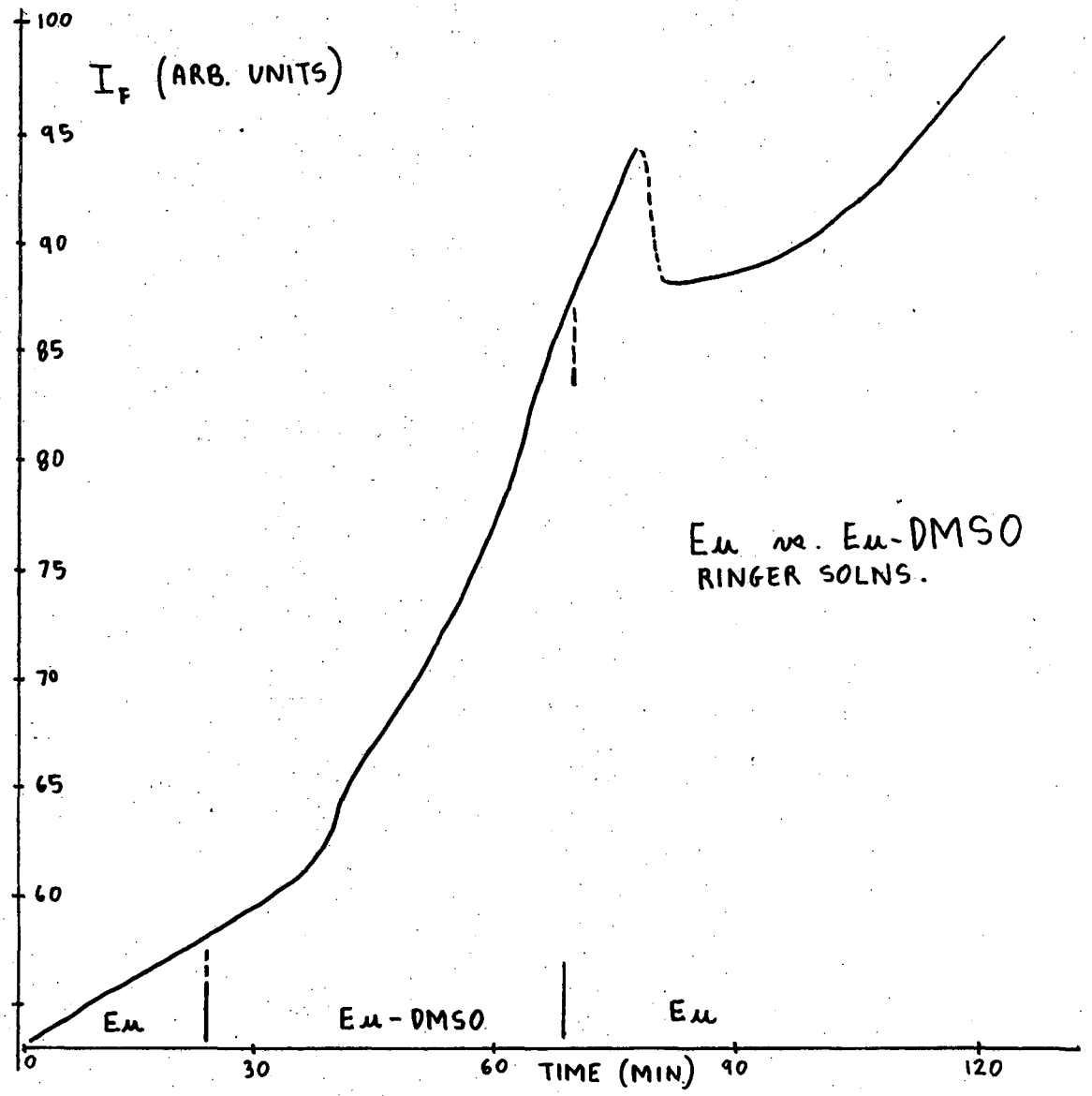

XBL 744-698

Fig. 30. Effect of DMSO on Eu-nerve fluorescence.
λ_a = 393 nm, λ = 614 nm.

Table 3 shows the percentage decrease of Eu-nerve fluorescence upon switching from the Ringer containing the pair of ions of column 1 to those of column 2.

Table 3

Ringer 1	Ringer 2	% Change
Eu-Gd	Eu-Nd	- 30
Eu-Gd	Eu-Tm	- 25
Eu-Gd	Eu-Dy	- 19
Eu-Gd	Eu-La	0

These results are exactly parallel to those found for energy transfer between rare-earth ions in inorganic glasses (104); i.e., Nd^{+3}, Tm^{+3}, Dy^{+3} can quench Eu^{+3} more efficiently than can Gd^{+3}, and La^{+3} and Gd^{+3} both have the same low quenching ability.

A typical Eu^{+3} fluorescence vs. time curve for these experiments, that for Eu-Gd vs. Eu-Tm Ringer is shown in Fig. 31. Note that sufficient time was not allowed for the Ringer solutions to reach equilibrium with nerve binding sites, so real percentage changes are probably even larger than those reported above. Scattered exciting light intensity was simultaneously monitored during these experiments as a control against artifacts; none of the experiments revealed any Ringer-dependent scattering changes.

We may conclude that at least some of the rare-earth binding sites in lobster nerve are more closely spaced than about 7Å (see Ref. 104). However, because of the likely multiplicity of types of binding

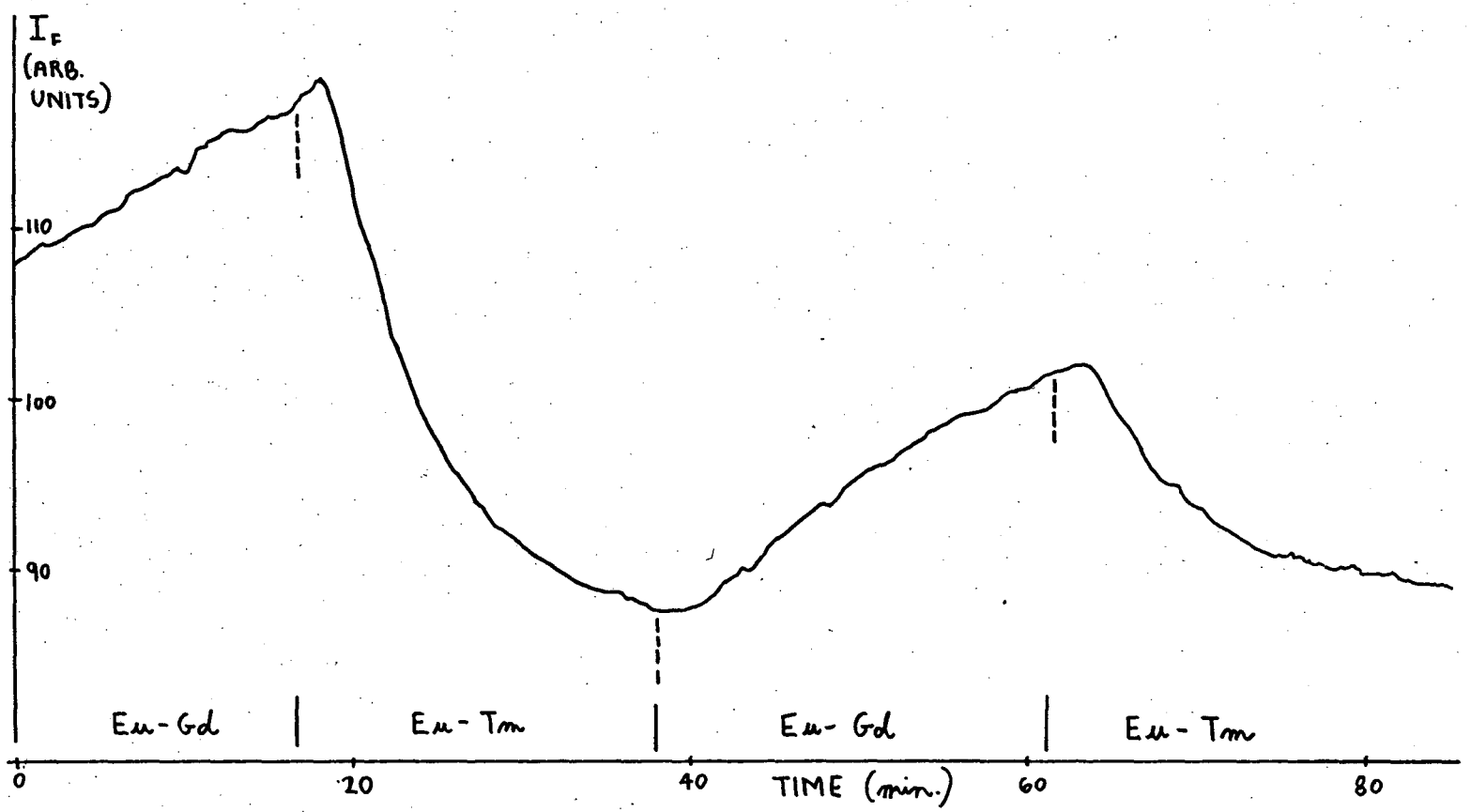

XBL 745-781

Fig. 31. Eu-lobster nerve fluorescence in Eu-Gd vs. Eu-Tm Ringer solutions. $\lambda_a = 393$ nm, $\lambda = 614$ nm.

sites and the difficulty of producing quantitative results on this structurally-complicated in vivo system, further conclusions may not be drawn. In a simpler system, the rate of fluorescence decrease from quenching after a rapid change of solutions as above may give information on the kinetics of rare-earth binding.

I. Protein Fluorescence Quenching by Transition Metals

As discussed in Chapter III, transition metals in complexes usually quench the intrinsic fluorescence of ligands. The protein fluorescence of nerve, excited at $\lambda_a = 285$ nm and observed at $\lambda = 310\text{-}380$ nm, was monitored during alternation of Ca-Ringer with transition metal-Ringer. Transition metals used were Ni^{+2}, Co^{+2} and Mn^{+2}. Although many experiments on both garfish and lobster nerve were attempted, results were not clear. Small (~1%) fluorescence decreases were occasionally noted, but it was difficult to determine whether these were artifacts of nerve movement or scattering changes, and these changes were not consistently reproducible. We therefore conclude that transition metal binding does not significantly quench nerve protein fluorescence. This conclusion does not necessarily contradict the previous observation (Chapter V) of energy transfer from protein to Tb^{+3} because (1) quenching of some protein fluorescence by transition metals may exist but only as a small fraction of the total protein fluorescence, and (2) the chemistries of Tb^{+3} and transition metal ions are not identical.

CHAPTER VIII

CONCLUSIONS AND DISCUSSION

The result that changes of bound rare-earth fluorescence synchronous with stimulation of garfish nerve are less than about ±0.01% of the total rare-earth fluorescence can lead to one or both of the following conclusions: (1) by far most of the chemical binding of rare-earth ions is not related directly to excitability, or (2) rare-earth ions do not change their binding state sufficiently to produce a fluorescence change, even if they are related directly to excitability. To the extent that rare-earths are a physiological substitute for Ca^{+2}, the same is true for Ca^{+2}.

Although the second conclusion above may be correct, the experiments using the flow-switching apparatus on a resting nerve tend to support the first conclusion. These experiments are all consistent with the interpretation that Eu^{+3} fluorescence is due primarily to Eu^{+3} binding to organelles and other substances in the axoplasm, especially the mitochondria, and that this binding is rate-limited by Eu^{+3} permeation through the axon membrane. Phospholipase-c and dimethylsulfoxide both irreversibly increase the permeability of the membrane to aqueous solutions, and therefore lead to a more rapid Eu^{+3} uptake. Apparently, trypsin, pronase, and neuraminidase do not act to break the main membrane barrier to Eu^{+3} permeation.

One of the main results of the Eu- and Tb-nerve fluorescence spectrum studies (Chapter V) is that Eu^{+3} binds to NADH and/or oxidized flavins in the nerve. This result also supports the view that much Eu^{+3}

fluorescence of Eu-nerve originates in the axoplasm, since little NADH or oxidized flavin is believed to be present in the nerve membrane.

The conclusion that the axon membrane is the rate limiter of Eu^{+3} uptake is consistent with the conclusions of Luxor and Yanez [92], that the rate constant for Ca^{+2} exchange across the axon membrane is an order of magnitude slower than the association of free Ca^{+2} with axoplasmic binding sites. Reynafarje and Lehninger [113] have shown that mitochondria of rat liver have a large capacity for Ca^{+2}, with both passive and active uptake. Numerous mitochondria appear to exist in several invertebrate of axons [48] as well as those of garfish olefactory nerve [42].

Is the known rate of transport of Ca^{+2} ions across the membrane into the axoplasm sufficient to account for the observed rate of Eu^{+3} uptake? Since no $^{45}Ca^{+2}$ tracer studies exist as yet for garfish nerve, we compare our results with $^{45}Ca^{+2}$ tracer studies on squid giant axon. The rate of Ca^{+2} influx in squid giant axon under normal conditions is about 0.2 pmol/cm^2-sec [72]. Using the data obtained in Section VI for total Eu^{+3} uptake in 48 hr, and the observations of Easton [42] on the total axon membrane surface area in garfish nerve, we can calculate an uptake rate of 0.0007 pmol/cm^2-sec for the garfish nerve. Thus, the rate of Eu^{+3} uptake we have observed in garfish nerve is at least two orders of magnitude smaller than the corresponding rate of Ca^{+2} uptake for giant squid axons, assuming that the uptake is entirely transport through the membrane into the axoplasm. Although the two figures are not really directly comparable, involving

different ions at different concentrations in different in vivo systems, they show that normal Ca^{+2} uptake is probably sufficient to account for all of the observed Eu^{+3} uptake.

The possibility that the observed Eu^{+3} uptake represents binding to, rather than permeation through, the axonal membranes, cannot be excluded completely. One might imagine that the phospholipase-c treatment exposes previously hidden ion binding sites on the membrane. However, the lack of effect of the protease and neuraminidase tend to weigh against this interpretation.

The sensitivity limit of 0.01% for transient changes is determined primarily by the shot noise of the total fluorescence, since the Xe lamp flicker is corrected for by the reference photomultiplier. Reduction of background fluorescence from substances not involved in excitation is therefore desirable. However, even when the experiments on transient changes were performed soon after bathing in Eu-Ringer and before much Eu^{+3} would have permeated into the axoplasm, negative results were still obtained. Apparently, if transient changes do exist, they are hidden by the flavin fluorescence shot noise. Since both the flavin background fluorescence and the bulk of Eu^{+3} binding originate in the axoplasm, the experiment may be more successful on internally perfused squid axons. Single squid axons, on the other hand, have the disadvantage of smaller total axon membrane surface area than garfish olefactory nerve trunk, so a smaller absolute signal, if any were to exist, would be expected.

The technique of in vivo Eu^{+3} substitution for Ca^{+2} and use as a fluorescent probe may still be valuable in biological systems where

either the Ca^{+2} involvement is quantitatively greater, as in muscle, or where one is interested in Ca^{+2} permeation through membranes or interaction with intracellular organelles.

There are properties of rare-earth fluorescence other than intensities and wavelengths which may be useful in indicating chemical environments in some biological systems. For example, the fluorescent lifetime of Eu^{+3} generally depends on the nature of the ligands [127]. The lifetime is fairly easily measurable since it is long (0.05-2.0 msec), and curve-fitting of a compound decay in a mixed system may indicate if Eu^{+3} is bound to more than one type of ligand system. Use of fluorescent lifetime measurements in systems where H_2O is replaced by D_2O may give information on the number of water molecules associated with the bound rare-earth [147]. Rare earths can also transfer excitation energy to each other [112, 104]. This property was applied here to determine that the separation of some rare-earth binding sites in lobster nerve is less than 7Å.

The technique's reliability is limited primarily by the faithfulness of Ca^{+2}-Eu^{+3} interchangeability. In nerve, it is clear that rare earths act like "super-calcium", and our results show that Eu^{+3} binding cannot be reversed by at least the normal concentration of Ca^{+2} in Ringer solution. Obviously, then, there is a functional chemical difference between Eu^{+3} and Ca^{+2}.

In our experiments, it is entirely possible that Eu^{+3} replaces Ca^{+2} at the binding sites associated with excitability, but its permeation through the membrane and binding to both the external membrane

and axoplasmic substances differs from Ca^{+2} in quantity and specificity.

> "Shall I teach you what knowledge is? When you know a thing, to hold that you know it; and when you do not know a thing, to allow that you do not know it. This is knowledge." —Confucius

ACKNOWLEDGMENTS

I am indebted to Dr. Melvin Klein for introducing me to scientific ideas and fields I previously had not known existed. Mel's guidance in the past four years has no doubt determined the direction of much of my future career. I also thank Dr. Melvin Calvin for his leadership of a well-equipped and remarkably diverse laboratory where work is both enjoyable and educational.

I thank Gary Smith and Mike Press for their advice on the building of the electronics, Dick O'Brien for building a nice home for the garfish, and Jo Onffroy, Evie Litton, Loretta Lizama, Carmen Hubbard, and Steve Gerber for production of this thesis.

Thanks also to Mike Kaplan for his generous advice about electrophysiology and microspectrophotometry. Roberto Bogomolni's suggestions on experimental technique and his uncanny knowledge of the hidden locations of all the equipment in the lab, were of great help to me. Joe Smith's and Jim Wurzbach's jokes and friendship, and the beautiful High Sierras, made even the most discouraging days tolerable.

Scientific exploration ideally is a very communal activity, where resources are commonly owned and shared and its fruits are openly disseminated, to be used for the betterment of the whole human community. Such an ideal structure survives best in a society similarly structured; I thank Prof. Charles Schwartz and the many other progressive people of Berkeley for their active efforts to move reality and the ideal a little closer together.

This work was supported by the U.S. Atomic Energy Commission.

REFERENCES

1. Baker, P.F., Hodgkin, A.L., Ridgeway, E.B. 1971. J. Physiol. 218, 709.
2. Ballhausen, C.J. 1962. "Introduction to Ligand Field Theory" McGraw-Hill, N. Y. Chap. 4.
3. Bangham, A.D. 1968. Prog. Biophys. Mol. Biol. 18, 29.
4. Bazanilla, F., Armstrong, C.M. 1972. J. Gen. Physiol. 60, 588.
5. Benson, A.A. 1966. J. Am. Oil Chem. Soc. 43, 265.
6. Benzer, T. I. and Raftery, M.A. 1972. Proc. Nat. Acad. Sci. 69, 3634.
7. Binstock, L. and Lecar, H. 1969. J. Gen. Physiol. 53, 342.
8. Blaustein, M.P. 1967. Biochim. Biophys. Acta 135, 653.
9. Blaustein, M.P., Goldman, D.E. 1968. J. Gen. Physiol. 51, 279.
10. Blumenthal, R., Changeux, J.P., Lefever, R. 1970. J. Memb. Biol. 2, 351.
11. Bretscher, M.S. 1973. Science 181, 622.
12. Brink, F. 1954. Pharmacol. Rev. 6, 243.
13. Brinley, F.J.,Jr. 1965. J. Neurophysiol. 28, 742.
14. Calvin, M., Wang, H.H., Entine, G., Gill, D., Ferruti, P., Harpold, M.A., Klein, M.P. 1969. Proc. Nat. Acad. Sci. 63, 1.
15. Capaldi, R. A., Green, D.E. 1972. FEBS Lett. 25, 205.
16. Caswell, A.H. 1972. J. Memb. Biol. 7, 345; Caswell, A.H. and Warren, S. 1972. Biochem. Biophys. Res. Comm. 46, 1757.

17. Caswell, A.H., Hutchison, J.D. 1971. Biochem. Biophys. Res. Comm. 42, 43.

18. Changeux, J.P., Thiery, J., Tung, Y., Kittel, C. 1967. Proc. Nat. Acad. Sci. 57, 335.

19. Chapman, D. 1965. N. Y. Acad. Sci. 137, 745.

20. Chapman, D. 1970. In "Membranes and Ion Transport" 1, ed. E. Bittar, Wiley-Interscience, N.Y. p. 23.

21. Chasteen, N. D., De Koch, R.J., Rogers, B.L., Hanna, M.W. 1973. J. Am. Chem. Soc. 95, 1301.

22. Chernitskii, Y.E., Lin, Y. I., Konev, S.V. 1969. Biofizika 14, 1023.

23. Cohen, L.B. 1973. Physiol. Rev. 53, 373.

24. Cohen, L.B., Davila, H.V., Waggoner, A.S. 1971. Biol. Bull. 141, 382.

25. Cohen, L.B., Keynes, R.D., Hille, B. 1968. Nature 218, 438.

26. Cohen, L.B., Hille, B., Keynes, R.D., Landowne, D., Rojas, E. 1971. J. Physiol. 218, 205.

27. Cohen, L.B., Keynes, R.D., Landowne, D. 1972. J. Physiol. 224, 701.

28. Cole, K.C. 1968. "Membrane, Ions, and Impulses" University of California Press, Berkeley, California.

29. Cole, K.S. 1949. Arch. Sci. Physiol. 3, 253.

30. Cone, R. 1972. Nature New Biol. 236, 39.

31. Conn, H. J. 1961. Biological Stains, 7th ed., p. 84. Williams and Williams, Baltimore, Md.

32. Conti, F. and Malerba, F. 1972. Biophysik 8, 326.

33. Curtice, R.E., Scott, A.B. 1964. Inorg. Chem. 3, 1383.

34. Dalton, J.C. 1958. J. Gen. Physiol. 41, 529.

35. Danielli, J.F., Davson, H. 1935. J. Cell. Comp. Physiol. 5, 495.

36. Darnall, D.W., Birnbaum, E.R. 1970. J. Biol. Chem. 245, 6484; Darnell, D.W., Birnbaum, E.R. 1973. Biochem. 12, 3489.

37. Dawson, R.M.C., Hauser, H. 1970. In "Calcium and Cellular Function" ed. A.W. Cuthbert. St. Martin's Press, N.Y., pg.17.

38. De Lorenzo, A.J.D., Brzin, M., Dettbarn, W.D. 1968. J. Ultrastructure Res. 24, 367.

39. Dettbarn, W.D., Davis, D.A. 1963. Biochim. Biophys. Acta 66, 397.

40. Dieke, G. 1968. "Spectra and Energy Levels of Rare-Earth Ions in Crystals" ed. H. M. Crosswhite and H. Crosswhite. Interscience, N.Y.

41. Doane, M.G. 1967. J. Gen. Physiol. 50, 2603.

42. Easton, D. 1965. Cold Spring Harb. Symp. 30, 15; Easton, D. 1971. Science 172, 952.

43. Eigen, M., DeMaeyer, L. 1970. Neurosci. Res. Prog. Bull. 9 (3), 301.

44. Eisenman, G., Sandblom, J.P., Walker, J.L. 1967. Science 155, 965.

45. Frankenhaeuser, B., Hodgkin, A.L. 1957. J. Physiol. 137, 218.

46. Frye, C.D. and Edidin, M. 1970. J. Cell Sci. 7, 313.

47. Gallagher, P.K. 1964. J. Chem. Phys. 41, 3061; 1965. J. Chem. Phys. 43, 1742.

48. Geren, B.B., Schmitt, F. O. 1954. Proc. Nat. Acad. Sci. 40, 863.

49. Gilbert, D.L. and Ehrenstein, G. 1969. Biophys. J. 9, 447; Gilbert, D.L. and Ehrenstein, G. 1973. Biophys. J. 13, 495.

50. Goldman, D.E. 1964. Biophys. J. 4, 167.

51. Gordon, H.T., Welsh, J.H. 1948. J. Cell. Comp. Physiol. 31, 395.

52. Hafemann, D.R. 1971. Biochim. Biophys. Acta 266, 548.

53. Hafeman, D. 1972. Soc. for Neurosci. Abst. 2nd Ann. Meeting, p. 97.

54. Hagiwara, S., Eaton, D.C., Stuart, A.E., Rosenthal, N.P. 1972. J. Memb. Biol. 9, 373.

55. Hagiwara, S., Takahashi, K. 1967. J. Gen. Physiol. 50, 583.

56. Hallett, M., Schneider, A.S., Carbone, E. 1972. J. Memb. Biol. 10, 31.

57. Helfferich, F. 1962. "Ion Exchange", McGraw-Hill, N.Y.

58. Hemmerich, P., Lauterwein, J.J. 1973. In "Inorganic Biochemistry", Vol. 2, ed. G. L. Eichhorn. Elsevier Scientific, N.Y., p. 1168.

59. Hille, B. 1970. Prog. Biophys. Mol. Biol. 21, 3.

60. Hille, B. 1972. J. Gen. Physiol. 59, 637.

61. Hille, B. 1972. Biophys. J. 12, 123a.

62. Hille, B. 1973. J. Gen. Physiol. 61, 669.

63. Hodgkin, A.L., Huxley, A.F. 1952. J. Physiol. 116, 473.

64. Hodgkin, A. L., Huxley, A.F. 1952. J. Physiol. 117, 500.

65. Hodgkin, A. L., Huxley, A.F., Katz, B. 1949. Arch. Sci. Physiol. 3, 129.

66. Hodgkin, A. L., Huxley, A.F., Katz, B. 1952. J. Physiol. 116, 424.

67. Hodgkin, A. L., Huxley, A.F., Katz, B. 1952. J. Physiol. 117, 500.

68. Hodgkin, A. L., Keynes, R. D. 1953. J. Physiol. 119, 513.

69. Hodgkin, A. L., Keynes, R. D. 1957. J. Physiol. 138, 253.

70. Hubbell, W. L., McConnell, H.M. 1968. Proc. Nat. Acad. Sci. 61, 12.

71. Howarth, J. V., Keynes, R.D., Ritchie, J.M. 1968. J. Physiol. 194, 745.

72. Hurlbut, W. P. 1970. In "Membrane and Ion Transport" 2, ed: E. E. Bittar. Wiley-Interscience, N.Y. p. 95.

73. Jobsis, F. F., O'Connor, M.J. 1966. Biochem. Biophys. Res. Comm. 25, 246.

74. Judd, B. R. 1963. "Operator Techniques in Atomic Spectroscopy" McGraw-Hill, N.Y.

75. Kajimoto, N., Kirpekar, S.M. Nature 235, 30.

76. Kaplan, M. 1972. Ph.D. thesis, Lawrence Berkeley Laboratory Report LBL-944, p. 45-56.

77. Katz, B. 1966. "Nerve, Muscle, and Synapse", McGraw-Hill, N.Y.

78. Kayushin, L. P., Ludkovskaya, R.G., Shmelev, I. P. 1960. Biofizika 5, 279.

79. Keynes, R.D., Lewis, P.R. 1956. J. Physiol. 134, 399.

80. Keynes, R.D., Ritchie, J.M., Rojas, E. 1971. J. Physiol. 213, 235.

81. Khodorov, B. L., Peganov, E. M. 1969. Biofizika 14, 474.

82. Korn, E. D. 1966. Science 153, 1496.

83. Krasnow, N. 1972. Biochim. Biophys. Acta 282, 187.

84. Landowne, D., Ritchie, J.M. 1971. J. Physiol. 212, 483.

85. Leake, C.D. 1967. Ann. N.Y. Acad. Sci. 141, 1-671.

86. Lehninger, A. L. 1968. Proc. Nat. Acad. Sci. 60, 1069.

87. Lehninger, A.L. 1970. "Biochemistry". Worth Publishers, N.Y. Chap. 10.

88. Lettvin, J. Y., Pickard, W. F., McCulloch, W.S., Pitts, W. 1964. Nature 202, 1338.

89. Loschen, G., Chance, B. 1971. Nature New Biol. 233, 273.

90. Lucy, J.A. 1968. In "Biological Membranes: Physical Fact and Function", ed. D. Chapman, p. 223.

91. Luk, C.K. 1971. Biochemistry 10, 2838.

92. Luxoro, M., Yañez, E. 1968. J. Gen. Physiol. 51, part 2, 1155.

93. Makarov, P.O., Krasovilskaya, M.V. 1968. Biofizika 15, 492.

94. Masters, B. 1973. Unpublished manuscript.

95. McConnell, H. 1970. In "Neurosciences Second Study Program," ed. F. O. Schmitt. Rockefeller Univ. Press. N.Y. p. 697.

96. Mela, L. 1968. Arch. Biochem. Biophys. 123, 286.

97. Mikulecky, D.C. 1963. Fed. Proc. 22.

98. Miledi, R. 1971. Nature 229, 411.

99. Moore, C., Pressman, B.C. 1964. Biochem. Biophys. Res. Comm. 15, 562.

100. Moore, J.W., Anderson, N., Blaustein, M., Takata, M., Lettvin, J. Y., Pickard, W.F., Bernstein, T., Pooler, J. 1965. N. Y. Acad. Sci. 137, 818.

101. Moore, J. W., Narahashi, T., Shaw, T. I. 1967. J. Physiol. 188, 99.

102. Mullins, L. J., De Weer, P. 1973. Nature New Biol. 243, 222.

103. Nachmansohn, D. 1970. Science 168, 1059.

104. Nakazawa, E., Shionoya, S. 1967. J. Chem. Phys. 47, 3211.

105. Narahashi, T., Moore, J.W., Shapiro, B. 1969. Science 163, 680.

106. Nash, H.A. and Tobias, J. M. 1964. Proc. Nat. Acad. Sci. 51, 476.

107. Offner, F.F. 1972. Biophys. J. 12, 1583.

108. Ohnishi, T., Ebashi, S. 1963. J. Biochem. 54, 506.

109. Pressman, B.C. 1968. Fed. Proc. 27, 1283.

110. Radda, G.K., Dodd, G.H. 1968. "Luminescence in Biochemistry". In: Luminescence in Chemistry. E. J. Bowen, editor, p.192. Van Nostrand, London.

111. Radda, G., Vanderkooi, J. 1972. Biochim. Biophys. Acta 265, 509.

112. Reisfield, R. 1973. Structure and Bonding 13. J. D. Dunitz, ed., Springer-Verlag, N.Y.

113. Reynafarje, B., Lehninger, A.L. 1969. J. Biol. Chem. 244, 584.

114. Robertson, J. D. 1959. Symp. Biochem. Soc. 16, 3.

115. Rojas, E., Atwater, I. 1967. Nature 215, 850.

116. Rojas, E., Atwater, I. 1968. J. Gen. Physiol. 51, 131.

117. Rojas, E., Lettvin, J. Y., Pickard, W. F. 1966. Nature, 209 886.

118. Scandella, C.J., Devaux, P., McConnell, H.M. 1972. Proc. Nat. Acad. Sci. 69, 2056.

119. Schmidt, P. P. 1971. Biochem. Biophys. Acta 233, 765.

120. Segal, J. R. 1968. Biophys. J. 8, 470.

121. Sherebrin, M. H. 1972. Nature 235, 122.

122. Sherebrin, M. H., MacClement, B.A.E., Franko, A.J. 1972. Biophys. J. 12, 977.

123. Shimomura, O., Johmon, F., Saiga, Y. 1963. Science 140, 1339.

124. Shmelev, I. P., Kayushin, L.P. 1961. Biofizika 6, 436.

125. Singer, S.J. 1971. In: "Structure and Function of Biological Membranes", ed. L. Rothfield. Acad. Press, N.Y., p.145.

126. Singer, S.J., Nicolson, G.L. 1972. Science 175, 720.

127. Sinha, S.P. 1967. "Europium". Springer-Verlag, N.Y.; Sinha, S.P., 1966. "Complexes of the Rare Earths". Pergamon Press, N.Y.

128. Smolka, G.E., Birnbaum, E.R., Darnall, D.W. 1971. Biochem. 10, 4556.

129. Spencer, T., Bygrave, F.L. 1972. FEBS Lett. 26, 225

130. Spyropoulos, C.S. 1968. Fed. Proc. 27, 1252.

131. Steinbach, H.B., Spiegelman, S., Kawata, N. 1944. J. Cell. Comp. Physiol. 24, 147.

132. Takata, M., Pickard, W.E., Lettvin, J. Y., Moore, J.W. 1966. J. Gen. Physiol. 50, 461.

133. Tasaki, I. 1959. J. Physiol. 148, 306.

134. Tasaki, I. 1968. "Nerve Excitation" Charles Thomas, Springfield, Ill.

135. Tasaki, I., Teorell, T., Spyropoulos, C.S. 1961. Am. J. Physiol. 200, 11.

136. Tasaki, I., Watanabe, A., Hallett, M. 1971. Proc. Nat. Acad. Sci. 68, 938.

137. Tasaki, I., Watanabe, A., Hallett, M. 1972. J. Memb. Biol. 8, 109.

138. Tasaki, R., Watanabe, A., Sandlin, R., Carmay, L. 1968. Proc. Nat. Acad. Sci. 61, 883.

139. Tasaki, I., Watanabe, A., Singer, I. 1966. Proc. Nat. Acad. Sci. 56, 1116.

140. Taylor, R.B., Duffus, W.P.H., Raff, M.C., de Petris, S. 1971. Nature New Biol. 233, 225.

141. Tobias, J. M. 1955. J. Cell. Comp. Physiol. 46, 183.

142. Tobias, J. M. 1964. Nature 203, 13.

143. Tosteson, D. C. 1968. Fed. Proc. 27, 1269.

144. Ungar, G., Romano, D.V. 1962. J. Gen. Physiol. 46, 267.

145. Van Breemen, C., deWeer, P. 1970. Nature 226, 760.

146. Vanderkooi, G., Green, D.E. 1971. Bioscience 21, 409.

147. Vinogradov, A., Scarpa, A., Chance, B. 1972. Arch. Biochem. Biophys. 152, 646.

148. Watanabe, A., Tasaki, I., Lerman, L. 1967. Proc. Nat. Acad. Sci. 58, 2246.

149. Watanabe, A., Tasaki, I., Singer, I., Lerman, L. 1967. Science 155, 95.

150. Wei, L. Y. 1969. Science 163, 280.

151. Wei, L. Y. 1972. Biophys. J. 12, 1159.

152. Weiss, D. E. 1969. Nature 223, 634; Aust. J. Biol. Sci. 22, 1355.

153. Williams, R.J.P. 1970. Quart. Rev. (Chem. Soc.) 24(3), 331.

154. Wybourne, B.G. 1965. "Spectroscopic Properties of Rare Earths", Interscience, N.Y.

155. Zambrano, F., Cellino, M., Canessa-Fischer, M. 1971. J. Memb. Biol. 6, 289.

LEGAL NOTICE

This report was prepared as an account of work sponsored by the United States Government. Neither the United States nor the United States Atomic Energy Commission, nor any of their employees, nor any of their contractors, subcontractors, or their employees, makes any warranty, express or implied, or assumes any legal liability or responsibility for the accuracy, completeness or usefulness of any information, apparatus, product or process disclosed, or represents that its use would not infringe privately owned rights.

TECHNICAL INFORMATION DIVISION
LAWRENCE BERKELEY LABORATORY
UNIVERSITY OF CALIFORNIA
BERKELEY, CALIFORNIA 94720